Drying Behavior of Oil Sand Mature Fine Tailings Pre-dewatered with Superabsorbent Polymer

Submitted by

Anis Roshani

Under the supervision of
Dr. Mamadou Fall

and

Co-supervision of
Dr. Kevin Kennedy

Thesis submitted in partial fulfillment of the requirements for the Doctorate in Philosophy in Environmental Engineering degree

Department of Civil and Environmental Engineering

University of Ottawa

To my Mother and Father

ABSTRACT

Oil sand processing to extract bitumen generates large volumes of slurry comprising water, silt, sand, clay, unrecovered bitumen, and residual chemical aides and solvents added during the extraction process. The by-product stream of the bitumen extraction is pumped into constructed tailings ponds. Managing these tailings is one of the most difficult environmental challenges for the oil sand industry. This study aims to develop a novel technique to assist in the assessment of the technologies for managing mature fine tailings (MFT) in oil sands. Innovative application of a superabsorbent polymer in the oil sands industry may provide a new method for tailings management. However, thus far, no study has addressed this research gap. In fact, fundamental knowledge of the behavior of MFTs pre-dewatered with the superabsorbent polymer could provide an important way to positively affect the speed of reclamation. To this end, comprehensive instrumentation, geo-environmental, and geotechnical analyses are carried out to obtain essential knowledge on the behavior of MFTs pre-dewatered with the polymer. The results of this study reveal that the mechanical, hydraulic, and thermal properties of the MFTs are related. Evaporation and drying shrinkage can affect the hydro-mechanical properties of the tailings and have a significant influence on the developed shear strength of the MFTs. In addition, the process-affected water includes a high concentration of the dissolved ions and organic chemicals that stem from ore extraction chemicals and tailings treatments, or that may be released from oil sands ores. Through the application of a superabsorbent polymer in the dewatering of oil sand MFTs, the chemical components are entrapped in the polymer chains, thus limiting the mobility of the major ions and trace metals in water bodies beneath the oil sand tailings pond. Results show that the application of the superabsorbent polymer considerably reduces the rate of drainage from the oil sand MFTs into water bodies, which can help mitigate the risk of seepage.

The author believes that the superabsorbent polymer dewatering technique can be considered as an environmentally friendly promising approach for management of oil sands MFTs. This new technique can accelerate the pace of reclamation and thus minimize the footprint of the oil industry in Canada.

ACKNOWLEDGEMENT

It would be a great pleasure to write a few words to acknowledge my supervisor Prof. Mamadou Fall and co-supervisor Prof. Kevin Kennedy whose consistent positive supports and guidance have truly allowed me the opportunity to complete this study. Indeed, their knowledge, understanding and dedication inspired me to continue to push forward and work hard. These words come as a small gesture of gratitude toward them.

I would like to express my deep gratitude towards Jean Claude Celestin (Technical officer, structures and geotechnical laboratory) who gave me his valuable suggestions and direction to proceed at every stage.

I also take the privilege to extend my hearty thanks to Samin and Parviz for their unconditional love and constant supports.

Table of contents

List of figures

List of tables

Symbols and Abbreviations

Symbols	Definition
ω	Water content
e	Void ratio
n	Porosity
S_r	Degree of saturation
γ_d	Dry density
γ_b	Wet density
τ	Undrained shear strength
Δ	Deflection
b	Spring constant
D	Measured diameter of the vane
H	Measured height of the vane
k	Hydraulic conductivity
ΔQ	Quantity of flow for a given time interval
L	Length of the specimen
A	Cross-sectional area of the specimen
Δt	Time interval
Δh	Head loss across the specimen
G_s	Specific gravity
M_d	Mass of dry soil
T	Torque

Acronym	Definition
CHWE	Clark Hot Water Extraction Process
MFTs	Mature Fine Tailings
PAH	Polycyclic Aromatic Hydrocarbons
ERCB	Energy Resource Conservation Board
SAP	Superabsorbent Polymer
DDA	Dedicated Disposal Area
SEM	Scanning Electron Microscopy
MIP	Mercury Intrusion Porosimetry
ASTM	American Standard Testing Material
CT	Composite Tailings
CTRW	Composite Tailings Recycle Water
SFR	Sand to Fine Ratio
CUF	Cyclone Under Flow
TT	Thickened Tailings
CFC	Coagulation-Flocculation-Coagulation
FC	Flocculation-Coagulation
FCF	Flocculation-Coagulation-Flocculation
ILTT	In Line Thickened Tailings
PE	Potential Evaporation
AE	Actual Evaporation
AA	Acrylic Acid
AM	Acrylamide
SPAN	Starch-graft-polyacrylonitrile
LL	Liquid Limit
PL	Plastic Limit
PI	Plasticity Index
A	Activity
XRD	X-Ray powder Diffraction
EC	Electrical Conductivity

VWC	Volumetric Water Content
TFT	Thin Fine Tailings
ICP-ES	Inductivity Coupled Plasma Emission Spectrometry
ICP-MS	Inductivity Coupled Plasma Mass Spectrometry
CEC	Cation Exchange Capacity
TD	Threshold Diameter
CIF	Crack Intensity Factor
PP	Polymer Paste
SL	Shrinkage Limit
BTEX	Benzene-Toluene-Ethylbenzene-Xylene
EDS	Energy Dispersive Spectroscopy

1

Introduction

1 Introduction

1.1 Oil sands composition and hot water process for bitumen extraction

The 1760s saw the first discovery of oil sand in Fort McMurray, northern Alberta. The high consumption of fossil fuel and the requirement for different forms of energy have prompted the expansion of this industry throughout the state. Certain areas of oil sand in northern Alberta are mined and processed for the production of bitumen. The Alberta oil sands consist of three deposits: Athabasca, Cold Lake, and Peace River. Together, these oil sand deposits contain approximately 170 billion barrels of mineable crude bitumen (Allen, 2008; Holden et al., 2011). In 2010, Alberta produced around 1.6 million barrels of raw crude bitumen per day from the oil sands. Alberta's 2010 yearly total of 589 million barrels of bitumen produced from oil sands was 8% higher than its 2009 oil sand production of bitumen (ERCB, 2011). The remaining established reserves as of December 31, 2013, are 26.56 billion cubic meters. Of this, 21.34 billion cubic meters (about 80 percent) is considered recoverable by in situ methods, while the remaining 5.22 billion cubic meters has an overburden of less than 65 m, which makes it suitable for surface mining technologies (ST98, 2014).

Oil sand is a mixture of bitumen, mineral matter and water in varying proportions. Bitumen content changes from 0 to 19 wt %, averaging 12 wt%, water is between 3-6 wt %, increasing as bitumen content decreases. Mineral content, predominantly quartz, silts and clay runs 84-86 wt %. The major clay mineral components in the region are 40-70 wt% kaolinite, 28-45 wt% illite and 1-15 wt% montmorillonite (Omotoso, 2004; Kaminsky et al., 2006). Among these clays montmorillonite clay has the highest affinity to water and swells when hydrated (Chalaturnyk et al., 2002).

Oil sands bitumen extraction was initially based on the pioneering work of Professor Karl Clark, who used a combination of hot water, water stream, and NaOH to separate the bitumen from the oil sands, and this process is called the Clark Hot Water Extraction Process (CHWE) (Clark and Pasternack, 1932). Figure 1.1 shows the typical commercial CHWE process used for bitumen extraction from oil sands. Oil sands are mined by trucks and shovels, digested at the extraction plant, and conditioned in large tumblers with the addition of hot water, steam, and NaOH. By using NaOH in the process, asphaltic acids in the bitumen become water-soluble and act as surfactants.

The concomitant reduction of the surface and interfacial tension with increasing pH of the suspension results in the disintegration of the oil sands ore structure and in the recovery of the bitumen (Chalaturnyk et al., 2002). As a result, the bitumen can be separated, and the silt and clay particles become well dispersed. The caustic use per ton of oil sand is about 0.11 kg at Syncrude Canada Ltd. and 0.04 kg at Suncore Inc. (Chalaturnyk et al., 2002). This is the first stage of extraction called conditioning. In the second stage, hot water is added to the solution for better separation of the sand particles and for floatation of the bitumen. In the separation unit, bitumen is separated as a froth that floats on the surface in large vessels. Sand settles to the bottom of the separation tank and is removed as a tailings stream. After the primary separation, a central portion of the slurry in the primary vessels, known as the middling, is removed and further processed to recover fine oil droplets that remain attached to the sand particles. The produced bitumen froth contains a significant amount of water and fine particles, which must be removed prior to the upgrading process where bitumen is converted into a light synthetic crude oil (Jeeravipoolvarn, 2009). The CHWE process achieves over 90% bitumen recovery efficiency at about 85°C and pH of 8.5 (Beier and Sego, 2008; Beier et al., 2013).

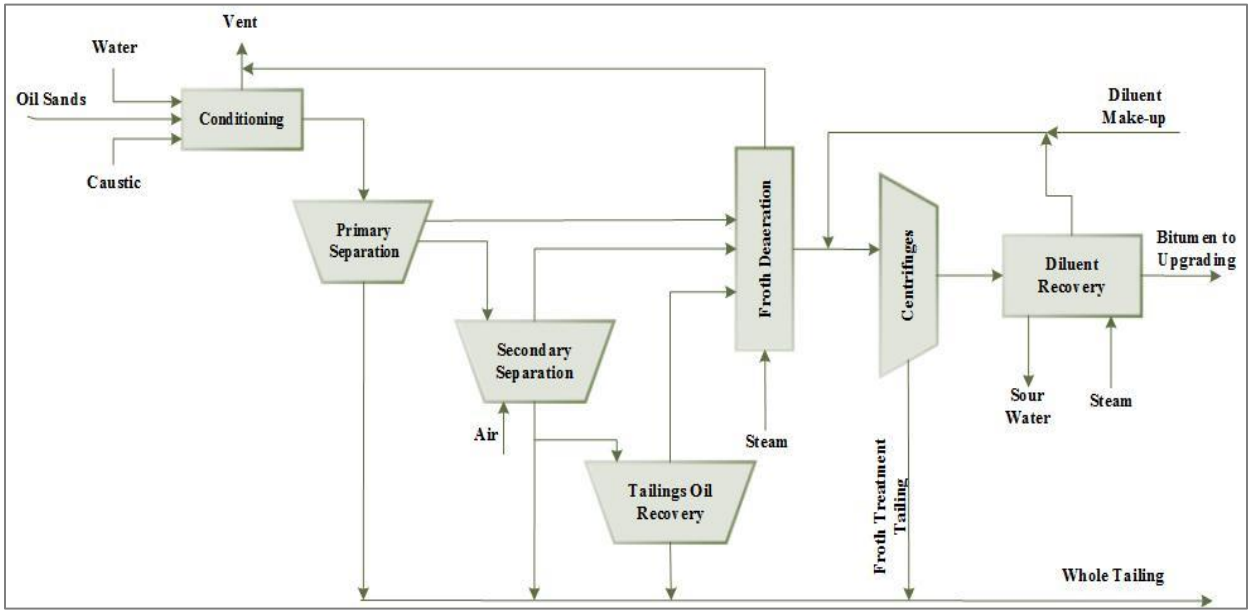

Figure 1.1, Bitumen extraction process from the oil sands (adapted from Chalaturnyk et al. 2002)

In the commercial oil sands operations using CHWE, the coarse tailings effluent, which is called "whole tailings", is in the form of a slurry, and it is a mixture of sand particles, dispersed fines, water, and residual bitumen. It has an about 55 wt% solid content, of which 82 wt% is sand, 17 wt% is fines smaller than 44 μm, and 1 wt% is residual bitumen (Table 1.1). The whole tailings are either discharged directly into a storage facility or classified through a cyclone separator and thickener before being discharged into the tailings pond.

In a conventional tailings deposition, the whole tailings are pumped into large tailings ponds. Here, the coarse particles settle out to form dykes and beaches, while much of the fines and residual bitumen flow into the pond as a thin and immature fine tailings stream at approximately 8% solid content (Jeeravipoolvarn, 2009). After a few years, the fines settle to 30%–35% solid content and are referred to as mature fine tailings (MFTs), which take several years for complete settlement (Eckert et al., 1996; Allen, 2008; Beier et al., 2013). The typical composition of MFTs is provided in Table 1.1.

For surface-mining operations, 1.0 m^3 of in-place oil sands will produce a tailings stream volume of 3.3 m^3 if the solid content of the tailings stream is 40% or a tailings stream volume of 1.9 m^3 if the solid content of the tailings is 60% (Jeeravipoolvarn, 2005). For every unit volume of bitumen recovered, 7 to 8 volume units of wet sand and MFTs (known as whole tailings) is produced that need to be handled. Ten volume units of water is added to the CHWE process, and three cubic meters of water per cubic meter of bitumen is trapped in the tailings pond and pores of the sands (Flint, 2005). On average, approximately 1 m^3 of sand and 0.25 m^3 of MFTs have been deposited for every barrel of bitumen that has been produced (Beier and Sego, 2008), and as of 2008, about 750 million cubic meters of MFTs exist within the tailings ponds (BGC Engineering Inc., 2010). If there is no change in the tailings management, the inventory of fluid tailings is forecast to reach two billion barrels per day in 2034 (Houlihan and Haneef, 2008). Therefore, MFTs storage requires large amounts of land, which has wide environmental and social concerns.

Table 1. 1, Whole tailings and MFTs properties (Beier et al. 2013)*

Parameter	Whole Tailings (typical values)	Mature Fine Tailings (typical values)
Solid content (%)	55	30-35
Sand content (% by mass)	82	<5
Fine content (% by total dry mass including bitumen)	17	>95
Clay content (% by dry mass of fine)	---	30-50

* It is noted that the solid content is the dry mass of solid divided by the total mass of the tailings. Sand content is the dry mass of sand divided by the dry mass of solid. Fine content is the dry mass of fine (silt < 44µm, clay < 2µm) divided by total dry mass of solids and clay content is the dry mass of clay divided by the dry mass of fine.

1.2 Statement of the problem

The inevitable expansion of oil sands development has and will continue to have a huge impact on land, water resource, ambient air, wild life and human health (Farkish and Fall, 2013; Hodson, 2013).

Land use for surface mining is comprised largely of the mine site, overburden storage, tailings ponds, and pit lakes. The Athabasca tar sand industrial footprint as of spring 2008 was 65040 ha (Timoney et al., 2009). Boreal coniferous, deciduous upland and riparian forests, water bodies, a diverse array of bog, and wetlands and shrub lands have been lost, and most of the native biota has been extirpated (Timoney et al., 2009).

As mentioned earlier, the extraction of bitumen from oil sands generates a huge amount of MFTs. MFTs have poor consolidation and water release characteristics (Chalaturnyk et al., 2002; Mikula et al., 1996). The depth of the MFTs zone varies from 15 to 20 m, and the pond can have a maximum depth of about 50 m in some areas (Guo, 2009). High depth of the ponds and low permeability of the tailings cause very slow densification, and it takes several decades to become trafficable under natural conditions (Eckert et al., 1996; Allen, 2008; Jeeravipoolvarn et al., 2009; Beier et al., 2013).

Tailings ponds contain a variety of harmful chemicals from heavy metals to naphthenic acids, which are of concern owing to their toxicity to aquatic organisms, birds, and wildlife in general (Renault et al., 1998; Allen, 2008; Pramanik, 2016).

Tailings pond seepage is another risk of pollution (Holden et al., 2011; Holden et al., 2013; Parajulee and Wania, 2014; Frank et al., 2014). Seepage of tailings water from Tar Island Pond One (Suncore's tailings pond) into the groundwater hydraulically connected to the Athabasca River has been quantified at 5.5–5.7 million L/day (Pramanik, 2016). Identified chemicals of potential ecological concern in the seepage are arsenic, ammonia, barium, chromium, bismuth, iron, lithium, manganese, naphthenic acids, selenium, strontium, tin, vanadium, zinc, methylnaphthalene, and polycyclic aromatic hydrocarbons (Allen, 2008; Timoney et al., 2009; Cui and Fall, 2015; Liang et al., 2011; Abolfazlzadehdoshanbehbazari et al., 2013). The projected peak seepage rate in 2012 was 26 million L/day (Environmental Defence, 2008). Sediment arsenic concentration in Lake Athabasca increased over the period 1970–1990 from 2 mg/kg to 10 mg/kg (Bourbonniere et al., 1996), while the interim freshwater guideline for protection of aquatic life is 5.9 mg arsenic/kg (CCME, 2002).

The impact of tailings ponds may be most evident for greenhouse gas production. Bacterial production of methane from tailings ponds increases greenhouse gas production. At the Mildred Lake settling basin, 60%–80% of the gas flux from the pond surface is due to methane, and 40 million litres of methane is released daily from these ponds (Holowenko et al., 2000; Parajulee and Wania, 2014).

To address and reduce the aforementioned environmental impacts and risks associated with the production and disposal of large amount of oil sand tailings, particularly MFTs, the Alberta Energy and Resources Conservation Board (ERCB) released new rules in 2009 to regulate the reclamation of oil sand tailings. Consequently, oil sand operators were required to submit their management plans in accordance with Directive 074 "Tailings Performance Criteria and Requirements for Oil Sand Mining Schemes". The key purpose of Directive 074 was to regulate tailings in the oil sands and to reduce the volume of produced fluid fine tailings. The ERCB wanted to hold minable oil sands operators accountable for the produced tailings by setting time-lines for the reduction in the amount of fluid tailings and the creation of a trafficable surface through consolidation, drying, drainage, etc. (ERCB, 2011). According to Directive 074, material deposited in dedicated disposal

areas (DDAs) must achieve a minimum undrained shear strength of 5 kPa within one year of deposition. If it does not meet this criterion, the material must be removed or remediated. Furthermore, the deposit in DDAs must be ready for reclamation within five years after active deposition, and at that time, the minimum shear strength must be 10 kPa (ERCB, 2011).

Therefore, over the years, the oil sands industry has expended significant effort in research on the development of technologies for the dewatering, densification, and speeding up of MFTs consolidation. Many dewatering and densification technologies/methods have been developed and applied for the dewatering and improvement of the settling properties of these MFTs (Farkish and Fall, 2013), as will be discussed in Chapter 2. Thin lift drying is one of the oil sand tailings management techniques that has been considered in recent years by active operators in this industry. Thin lift involves tailing deposition in thin lifts. Each lift is allowed to dry before deposition of the next lift. Successive deposition of tailings in thin lifts can maximize the influence of evaporation on the dewatering process. Multi-layer deposition has a high impact on minimizing dedicated disposal area. However, there are some issues associated with this technique. Sequential lifts act as a cover for the former lifts and prevent their evaporation. Drainage water that goes through the last layer (due to gravity) has a negative impact on the shear strength of the deposition. Therefore, the thin-lift deposition technique cannot be applicable if the developed strength in each lift is compromised by the freshly deposited layer. To address this issue, a novel dewatering technique was introduced in 2013, which consists of dewatering and densifying MFTs by using a superabsorbent polymer (SAP) before their disposal (Farkish and Fall, 2013). Previous studies (e.g., Farkish and Fall, 2013) have demonstrated that the use of SAP results in rapid dewatering and densification of MFTs as well as in significant strength increase of the deposition. However, these previous investigations on the SAP-based dewatering technique considered only small (size) MFT samples and multi-layer deposition of MFTs was excluded. To the best of our knowledge, no study has addressed the combined effect of atmospheric drying and SAP in multi-layer deposition of MFTs. The understanding and assessment of the impact of atmospheric drying on the desiccation behavior and properties of MFTs dewatered with SAP in multi-layer deposition are critical for the field application of the SAP-based dewatering technique. Furthermore, to assess the field efficiency of the aforementioned approach, i.e., multi-lift deposition of MFTs pre-dewatered with SAP, it is important to investigate the desiccation behavior of MFTs pre-dewatered with SAP under prevalent climatic condition in summer (the period in which atmospheric drying

is more effective). A key climatic factor that can affect the desiccation behavior of multi-lifts of MFTs pre-dewatered with SAP during summer in northern Alberta is the alternation and duration of dry and wet (rainfall) weather periods. However, no previous studies have attempted to assess and understand the effect of wetting and drying cycles on the desiccation behavior of multi-lifts of MFTs pre-dewatered with SAP.

The main objectives of this thesis are:

(i) To assess and better understand the effect of atmospheric drying on the desiccation and geo-environmental behavior or properties of raw MFTs in a multi-lift deposition system.

(ii) To assess and understand the effect of atmospheric drying on the desiccation and geo-environmental behavior or properties of MFTs pre-dewatered with SAP in a multi-lift deposition system.

(iii) To assess and understand the effect of wetting and drying cycles on the desiccation and geo-environmental behavior or properties of MFTs pre-dewatered with SAP in a multi-lift deposition system.

The specific objectives of the present thesis are:

(i) To develop an appropriate experimental setup and testing method for assessing the effect of atmospheric drying on the desiccation process in a multi-lift deposition system for raw MFTs as well as MFTs pre-dewatered with a superabsorbent polymer (SAP).

(ii) To develop an appropriate experimental setup and testing method for assessing the effect of wetting and drying cycles on the desiccation process in a multi-lift deposition system for MFTs pre-dewatered with SAP.

(iii) To conduct column experiments to investigate the desiccation and geo-environmental behavior of two lifts of MFTs under atmospheric drying

(iv) To conduct column experiments to investigate the desiccation and geo-environmental behavior of two lifts of MFTs pre-dewatered with SAP under atmospheric drying

(v) To conduct column experiments to investigate the effect of wetting and drying cycles on the desiccation behavior of two lifts of MFTs pre-dewatered with SAP.

1.3 Research approach and methods

The geotechnical and geo-environmental behavior of raw MFTs and MFTs pre-dewatered with SAP have been experimentally studied in order to achieve the research objectives. For this research, MFTs were derived from northern Alberta, and the physical properties of these MFTs will be presented in subsequent chapters. This research was carried out in four separate phases. (i) The effect of atmospheric evaporation on the geotechnical behavior of **raw MFTs** in a two-lift deposition system (25 cm each) was investigated. Four columns in total were engineered and filled with raw MFTs, including one column for monitoring purposes and three columns for sampling. Each column was dismantled at specific elapsed times of 5, 10, 20, and 30 days. The samples were taken from different heights of the columns and then subjected to different tests. (ii) **Modified MFTs with 1% superabsorbent polymer** were casted in the columns as a two-lift deposit (25 cm each), and samples were collected after the same elapsed times as in the first phase. The samples were also taken from the same heights as in the first phase, and then, the effect of SAP on the desiccation behavior of MFTs was analyzed. (iii) The negative impact of precipitation on the desiccation behavior of MFTs was studied in the third phase of the research. A thin-lift deposition system (two lifts of 15 cm) of **raw MFTs** was subjected to five cycles of wetting–drying. For this purpose, one column with a large surface area was manufactured. Five cycles of wetting–drying were applied in a 30-day period, and samples were then collected and subjected to geotechnical analysis. (iv) The effect of the wetting–drying cycles on the geotechnical desiccation behavior of **MFTs pre-dewatered with SAP** in a two-lift deposition system (15 cm each) was studied. The experimental setup and procedure was the same as that in the third phase. Samples collected from different heights after specific elapsed times were subjected to different tests. Two types of tests were performed: (i) Monitoring tests, which refers to collection of results from embedded sensors in the monitoring column. The monitored parameters include suction, water content, electrical conductivity, and temperature, as well as evaporation rate, drainage rate, and settlement. (ii) Sampling tests, which include measurement of undrained vane shear strength and hydraulic conductivity, scanning electron microscopy (SEM), mercury intrusion porosimetry (MIP), and evaluation of index properties (solid content, void ratio, porosity, density, and saturation). All

experiments were conducted in accordance with the latest version of ASTM (American Society for Testing and Materials). The obtained experimental results provide fundamental knowledge and information about a novel technology for multi-lift deposition of MFTs. For sustainable development of the oil sands industry, it is important to develop a technically and economically applicable solution for managing the large inventory of oil sand fine tailings.

1.4 Tasks and organization of the thesis

A description of the experimental setup, testing procedure, discussion, and conclusion for each tasks and objectives of the research, as well as the relevant technical and theoretical background, are provided in nine chapters of this thesis. **Chapter one** gives a general introduction. It also presents the problem statement, objectives, and methods. **Chapter two** includes a comprehensive literature review on different techniques in MFTs management and on previous studies on SAP-based dewatering of MFTs. **Chapters three to seven** consist of five technical papers. Each paper includes an introduction, material and methods, experimental results and discussion, and conclusion. **Chapter three** describes the hydro-mechanical behavior of raw MFTs under atmospheric drying in a two-lift deposition. The effect of newly added lift on the developed suction and strength is well discussed in this chapter. **Chapter four** presents the microstructural, hydraulic conductivity, and geochemical changes during atmospheric drying of raw MFTs in a two-lift deposition system. The interaction of the former lift and the fresh lift and its impact on the aforementioned parameters will be fully explained. In **Chapter five**, the impact of pre-dewatering MFTs with SAP on the mechanical, physical, and hydraulic properties of the MFTs in a two-lift deposition is studied. This chapter also provides a comparison between the drying behavior of raw MFTs and MFTs pre-dewatered with SAP. **Chapter six** highlights the effect of SAP on the water content, geo-chemistry, microstructure, and permeability of the MFTs. In addition, a comparison between raw MFTs and MFTs pre-dewatered with SAP with respect to these parameters is discussed. **Chapter seven** studies the effect of cyclic wetting–drying on the water distribution, strength gain and loss, and settlement in a two-lift deposition system of raw MFTs as well as MFTs pre-dewatered with SAP. Further, the initiation and evolution of cracks in periodical wetting–drying cycles induced by seasonal rainy and sunny weather were monitored, and the image processing and other techniques involved are discussed. **Chapter eight** synthesizes and integrates

the results obtained, and proposes further insights. **Chapter 9** presents conclusions and recommendations for future research.

1.5 Statement of authorship

Paper Title	Publication Status	Publication Details
A column study of the hydro-mechanical behavior of mature fine tailings under atmospheric drying	Published	International journal of mining science and technology, 2017, 27(2), 203-209
Microstructural, hydraulic conductivity and geochemical changes of drying mature fine oil sand tailings in column experiment	Published	International journal of mining, reclamation and environment, ISSN: 1748-0930, 2017, 1-15
Drying behavior of mature fine tailings pre-dewatered with superabsorbent polymer (SAP): column experiment	Published	Geotechnical testing journal, 2017, 40(2), 210-220
Impact of drying on geo-environmental properties of mature fine tailings pre-dewatered with superabsorbent polymer	Published	International journal of environment, science and technology, 2016, 14 (3), 453-462.
Effect of wetting-drying cycles on drying behavior of mature fine tailings pre-dewatered with superabsorbent polymer.	under review	submitted

Author Contributions

Name of the principal Author	Anis Roshani
Contribution to the papers	Performed analysis and tests on all samples; interpreted data; wrote first draft of the manuscript.

Name of the first co-Author and role	Dr. Mamadou Fall; supervisor
Contribution to the papers	Supervised development of work; provided significant help in data interpretation, manuscript writing and evaluation; acted as corresponding author.

Name of the first co-Author and role	Dr. Kevin Kennedy; supervisor
Contribution to the papers	Co-supervised development of work and review the manuscripts

1.6 References

Abolfazlzadehdoshanbehbazari, M., Birks, S., Moncur, M. C., and Ulrich, A. (2013). Fate and transport of oil sand process-affected water into the underlying clay till: A field study. Journal of Contaminant Hydrology, 151, 83–92.

Allen, E. (2008). Process water treatment in Canada's oil sands industry: II. A review of emerging technologies. Journal of Environmental Engineering and Science, 7(5), 499–524.

Beier, N., and Sego, D. (2008). The oil sands tailings research facility. Journal of Geotechnical News, 26(2), 72–77.

Beier, N., Wilson, W., Dunmola, A., and Sego, D. (2013). Impact of flocculation-based dewatering on the shear strength of oil sands fine tailings. Canadian Geotechnical Journal, 50, 1001–1007.

BGC Engineering Inc. (2010). Oil sands tailings technology review. Oil Sands Research and

Information Network, OSRIN Report No. TR-1.

Bourbonnier, R., Telford, S., and Kemper, J. (1996). Depositional history of sediments in Lake Athabasca: geochronology, bulk parameters, contaminants and biogeochemical markers. Repoar No. 72, Edmonton: Northern River Basins Study.

CCME (Canadian Council of the Ministers of the Environment). (2002). Canadian Enviromental Quality Guidelines, Ottawa. Ontario, Canada.

Chalaturnyk, J., Scott, D., and Ozum, B. (2002). Mnagement of oil sands tailings. Journal of Petrolumn Science and Technology, 20(9-10), 1025-1046.

Clark, K. A, and Pasternack, D. S. (1932). Hot water separation of bitumen from Alberta bituminous sand. Journal of Industrial and Engineering Chemistry, 1410–1416.

Cui, L., and Fall, M. (2015). A coupled thermo–hydro-mechanical–chemical model for underground cemented tailings backfill. Journal of Tunnelling and Underground Space Technology, 50, 396–414.

Eckert, W. F., Masliyah, J. H., Gray, M. R., and Fedorak, P. M. (1996). Prediction of sedimentation and consolidation of fine tails. AIChE Journal, 42(4), 960–972.

Energy Resource and Conservation Board (ERCB), 2011. Government of Alberta.

Environmental Defence. (2008). The tar sands' leaking legacy; Environmnet Defence, Toronto, Ontario, Canada.

Kaminsky, H., Etsell, T., Ivey, D., and Omotoso, O. (2006). Fundamental particle size of clay minerals in Athabasca oil sands tailings. Journal of Clay Sience, 12 (2), 217-222.

Farkish, A., and Fall, M. (2013). Rapid dewatering of oil sand mature fine tailings using super absorbent polymer (SAP). Journal of Minerals Engineering, 50–51, 38–47.

Flint, L. (2005). Bitumen recovery technology: a review of long term R&D opportunities. LENEF Cnsulting, Calgary, Alberta, Canada.

Frank, R., Roy, j., Bickerton, G., Rowland, S., Headley, J., Scarlett, A., West, C., Peru, K., Parrott, J., Conly, M., and Hewitt, L. (2014). Profiling oil sands mixtures from industrial developments and natural groundwaters for source identification. Journal of Environmental and Science, 48(5), 2660–2670.

Guo, C., (2009). Rapid densification of the oil sands mature fine tailings (MFT) by microbial activity. Ph.D. thesis in Geothechnical Engineering, University of Alberta, Edmonton, Alberta, Canada.

Hodson, P. V. (2013). History of environmental contamination by oil sands extraction. Proceedings in the National Academy of Sciences of the United States of America, 110(5), 1569–1570.

Holden, A. A., Haque, S. E., Mayer, K. U., and Ulrich, A. C. (2013). Biogeochemical processes controlling the mobility of major ions and trace metals in aquitard sediments beneath an oil sand tailings pond: Laboratory studies and reactive transport modeling. Journal of Contaminant Hydrology, 151, 55–67.

Holden, A. A., Donahue, R. B., and Ulrich, A. C. (2011). Geochemical interactions between process-affected water from oil sands tailings ponds and North Alberta surficial sediments. Journal of Contaminant Hydrology, 119(1–4), 55–68.

Holowenko, F., Mackinnon, M., and Fedorak, P. (2000). Methanogens and sulfate-reducing bacteria in oil sands fine tailings waste. Canadian Journal of Microbial, 46, 927-937.

Houlihan, R., and Haneef, M. (2008). Past, present, future tailings regulatory perspective. Proceeding in the international conference of oil sands tailings, Edmonton, Alberta.

Jeeravipoolvarn, S. (2005). Compression behavior of thixotropic oil sands tailings, MASc thesis in Geotechnical Engineering, Department of Civil and Environmental Engineering: University of Alberta, Canada.

Jeeravipoolvarn, S., Scott, J. D., and Chalaturnyk, R. J. (2009). 10 M standpipe tests on oil sands tailings: Long-term experimental results and prediction. Canadian Geotechnical Journal,

46(8), 875–888.

Liang, X., Zhu, X., and Butler, E. C. (2011). Comparison of four advanced oxidation processes for the removal of naphthenic acids from model oil sands process water. Journal of Hazardous Materials, 190(1–3), 168–176.

Mikula, R., Kasperski, K., and Burns, R. (1996). Nature and fate of oil sands fine tailings. Journal of American Chemical Society, 677-723.

Omotoso, M. (2004). High surface areas caused by smectitic interstratification of kaolinite and illite in Athabasca oil sands. Journal of Applied Clay Science, 25(1–2), 37–47.

Parajulee, A., and Wania, F. (2014). Evaluating officially reported polycyclic aromatic hydrocarbon emissions in the Athabasca oil sands region with a multimedia fate model. Proceedings of the National Academy of Sciences of the United States of America, 111, 3344–9.

Pramanik, S. (2016). Review of biological processes in oil sands: a feasible solution for tailings water treatment. Environmental Reviews, 24, 274-284.

Renault, S., Lait, C., Zwiazek, J., and MacKinnon, M. (1998). Effect of high salinity tailings waters produced from gypsum treatment of oil sands tailings on plants of the boreal forest. Journal of Environmental Pollution, 102(2–3), 177–184.

ST98 (2014). Alberta energy reserves and supply/demend outlook. p. 72.

Timoney, K., and Lee, P. (2009). Does the Alberta tar sands industry polute? The scientific evidence. Journal of Open Conservation Biology, 3, 65-81.

2
Theoretical and technical background

2 Theoretical and technical background

2.1 Introduction

To better understand the results presented in this thesis, the relevant background on the main technologies of treatment of oil sand tailings as well as on SAP and its use in dewatering technology are described and discussed in this chapter. Moreover, a review of previous studies on SAP-based dewatering or densification of MFTs is provided.

2.2 Tailings treatment technologies

Management of a large quantity of MFTs is a real challenge for the oil sands industry. Various techniques have been developed over the past 40 years by several oil sands operators and researchers for removing the water and land reclamation. These technologies have been divided into five groups (BGC Engineering Inc., 2010):

1. Physical/Mechanical processes: filtration, centrifugation, and wick drain.
2. Mixture/Co-disposal: consolidated tailings, MFTs spiked tailings, and MFTs mixed with Clear water overburden.
3. Chemical amendment: thickened tailings, in-line thickened tailings, coagulation, and flocculation.
4. Natural processes: evaporation, and freeze-thaw.
5. Permanent storage: water capped tailings, and pit Lake.

2.2.1 Physical/Mechanical processes

In physical and mechanical processes, several technologies for separating water from solids are applied. Some of them will be described below.

2.2.1.1 Filtered whole tailings

Filtration is one of the most traditional and useful methods for separating liquids from solids in different industries. Filtration takes place under pressure or vacuum force. In the mid-1990s, pilot-scale tests were conducted on different bitumen extraction processes in Alberta. Many of these

experiments were unsuccessful. The coarse particles settled quickly and formed a thick porous filter cake, and the fines eventually settled onto the surface of this cake and blind it (BGC Engineering Inc., 2010).

2.2.1.2 Centrifugation of fine tailings

A centrifuge applies up to thousands of times the force of gravity to extract fluids from solids. The use of centrifugation to produce dry tailings was tested in the past with robust results but the cost was too high at that time. This technology was developed at the bench scale at Syncrude as a two-step process. The first step is MFTs dewatering using a horizontal bowl scroll with flocculation to form a relatively free water-free cake. The cake has a solid content of 55% -60%. The second step involves subsequent dewatering of the cake by natural processes, such as desiccation and freeze-thaw, via 1 to 2 m thick annual lifts in order to increase the strength of the soil and reclamation of the land (BGC Engineering Inc., 2010). However, this method requires high upfront capital and high operating costs, which may be challenging.

2.2.1.3 Wick drains

Prefabricated vertical drains (wick drains or band drains) facilitate the dewatering process by providing a suitable conduit to allow the exit of pore water. In 2009, Suncor conducted field trials of vertical wick drains installed in tailings with very high fine content and low density. Preliminary tests were successful, and laboratory data indicated that there was no clogging of nonwoven geo-textiles with apparent opening sizes of 90 µm and 210 µm (Wells and Caldwell, 2009). However, wick drains may not retain their shape over time owing to large settlement. Further, the high cost of close spacing of wick drains is another issue associated with this technology.

2.2.2 Mixture/Co-disposal

Mixture or co-disposal technologies involve mixing tailings streams with available soil materials and waste products to increase the solid content and density of the tailings.

2.2.2.1 Composite tailings (CT)

In the oil sands industry, composite tailings (CT) is a process in which the coarse sand fractions are mixed with the clay fraction of extracted tailings (Caughill et al., 1993; Chalaturnyk et al.,

2002; Matthews et al., 2002; Mackinnon et al., 2010). The CT process rapidly releases water after deposition and binds the MFTs in a coarse tailings deposit. This technology creates non-segregating slurry with higher fine content and results in consumption of MFTs (Matthews et al., 2002). The CT process enhances the permeability of the mixture, and the sands acts as a stress or load that increases the de-watering of the deposit (Mackinnon et al., 2001).

Caughill et al. (1993) tested tailings supplied by Syncrude and investigated the use of lime and sulphuric acid to prevent segregation of the tailings stream. They reported that 800 ppm CaO appeared to be the optimum concentration in terms of the rate of settlement and final void ratio after self-weight consolidation, and that the tailings treated with 600 and 800 ppm CaO showed no segregation. The optimum acid concentration was in the range of 10 mL/L, but the acid-treated tailings did not consolidate to quite as low a final void ratio as did the lime-treated tailings.

Mackinnon et al. (2010) studied the effects of some coagulants aids on the CT release water (CTRW) quality of a CT mixture with 60% solid content and 20% fine content, with a sand to fine ratio (SFR) of 4:1. According to their results, for sulphuric acid, a non-segregating deposit was produced at a dosage of 1000–1200 mg/L. In the case of lime treatment, 1500 g/m^3 was considered as an effective dosage, while the increase in Ca^{+2} in the water and the high pH were considered as risks associated with the recycling of the water back into the process. In that study, gypsum was considered as another coagulant aid to produce non-segregating deposit at a concentration of 1000 g/m^3, but the large increase in salinity in gypsum–CT water was considered as a challenge. The aim of that study was to find a chemical that would be as effective as gypsum but have less impact on water quality. One chemical that seemed to meet this requirement was alum (Al_2 $(SO_4)_3$.14.3 H_2O). The effective concentration of alum was found to be in the 1000–1250 g/m^3 range. With alum, there is some release of Ca^{2+}, although not from the chemical added but through cation exchange. The increase in Ca^{2+} from the alum treatment would be about 25% that of gypsum. At Syncrude, gypsum was chosen as the base case for planning and implementation of CT at a dosage of 1400 g/m^3 (Chalaturnyk et al., 2002), and the use of alternative chemicals, such as alum, will require field testing to ensure that they perform comparably to gypsum and produce a CT product with the desired properties (Mackinnon et al., 2010).

The advantages of the CT process include the consumption of MFTs and the formation of trafficable deposits. Moreover, approximately 80% of the released water is recycled back into the process (Pramanik, 2016). Although the CT process reduces the fresh water requirement, the water released by the CT process has a high concentration of dissolved ions and toxic compounds, and hence, recycling the water into the extraction process could affect the efficiency of the process (Allen, 2008; BGC Engineering Inc., 2010). In addition, the CT process has more challenges. Production of CT is linked to the extraction process because of cyclone under flow (CUF). This means that after the mine life, the tailings treatment cannot be applicable. A precise formula of MFTs, coarse tailings, and coagulant is required for creating a non-segregating deposit (Azam and Scott, 2005), and thus, any deviation can result in the failure of this process. Because of these issues, some operators have investigated other technologies (BGC Engineering Inc., 2010).

2.2.3 Chemical amendments

In chemical and biological amendments, the chemical properties of the tailings are changed, and as a result, the water is removed and the strength is increased.

2.2.3.1 Thickening process

Thickened tailings (TT) or paste technology involves rapid settling and sedimentation of the suspended fines in a thickener by addition of chemicals that aid in flocculating the fine solids, and the released water is suitable for reuse in the extraction process. Less make-up heating (for warming up the water) is required, which results in lower energy costs and greenhouse gas emissions. The accelerated settling rate of the fines produces a concentrated stream of fine solids. This stream can be deposited with less land disturbance and more chance of land reclamation (BGC Engineering Inc., 2010). The resulting material is still a slurry, and further treatments are required. Syncrude has prepared several large-scale thickened tailings and considered it as a commercially viable (Fair, 2008).

2.2.3.2 Flocculation and coagulation

Flocculation and coagulation are used widely in different stages of oil sand tailings management in order to increase the density of the slurry and reduce the potential for segregation (BGC Engineering Inc., 2010). Flocculation is a technique in which discrete, colloid-sized particles

agglomerate by forming bridges between individual particles. Coagulation is a process by which cationic coagulants collapse the electric double layer around extremely fine particles left after flocculation and make them agglomerate (Yuan and Shaw, 2007).

Beier et al. (2013) explored the geotechnical aspects of meeting regulatory strength performance criteria (Directive 074) by applying flocculation-based dewatering of fine tailings. They revealed that chemically amended tailings develop the strength at much lower solid content when compared to un-amended tailings.

Yao et al. (2012) analyzed the effect of flocculation on MFTs originating from the Shell Muskeg River Mine. A series of vane shear tests were performed in order to compare the strength of the treated and untreated MFTs. For the untreated MFTs with a void ratio of 1.35, the shear strength was about 1 kPa, which increased to 190 kPa when the void ratio decreased to 0.48, and the MFTs curve for the flocculated MFTs was slightly higher than that for the untreated MFTs. In other words, at the same void ratio, the untreated MFTs exhibited lower shear strength, or at the same shear strength, the flocculated MFTs had a higher void ratio than the untreated MFTs. According to their data, the undrained shear strength of 5 kPa for flocculated MFTs was obtained at void ratios of 1.1, which is 10% higher than that of the untreated MFTs (1.0).

Flocculation of fine suspensions depends on a number of factors, such as the type, degree of ionization, and molecular weight of the flocculants; the particle size and mineralogical composition of the solid particles; and the pH and chemical composition of the solution. Sworska et al. (2000) studied the effect of pH, polymer dosage, and the presence of divalent cations (Mg^{2+} and Ca^{2+}) on the flocculation of Syncrude tailings. They found that the optimum solid content and optimum settling rate occurred at low pH, below 6. The optimum solid content is an important parameter since the water is recycled back to the extraction process. In this pH range, clays form an unstable suspension and coagulate. With decreasing pH, a higher polymer dosage is required to have a reasonable settling rate. They noted that since clays form a stable suspension in alkaline media, the addition of Ca^{2+} and Mg^{2+} is required to destabilize the suspension before the addition of the flocculent. However, at a practical commercial scale, this cannot be applicable owing to the negative effects of a high cation concentration and acidic water recycled back into the extraction process.

Yuan and Shaw (2007) studied the effect of using a single flocculent, a single coagulant, or a binary coagulant–flocculent in a conventional process thickener, and they showed that these methods were ineffective to obtain the target solid content of <0.5% in the thickener over flow water. They tested new processes, such as coagulation-flocculation-coagulation (CFC), flocculation-coagulation (FC), and flocculation-coagulation-flocculation (FCF), and reported that the FCF process produced huge flocs resulting in fast initial settling rates and a clear supernatant of less than 0.13%. In the first stage of this process, the addition of flocculants was believed to bind the relatively larger particles by a bridging mechanism that results in bimodal flocculation, with larger flocs and extremely fine particles left in dispersion. The subsequent addition of a cationic coagulant collapses the electric double layer around the particles left in stage 1, making them aggregate. The addition of a flocculent again in the third stage binds the flocculated larger grained particles formed in stage 1 with the coagulated finer grained particles formed in stage 2 together, thus increasing the settling rate.

2.2.3.3 In-line thickened tailings (ILTT) technology

MFTs dewatering may be applied through a combination of chemical addition and strategic deposition. In-line thickened tailings (ILTT) is a process in which a polymer solution is injected into the MFTs transfer pipelines. When fine particles at low solid content bind into flocs, hydraulic conductivity increases. Flocculated MFTs can be discharged in thin layers at a solid content of 30%. Aggregation of fine particles into flocs enhances the water release properties of MFTs. Moreover, a combination of settlement, seepage, desiccation, and freeze–thaw achieves additional dewatering (BGC Engineering Inc., 2010). This technology is commercially being implemented by Syncrude (Jeeravipoolvarn, 2008), Suncor (Beier and Sego, 2008), and Shell Muskeg River (Kolstad et al., 2012)

Chemically amended oil sands fine tailings may exhibit sensitive, metastable behavior upon deposition, and hence, mitigation measures should be taken into consideration (Beier et al., 2013).

2.2.4 Natural processes

Natural processes are processes in which environmental and geophysical phenomena remove water from solids.

2.2.4.1 Evaporation

The rate of evaporation has a significant effect on the rate at which the strength and density of the tailings increase. Prediction of the flux boundary condition and water flow across the soil–atmosphere boundary is essential for addressing many problems in geotechnical engineering (Wilson, 1994). Water moves into the soil surface as a liquid through the process of infiltration, and it ex-filtrates from the soil surface as vapour through the process of evaporation. Infiltration depends primarily on soil properties, such as hydraulic conductivity, but the rate of evaporation depends on both soil properties and climatic conditions (Wilson, 1994). Therefore, analysis of the evaporative fluxes from the soil surface is more difficult. Engineers traditionally use a term defined as potential evaporation (PE) to estimate the evaporation or evapotranspiration rate. PE may be defined as the maximum rate of evaporation from a pure water surface under given climatic conditions (Thornthwaite, 1948). In other words, the surface is considered as an open water surface or a saturated soil surface. The actual rate of evaporation (AE) begins to decline as the surface becomes unsaturated and as the motion of water to the surface becomes restricted. The shape of the drying curve is shown in Figure 2.1. In general, the curve is described as having three stages of drying. Stage 1 drying is the maximum rate of drying that occurs when the soil surface is at or near saturation, and it also depends on the climatic conditions. Stage II drying begins when the conductive properties of the soil cannot permit a sufficient flow of water to the surface to continue the maximum potential rate of evaporation (Wilson, 1994).

The rate of evaporation continues to decline during stage II drying owing to surface desiccation, and it reaches a slow residual value defined as stage III drying. The slow rate of evaporation during stage III drying occurs after the soil surface becomes sufficiently desiccated, and the liquid water phase becomes discontinuous. The flow of liquid water to the surface declines, and water molecules may only migrate to the surface through the process of vapour diffusion. To sum up, the rate of AE from the soil surface is controlled by both climatic conditions, which define the potential rate of evaporation, and soil properties, such as hydraulic conductivity and vapour diffusivity. The vapour pressure in the soil is a function of the soil temperature and soil suction (Wilson, 1994).

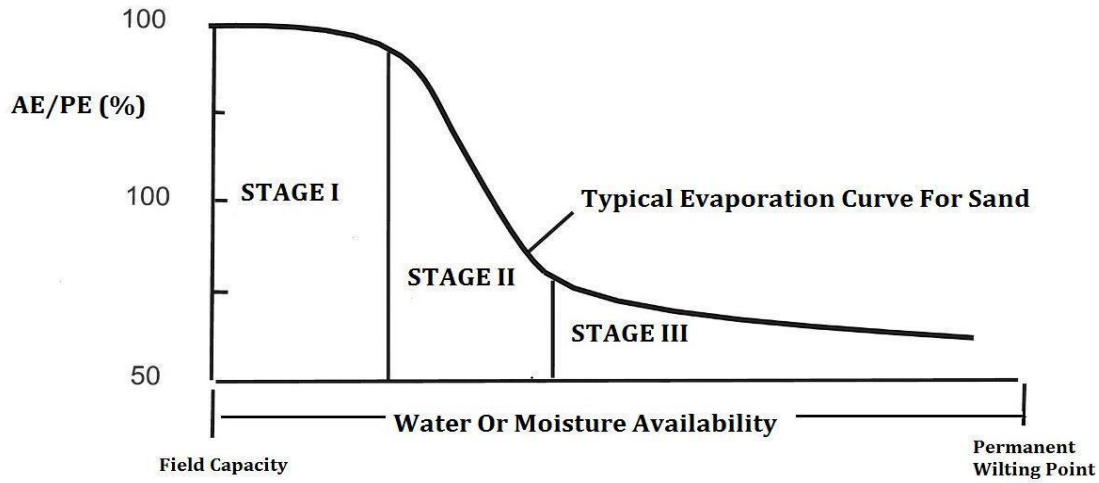

Figure 2.1, Relationship between the rate of actual evaporation and potential evaporation (Wilson, 1994)

The rate of evaporation is a critical parameter in the geotechnical and geo-environmental performances of the tailings stack. Evaporation promotes desiccation and strength gain. The increase in density and the decrease in void ratio due to desiccation not only reduce the total volume of tailings but also allow for steeper deposition and increase the resistance of the tailings stack to seismic events (Crowder, 2004; Wijewickreme et al., 2005; Simms and Sivathayalan, 2007; Fisseha et al., 2010). The rate of drying of the tailings depends on climatic parameters as well as the thickness of the deposited fresh layer (Fisseha et al., 2010).

Evaporation is a function of salinity, and the evaporation rate from saline water is lower than that from a freshwater surface. Salts are known to suppress evaporation in soils and tailings through at least three phenomena: increase in albedo (the ratio between the measured reflected short wave radiation and the incoming radiation from a lamp) due to the increased reflectivity of salt precipitates, suppression of vapor pressure at the surface due to osmotic suction induced by the high ion concentration of pore water, and the formation of a salt crust that acts as a physical barrier to water flow (Fujiyasu and Fahey, 2000; Simms and Sivathayalan, 2007; Fisseha et al., 2010).

2.2.4.2 Freeze-thaw

The dewatering of fine-grained slurries by freeze–thaw has been applied in different industries for several decades (Stahl and Sego, 1995; Chamberlain and Gow, 1979; Dawson et al., 1999; Beier and Sego, 2008; Proskin et al., 2010; Proskin et al., 2012; Farkish and Fall, 2013).

When water saturated, fine-grained slurries are subjected to temperatures below freezing, negative pore-water pressures are developed between the unfrozen water surrounding the mineral particles,

and ice fills the voids. During phase transition, water expands by about 9% as the lattice of its hexagonal crystal structure opens. The crystals grow until they interfere with each other and the adjacent soil particles. The pressure applied on the soil particles owing to expansion of pore water while freezing causes them to move, rearrange, and consolidate (Chamberlain and Blouin, 1976). Negative pore pressures develop as a result of the difference in surface tension between the ice and the liquid pore water. These negative pressures (suctions) cause water to migrate to the growing ice crystals, which results in distinct segregated reticulate ice – fine grained "ped" – structure in the resulting frozen mass (Dawson et al., 1999).

In an open system where the soil accesses free water, steady state conditions will be setup between the advancing freezing front and the warmer soil beneath, which results in the formation of horizontal ice lenses. In a closed system where there is no free water, complete freezing is permitted to occur, and horizontal ice lenses comprised of externally derived water cannot form (Dawson et al., 1999). However, a reticulated ice structure forms through the growth of ice crystals in place of water from the matrix of the freezing soil (Dawson et al., 1999). A freeze–thaw-controlled dewatering system has the best efficiency when thin layers (less than 0.5 m thick) are frozen under a closed freezing system. This prevents the formation of ice lenses owing to water migration in an open freezing system (Dawson et al., 1999).

Figure 2.2 depicts the void ratio versus the effective stress in a closed freeze–thaw system. Fine-grained, frost-susceptible tailings exist at point A with some sedimentation and consolidation in a settling basin. After removal from the pond, the fine tailings sample swells to point B and has approximately zero effective stress. By freezing the sample at B into a thin layer, an increase in volume to point C is caused by the expansion of the pore water as ice forms in the void spaces between the mineral particles. As the frozen material thaws, a volume change from B to D occurs, which is known as thaw strain. Further post-thaw loading causes the material to consolidate along path D-E.

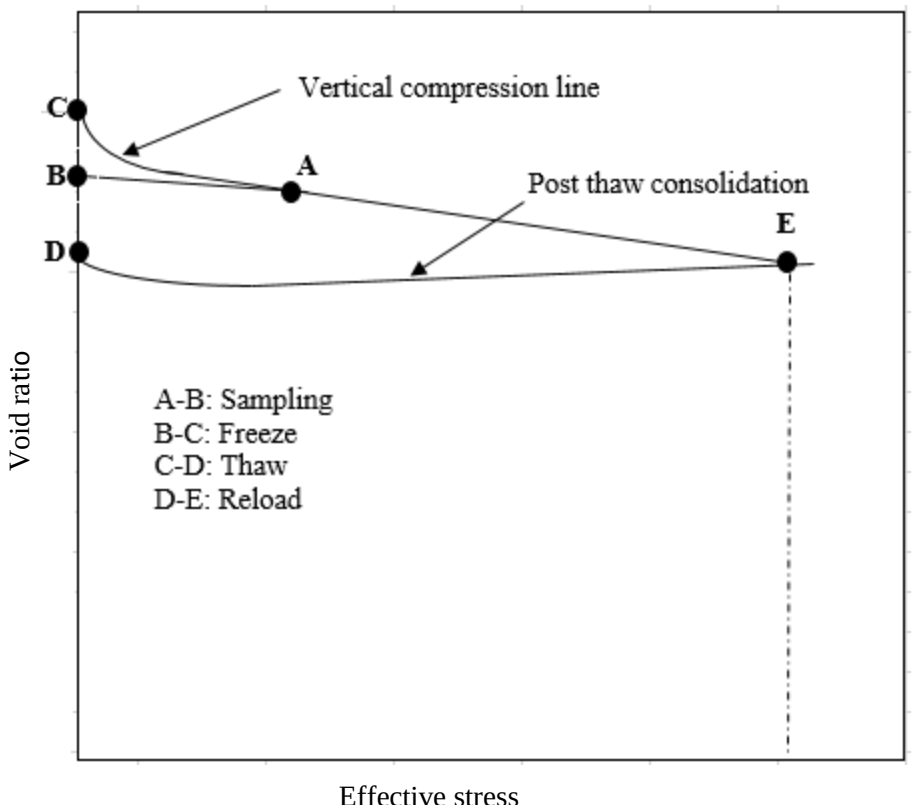

Figure 2.2, Void ratio versus effective stress in a close system freeze-thaw (Dawson et al., 1999)

Freeze–thaw affects the geotechnical properties of the soils (Luckham and Rossi, 1999; Proskin et al., 2010). It changes the soil fabric on both the macroscopic and microscopic scales. In the frozen state, the MFTs soil fabric consists of a reticulate ice network and soil peds. Upon thawing, the soil fabric consists of interconnected voids, formerly occupied by ice but now filled with pore fluid and soil peds with a new arrangement (Othman and Benson, 1993).

Freezing and thawing increases the hydraulic conductivity of the clay, especially in the first to third cycles (Chamberlain and Gow, 1979; Othman and Benson, 1993). Permeability of thawed MFTs is increased by two orders of magnitude compared to the unfrozen samples at a similar void ratio (Dawson et al., 1999). By melting the ice lenses, the network of cracks left behind and the extended pores during freezing increase the permeability of the soil matrix. Chamberlain and Gow (1979) found that the largest increase in permeability of four different fine-grained soils occurred for samples with a higher plasticity index.

Farkish and Fall (2013) studied the effect of freeze–thaw cycles on MFTs pre-dewatered with SAP. Their results showed that freeze–thaw cycles can increase the solid content and subsequently the

strength of the MFTs. One freeze–thaw cycle increased the solid content of MFTs from 38% to nearly 45%. After 3 days of mixing MFTs with 1% and 3% SAP, followed by two freeze–thaw cycles, the vane shear strength of the MFTs was 2.9 and 6 kPa, respectively. The effect of evaporation was not considered in their study.

2.2.5 Permanent storage

Permanent storage involves tailings storage below ground in their original form.

2.2.5.1 MFT water capped lake

MFT water capping is the placement of MFTs in a mined-out pit and the addition of water over the deposit. The water used in this process can be from natural surface water or affected water. Different bacteria result in active and passive bioremediation of different components of the tailings to sufficiently reduce the concentration of harmful components within five to ten years (BGC Engineering Inc., 2010).

2.3 Superabsorbent polymer and its use as dewatering technology

A superabsorbent polymer (SAP) is a high-molecular-weight, cross-linked hydrophilic network that can absorb and retain large amounts of water or aqueous solutions, as high as 10–1000 grams per gram of polymer. Unlike SAP, traditional absorbent materials (such as tissue papers and polyurethane foams) will lose most of their absorbed water through squeezing under pressure. This is not the case for SAP because the water imbibing mechanisms of SAP are the physical entrapment of water via capillary forces in their macroporous structure and the hydration of functional groups (Zohuriaan and Kabiri, 2008). SAPs are classified based on the type of monomeric unit used in their chemical structure, and most conventional SAPs fall into one of the following categories (Po, 1994; Zohuriaan and Kabiri, 2008):

1. Cross-linked poly-acrylates and poly-acrylamides
2. Hydrolyzed cellulose-poly-acrylonitrile
3. Cross-linked copolymers of maleic anhydride

Acrylic acid (AA) with sodium or potassium salts and acrylamide (AM) are most frequently used for SAP industrial production. Figure 2.3 depicts the water absorption process of sodium poly-acrylate ([CH_2-CH-(COONa)-]). When the powder is dry, the polymer chains are coiled. When hydrated, the sodium ion detaches so that the carboxyl groups (CO_2H) become negatively charged and repel one another, thus uncoiling the polymer chain and allowing more water to associate with more carboxyl groups or sodium atoms (Hu et al., 2004).

Dry

In water

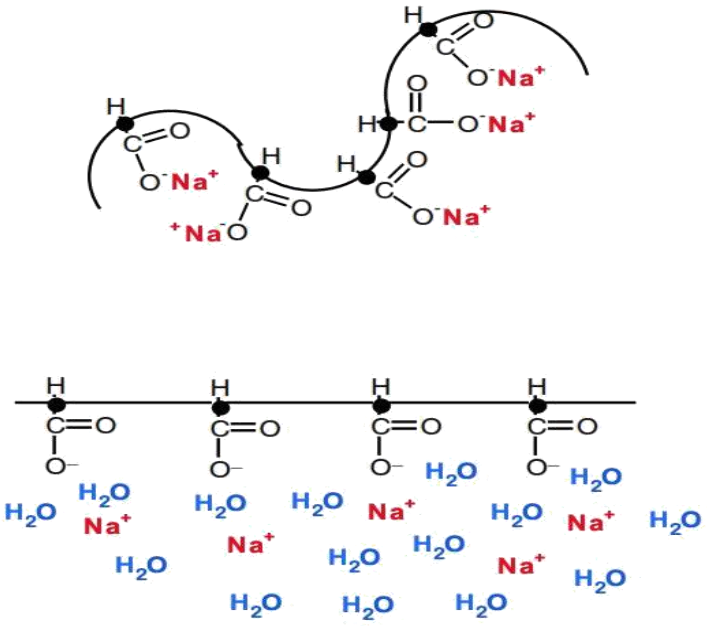

Figure 2.3, Schematic presentation of the SAP swelling (Hu et al., 2004)

The first commercial SAP was produced through alkaline hydrolysis of starch-graft-polyacrylonitrile (SPAN). The hydrolyzed product was developed in the 1970s at the Northern Regional Research Laboratory of the US Department of Agriculture. However, this product was unsuccessful owing to the high costs and the inherent structural disadvantage (lack of sufficient gel strength) of this product. Commercial production of SAP began in Japan in 1978 for use in feminine napkins. Further developments lead to SAP materials being employed in baby diapers in Germany and France in 1980 (Zohuriaan and Kabiri, 2008). SAP has several applications in hygienic and agricultural areas (Bowman et al., 1990; Levy et al., 1995; Kenawy et al., 1998). SAP is also used in many other applications, such as entertainment toys and tools, interior decoration,

cryogenic gels, food /meat packaging, concrete strengthening, and reduction of ground-resistance in the electrical industry (Po, 1994; Gao et al., 2011; Yamane et al., 1994).

High water removal efficiency of SAP has been approved for dewatering of fine coal slurry and domestic sludge (Masuda and Iwata, 1990; Kuai, 2000). Dzinomwa et al. (1997) used SAP to reduce the moisture content of fine coal cakes produced by conventional dewatering equipment in Queensland, Australia. Dewatering of the fine coal to low water content is often a problem. They used Alcosorb AB3C, a sodium acrylate/acrylamide copolymer, as the SAP. The initial water content of the samples was around 30%. Regeneration of the polymer, which is essential to the economic viability of the process, was investigated in that study. Regeneration helps reduce the costs of the process to an acceptable level. The polymer regenerating techniques were pH-induced and temperature-induced. In pH-induced regeneration, hydrochloric acid (32 wt%) was used, and the mass of acid added was approximately 0.01 times that of the total absorbed water in the polymer. After 4 h, the collapsed polymer was recovered and washed, followed by addition of a basic solution to neutralize any remaining acid. In temperature-induced regeneration, the swollen polymer was placed into oven at 60 °C. A gradual decrease in the amount of water absorbed by the unit mass of the polymer was observed as the number of cycles increased, which was attributed to a gradual increase in the concentration of ions retained in the polymer matrix. The authors noticed that despite this slight decrease in absorption characteristics of the polymer granules, the use of SAP to dewater coal is feasible in this industry with significant economic savings (Dzinomwa et al., 1997).

Peer and Venter (2003) investigated the effectiveness of SAP polymer that demonstrated significant decreases in the moisture content of fine coal slurries. Coal slurry containing 45% moisture was observed to lose 80% of its moisture with a 1% polymer dosage. The slurry with 60% water content was observed to lose a maximum of 88% of its water content with a 2% polymer dosage. They noted that mixing caused a further decrease in the water content. They claimed that without mixing, the moisture content is reduced at a very slow rate and the final moisture content is also not as low as when the slurry is mixed. They also found that the SAP with 3.09 g dry mass per sachet absorbed 95% of added distilled water and about 85% of added tap, and after regeneration through thermal drying (70°C for 24 h), in the 7^{th} cycle, 92.5 ml of distilled water

was absorbed (out of 100 ml distilled water). Temperature-induced regeneration was more successful than pH-induced regeneration (Peer and Venter, 2003).

2.4 Review of previous studies on SAP-based dewatering of MFTs

There is a paucity of previous studies on superabsorbent polymer (SAP)-based dewatering of mature fine tailings (MFTs). The only previous studies were conducted by Farkish and Fall (2013, 2014), who proposed a novel method of using SAP to dewater and produce dense MFTs. They compared the capacity of SAP to absorb distilled water, tap water, and MFTs water. Farkish and Fall (2013, 2014) showed that SAP can absorb a significant amount of MFTs water, and despite the observed drop in SAP absorption capacity for MFTs, absorption capacity still remained high (see Figure 2.4). They applied two different methods of mixing MFTs and polymer. In the first method (direct method), polymer was directly added to MFTs. In the second method (indirect), sachets containing polymer were added to MFTs. The main results of the previous studies on SAP-based dewatering of MFTs performed by Farkish and Fall (2013, 2014) are discussed below.

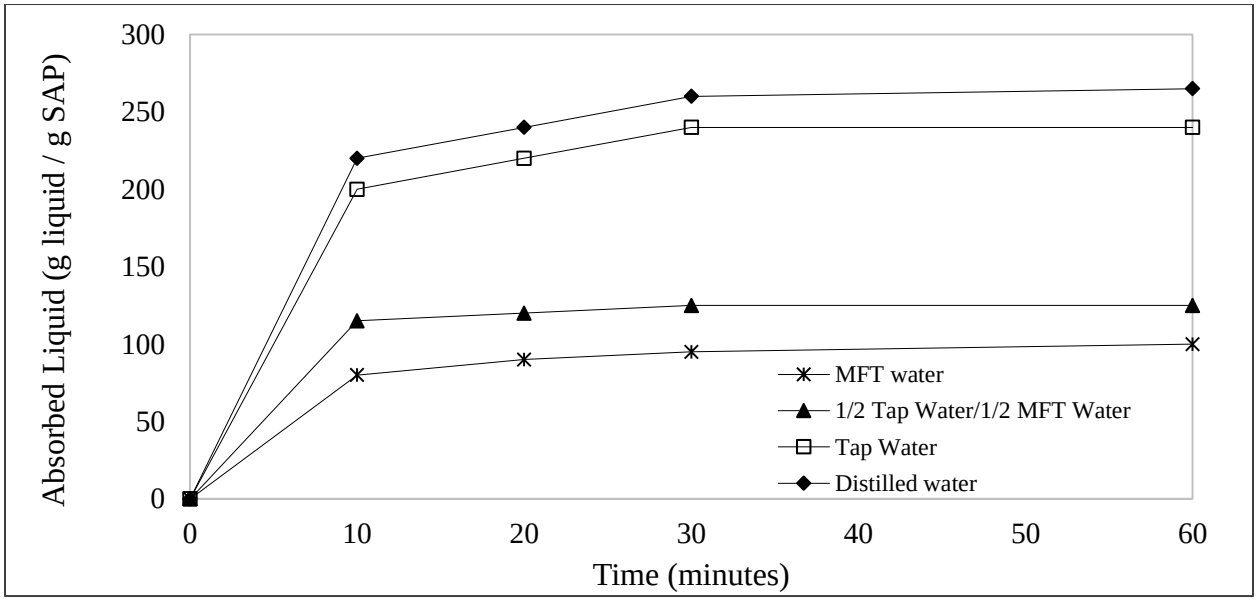

Figure 2.4, Absorption capacity of the SAP (Farkish and Fall, 2013)

2.4.1 Solid content and vane shear strength

Figure 2.5 shows the results of the vane shear test carried out on MFTs dewatered with SAP sachets. The initial shear strength of MFTs that was mixed 4 days with polymer and allowed to rest for 3 days (with SAP sachets) was significantly different from the sample that rested for an

extra 7 days (after removing the polymer bags). The samples mixed with 3% SAP showed the highest strength (9 kPa) after 7 days, whereas the samples mixed with 1% and 0.5% had a low strength (less than 1 kPa). MFT samples that were allowed to rest for an extra week had higher strength believed to be due to the formation of the structure within MFTs (Farkish and Fall, 2013).

Mixing MFT sachets within the first 4 days disturbed all the bounds between the aggregates. Thus, the samples that had more time to rest and form a stronger structure showed higher shear strength. The authors also mentioned that the shear strength of MFTs dewatered with SAP sachets was higher than samples in which SAP was directly (with no sachet) mixed with MFTs (Farkish and Fall, 2013). They explained that when the swollen polymer bags were separated from MFTs, the solids content of MFTs increased, and, consequently, shear strength improved. They also measured the evolution of solids content for specimens dewatered with different proportions of SAP (0%, 0.5%, 1%, and 3%), which is shown in Figure 2.6.

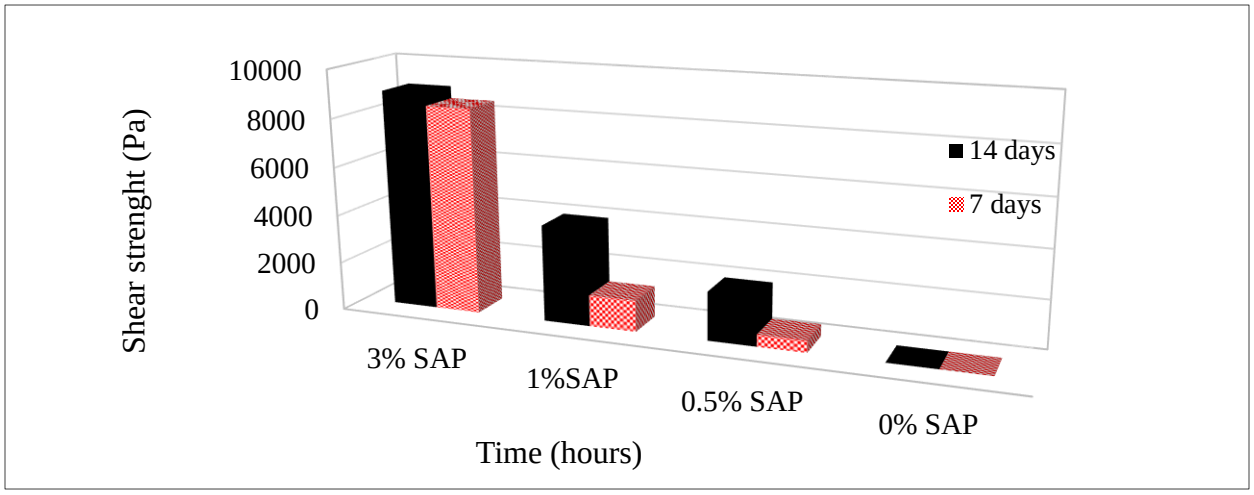

Figure 2.5, Vane shear strength of MFTs dewatered by SAP sachets (Farkish and Fall, 2013)

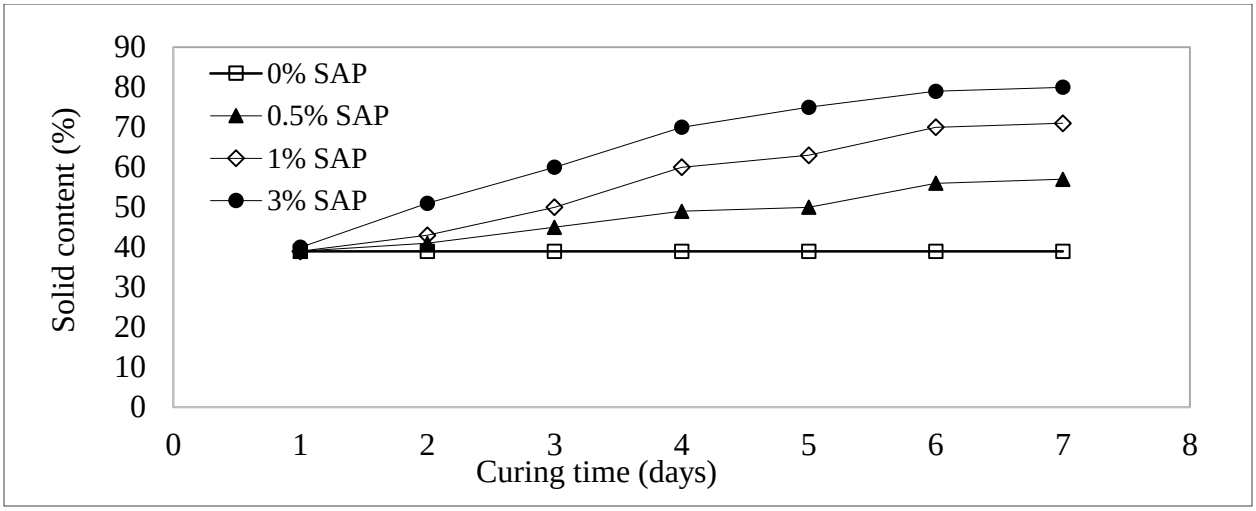

Figure 2.6, Solid content of MFTs dewatered by SAP sachets (Farkish and Fall, 2013)

It was found that MFTs dewatered with SAP sachets (indirect method) showed a significant increase in solids content compared to the direct method. The solids content for MFTs with 3% SAP increased up to 61% in the direct method versus 80% in the indirect method. Farkish and Fall (2013) stated that in the direct method, swollen polymer can hold the water in the tailings within the polymer chain. It should be mentioned that all the samples were completely sealed, and the effect of evaporation was not considered in their research.

2.4.2 Effect of freeze-thaw

One dimensional freeze-thaw was applied on MFTs dewatered with SAP. Dewatered MFTs was stored in a rectangular container with a 40 cm × 20 cm surface area and 20 cm depth. Samples were frozen at –24°C for 24 h, and thawing was carried out at room temperature until the entire frozen matrix was melted. According to the results for MFTs dewatered in the direct method, the first cycle of freeze-thaw is more efficient than the second in terms of increasing the solid content because the water content in the first cycle of freeze-thaw is higher than that in the second cycle. After 3 days of MFTs dewatering with 0.5%, 1%, and 3% SAP, the vane shear strength measurements in the second cycle of freeze-thaw were 2.1, 2.9, and 6kPa, respectively (Farkish and Fall, 2013).

The effect of freeze-thaw on MFTs dewatered with SAP sachets (indirect method) was also studied. The dewatered samples after 4 days of mixing followed by 3 days of rest with sachets and then 7 days of rest without sachets were subjected to two freeze-thaw cycles. Dewatered samples

with 3% SAP showed a dramatic increase of 5kPa in the first cycle and 14kPa at the end of the second cycle. It is worth mentioning that MFTs dewatered with 1% SAP reached 5kPa strength after two cycles of freezing and thawing (Farkish and Fall, 2013).

2.4.3 SAP regeneration

SAP was regenerated according to the approach proposed by et al. (1997). Temperature-controlled regenerated SAP showed higher efficiency after ten regeneration cycles in comparison with pH-induced regenerated polymer. The results revealed that the shear strength of the dewatered MFTs by regenerated SAP decreased as the number of regeneration cycles increased. A significant decrease in shear strength—from 14 kPa to 5.5 kPa—occurred after the first regeneration cycle in the MFTs sample dewatered with 3% SAP. This decrease is due to the reduction in the absorption capacity of the regenerated polymer. This reduction in the absorption capacity of SAP results from the trapped water that is tightly bound to the polymer chains (Farkish and Fall, 2013).

2.4.4 Hydraulic conductivity of MFTs dewatered with SAP

The effects of initial solids content and void ratio on hydraulic conductivity were studied in this research (Farkish and Fall, 2014). Figure 2.7 shows the void ratio versus hydraulic conductivity for MFTs dewatered by SAP sachets.

The obtained data indicated that a decrease in void ratio also decreased the hydraulic conductivity. These data seemed to follow the same trend captured by Suthaker and Scott (1996). In general, the hydraulic conductivity of MFTs was very low due to the high concentration of fine particles (Farkish and Fall, 2014).

The hydraulic conductivity of MFTs dewatered with recycled SAP was also studied. MFTs dewatered by recycled SAP showed higher hydraulic conductivity because the water content of MFTs dewatered by recycled SAP was higher (Farkish and Fall, 2014).

Figure 2.8 shows the results of the hydraulic conductivity of MFTs dewatered with SAP and subjected to the freeze-thaw cycles. According to the data, the hydraulic conductivity of MFTs decreased as effective stress increased. However, this reduction was slower for samples subjected to freeze-thaw because the freeze-thaw cycle altered the soil fabric. Ice networks formed during

the freezing period created interconnected voids that worked as drainage channels during thawing. Under low effective stress, these voids resulted in a higher void ratio and consequently higher hydraulic conductivity. However, under high effective stress, these inner structures would collapse and cause significant reduction in hydraulic conductivity (Farkish and Fall, 2014).

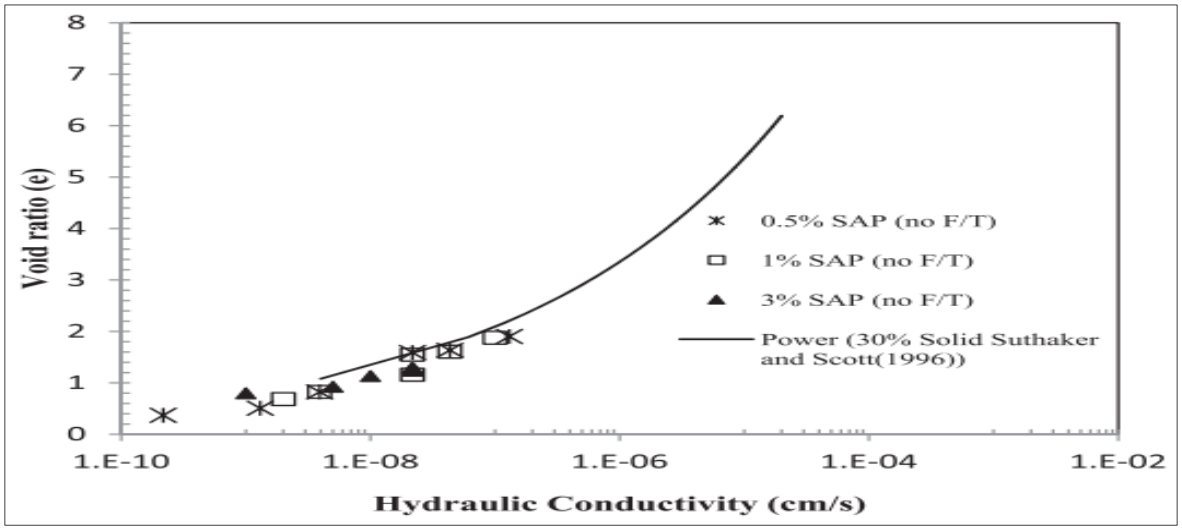

Figure 2.7, Hydraulic conductivity for MFTs dewatered by SAP (Farkish and Fall, 2014)

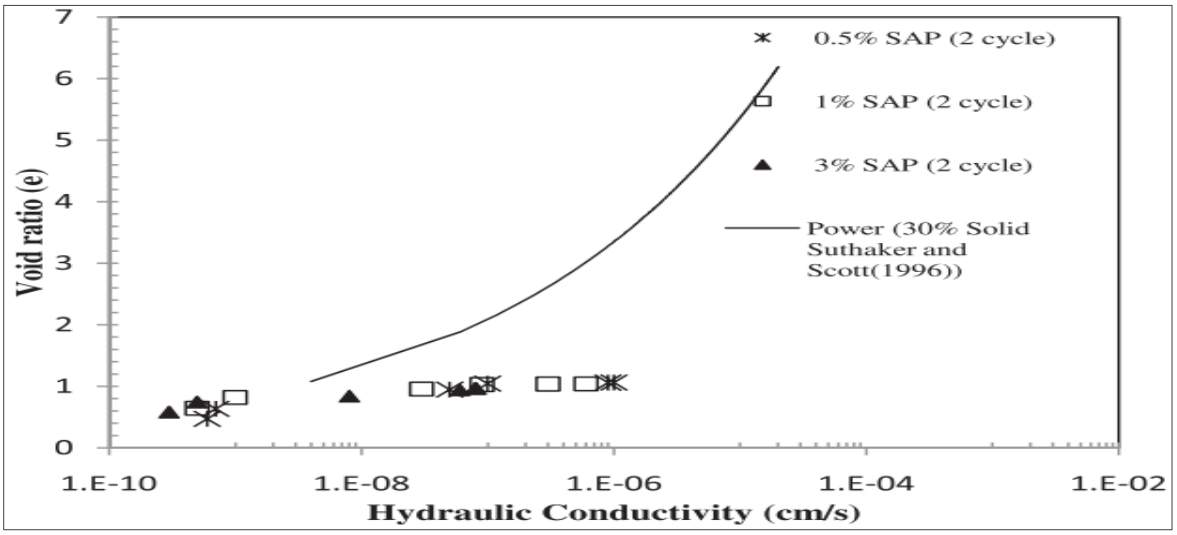

Figure 2.8, Hydraulic conductivity for MFTs dewatered by SAP after two freeze-thaw cycles (Farkish and Fall, 2014)

2.5 Conclusions

Large quantities of liquid waste products generated by the oil sand industry have intensified the necessity for a viable tailings dewatering technology. A review of the existing tailings technologies

reveals no single method for dewatering all types of tailings. Moreover, based on the previous study, extensive laboratory tests on densification of MFTs by SAP revealed that rapid increases in strength can be achieved by applying SAP as a novel dewatering technique. SAP regeneration through light thermal drying is also viable to reduce the cost of the process. In addition, freeze-thaw cycles can generate additional strength of dewatered MFTs with SAP. This natural dewatering process can reduce the amount of SAP used in the process as well. These results position the SAP densification technique as a promising approach to increase the speed of reclamation and minimize the environmental footprint of the oil sand industry in Canada.

However, to date, no studies have addressed the effect of atmospheric drying, as well as wetting and drying cycles, on the geo-environmental and geotechnical behavior of MFTs pre-dewatered with SAP in large column experiments. In an effort to understand the atmospheric drying behavior of raw MFTs and MFTs pre-dewatered with SAP as well as the impact of wetting-drying cycles on the geotechnical properties of MFTs, a lab scale setup with a two-lift MFTs deposit will be developed in the coming chapters. Addressing this research gap is essential for a potential field application of a SAP-based MFTs dewatering technique. The comprehensive assessment will be discussed in the coming chapters.

2.6 References

Allen, E. W. (2008). Process water treatment in Canada's oil sands industry: II. A review of emerging technologies. Journal of Environmental Engineering and Science, 7(5), 499–524.

Azam, S. and Scott, J. (2005). Revisiting the ternary diagram for tailings characterization and management. Journal of Geotechnical News, 23(4), 43–46.

Beier, N., Wilson, W., Dunmola, A., and Sego, D. (2013). Impact of flocculation-based dewatering on the shear strength of oil sands fine tailings. Canadian Geotechnical Journal, 50, 1001–1007.

Beier, N., and Sego, D. (2008). The oil sands tailings research facility. Geotechnical News, 26(2), 72–77.

BGC Engineering Inc. (2010). Oil sands tailings technology review. Oil Sands Research and

Information Network, OSRIN Report No. TR-1.

Bowman, D., Evans, R., Paul, J. (1990). Fertilizer salts reduce hydration of polyacrylamide gels and affect physicl properties of gel-amended container media. Journal of American Society of Horticultural Science, 115(3), 382-386.

Caughill, D., Morgenstern, N. and Scott, J. (1993). Geotechnics of nonsegregating oil sand tailings. Canadian Geotechnical Journal, 30(5), 801–811.

Chalaturnyk, J., Scott, D., Ozum, B. (2002). Mnagement of oil sands tailings. Journal of Petrolumn Science and Technology, 20 (9-10), 1025-1046.

Chamberlain, E. and Gow, A. (1979). Effect of freezing and thawing on the permeability and structure of soilds. Journa of Engineering Geology, 13, 73-92.

Chamberlain, E., and Blouin, S. (1976). Freeze-thaw enhancement of the drainage and consolidation of fine-grained dredged material in confined disposal areas. United States Army. Corps of Engineering, Cold Region Research and Engineering Laboratory, Hanover.

Crowder, J. (2004). Deposition, consolidation and strength of a non-plastic tailings paste for surface disposal. Ph.D. thesis, department of Civil Engineering, University of Toronto, Ontario, Canada.

Dawson, R., Sego, D. and Pollock, G. (1999). Freeze-thaw dewatering of oil sands fine tails. Canadian Geotechnical Journal, 36(4), 587–598.

Dzinomwa, G., Wood, C., and Hill, D. (1997). Fine coal dewatering using pH- and temperature-sensitive superabsorbent polymers. Journal of Polymers for Advanced Technologies, 8, 767–772.

Fair, A. (2008). The past, present and future of tailings at Syncrude. Proceeding in 3th International oil sands tailings conference, Edmonton, Alberta, Canada.

Farkish, A., Fall, M., (2014). Consolidation and Hydraulic Conductivity of Oil Sand Mature Fine Tailings Dewatered by using Superabsorbent Polymer. ASCE Journal of Geotechnical and Geoenvironmental Engineering 140(7): 06014006.

Farkish, A., and Fall, M. (2013). Rapid dewatering of oil sand mature fine tailings using superabsorbent polymer (SAP). Minerals Engineering, 50–51, 38–47.

Fisseha, B., Bryan, R., and Simms, P. (2010). Evaporation , unsaturated flow, and salt accumulation in multilayer deposits of " Paste " gold tailings. Journal of Geotechnical and Geoenvironmental Engineering, 136, 1703–1712.

Fujiyasu, Y., and Fahey, M. (2000). Experimental study of evaporation from saline tailings, Jornal of Geotechnical and Geoenvionmental Engineering, 126, 18-27.

Gao, D., Heimann, R., and Alexander, S. (1997). Box-Behnken design applied to study the strengthening of aluminate concrete modified by a superabsorbent polymer/clay composite. Journal of advances in Cement Research, 9 (35), 93-97.

Hu, Y., Beach, J., Raymer, J., and Gardner, M. (2004). Disposable diaper to collect urine samples from young children for pyrethroid pesticide studies. Journal of Exposure Analysis and Environmental Epidemiology, 14(5), 378–84.

Jeeravipoolvarn, S. (2008). Sedimentation and consolidation of in-line thickened fine tailings. Proceedings of International Oil Sands Tailings Conference, At Edmonton, AB, Canada, 1-14.

Kenawy, E. (1998). Recent advances in controlled release of agrochemicals. Journal of Macromolecular Science, 38 (3), 365-390.

Kolstad, D., Dunmola, A., Dhadli, N., O'Kane, M., Song, J., and Masala, S. (2012). Toward the improvement in geotechnical perfomance of atomospheric fines drying (AFD) deposits at Shell's Muskeg River mine. Proceeding in the third international oil sands tailings conference, Edmonton, Alberta, 411–420.

Kuai, L., 2000. Sludge treatment and reuse as soil conditioner for small rural communities. Journal

of Bioresource Technology, 73(3), 213–219.

Levy, R., Nichols, M., and Miller, T. (1995). Evaluation of superabsorbent polymer-pesticide formulations for prolonged insect control. Proceeding in the 14th Symposum on Pesticide Formulation and Application Systems, Dallas, US.

Luckham, P. and Rossi, S. (1999). Colloidal and rheological properties of bentonite suspensions. Journal of Advances in Colloid and Interface Science, 82(1), 43–92.

Mackinnon, M., Matthews, J., Shaw, W., and Cuddy, R. (2010). Water quality issues associated with composite tailings (CT) technology for managing oil sands tailings. International Journal of Surface Mining, Reclamation and Environment, 15 (4), 235–256.

Masuda, K., and Iwata, H. (1990). Dewatering of particulate materials utilizing highly water-absorptive polymer. Journal of Powder Technology, 63(2), 113–119.

Matthews, J., Shaw, W., Mackinnon, M., and Cuddy, R. (2002). Development of composite tailings technology at Syncrude. International Journal of Surface Mining, Reclamation and Environment, 16(1), 24–39.

Othman, M. and Benson, C. (1993). Effect of freeze–thaw on the hydraulic conductivity and morphology of compacted clay. Canadian Geotechnical Journal, 30(2), 236–246.

Peer, F., and Venter, T. (2003). Dewatering of coal fines using a superabsorbent polymer. Journal of the South African Institude of Mining and Metallurgy, 403–410.

Pó, R. (1994). Water-Absorbent polymers: A patent survey. Journal of Macromolecular Science, 4(4), 607–662.

Pramanik, S. (2016). Review of biological processes in oil sands: a feasible solution for tailings water treatment. Journal of Environmental Reviews, 24, 274-284.

Proskin, S., Sego, D. and Alostaz, M. (2010). Freeze-thaw and consolidation tests on Suncor mature fine tailings (MFT). Journal of Cold Regions Science and Technology, 63(3), 110–120.

Proskin, S., Sego, D., and Alostaz, M. (2012). Oil sands MFTs properties and freeze-thaw effects. Journal of Cold Regions Engineering, 26(2), 29–54.

Stahl, R., and Sego, D. (1995). Freeze-thaw dewatering and structural enhancement of fine coal tails. Journal of Cold Regions Engineering, 9(3), 135–151.

Sworska, A., Laskowski, J., Cymerman, G. (2000). Flocculation of the Syncrude fine tailings part I. Effect of pH, polymer dosage and Mg^{2+} and Ca^{2+} cations. International Journal of Mineral Processing, 60, 143-152.

Tarhouni, M., Simms, P., and Sivathayalan, S. (2011). Cyclic behavior of reconstituted and desiccated – rewet thickened gold tailings in simple shear. Canadian Geothecnical Journal, 48(7), 1044–1060.

Thornthwaite, C. (1948). An approach toward a rational classification of climate. Journal of Geographical Review, 38, 55-94.

Yamane, H., Ideguchi, T., Tokuda, M., Koga, H. (1994). A new ground resistance-reducing material based on water-absorbent polymer. Journal of Electronics and Communictaion in Japan, 77(5), 68-78.

Yao, Y., Tol, F., and Paassen, L. (2012). The effect of flocculant on the geotechnical properties of mature fine tailings : an experimental study. Proceeding in the 3rd International Oil Sand Tailings Conefernce, Edmonton, Canada, 391–398.

Yuan, X., and Shaw, W. (2007). Novel processes for treatment of Syncrude fine transition and marine ore tailings. Journal of Canadian Metallurgical Quality, 46(3), 265-272.

Wells, P., and Caldwell, J. (2009). Vertical wick drains and accelerated dewatering of fine tailings in oil sands. Proceeding in the 9th Tailings and Mine Waste, Banff, Alberta, Canada.

Wijewickreme, D., Sanin, M., and Greenaway, G. (2005). Cyclic shear response of fine-grained mine tailings. Canadian Geothecnical Journal, 42, 1408-1421.

Wilson, G. (1994). Coupled soil-atmosphere modelling for soil evaporation. Canadian Geotechnical Journal, 31, 151-161.

Zohuriaan-mehr, J., and Kabiri, K. (2008). Superabsorbent polymer materials: A Review. Journal of Iranian Polymer, 17(6), 451-477.

3 A column study of the hydro-mechanical behavior of mature fine tailings under atmospheric drying

Anis Roshani, Mamadou Fall, Kevin Kennedy
International journal of mining science and technology,27(2): 203–209

ABSTRACT

In this paper, the hydro-mechanical behavior and physical properties of the mature fine tailings (MFTs) under atmospheric drying were investigated by column study. Evaporation resulted in the development of suction in the upper parts of the column and increasing suction led to higher strength. After 5 days, suction in the first lift developed to around 17 kPa at the upper part of the column. By adding the second load, the former lift initially lost strength but over a 30 days period, recovered to prior values and suction in the later lift reached 500 kPa. Vane shear strength values show a high increase in strength of mature fine tailings after 30 days under atmospheric drying and drainage. The 90 percent strength of the column exceeded the threshold (5 kPa). The hydraulic-mechanical properties of the deposit are closely coupled due to several mechanisms, such as evaporation, drainage, self-consolidation, suction and crack development. The findings of this study will provide a better understanding of the placement behavior of multiple lifts of MFTs and thus contribute to reclamation design standards and reduce the use of dedicated disposal areas.

Keywords: Tailings; Oil Sand; Environment; Drying; Multi-lift deposition

3.1 Introduction

Oil sand extraction processes in Northern Alberta produce large volumes of tailings with high water content. The tailings (known as "whole tailings") are a mixture of sand, silt, clay, and a small amount of bitumen. For each barrel of synthetic crude oil produced, around two tons of ore must be processed, which results in the production of around 1.8 tons of solid tailings and about 2 m^3 of waste water (Mikula et al., 1996). After deposition, the fine tailings (< 45μm) settle to about 30% solid content (water content of 186% to 233%) within 2 years and are then referred to as mature fine tailings (MFTs). Extensive clay dispersion from the extraction processes due to sodium hydroxide (NaOH) causes chemical interaction between clay, water and residual bitumen that leads to a significant reduction of the MFTs' hydraulic conductivity and consolidation (e.g., Jeeravipoolvarn et al., 2009; Beier et al., 2013). The average solid content of MFTs increased from 30.6% to 41.8% in approximately 26 years (Jeeravipoolvarn et al., 2009) and full consolidation of untreated tailings could take up to thousands of years (Mikula et al., 1996; Beier et al., 2013) which requires long-term storage consideration in constructed containments. The continuing accumulation of MFTs is therefore causing enormous economic and environmental concerns (Farkish and Fall, 2013).

Applying practical methods to manage and reduce the MFTs has been an ongoing challenge for oil sands industry. The industry has developed several types of technologies to manage MFTs. For instance, composite tailings or consolidated tailings (CT) were used by Suncor and Syncrude. However, CT has a number of challenges associated with the process. Any deviation from the sand to fine ratio (SFR), which is approximately 4:1, could produce segregated material that would not be trafficable and cannot be reclaimed (Beier et al., 2013). An increasing trend in this industry is to manage the fine tailings stream by using chemical additives. Polymer solutions are injected into transfer pipelines and the flocculated mixture is discharged in thin layers to form a gently sloping beach. Flocculants are added in a thickening process to create thickened tailings, which allow them to spread in layers and consolidate (BGC Engineering Inc., 2010). However, chemically amended tailings may exhibit shear-sensitive and metastable behavior after deposition, unless mitigative measures are applied (Beier et al., 2013).

In 2009, the implementation of Directive 074 by the Energy Resource Conservation Board (ERCB) compelled operators to review current technologies and techniques and investigate alternative technologies and process to manage oil sands tailings and their reclamation (Farkish and Fall, 2014). The key requirement of Directive 074 was that oil sands operators were to deposit a substantial percentage of their annual production of fine tailings in designated disposal areas (DDAs). The DDAs must be constructed in a manner that guaranteed trafficable deposits (ERCB 2009; Farkish and Fall, 2013). However, a promising alternative approach to effectively manage MFTs instead is through atmospheric drying (thin-lift drying). Thin-lift drying consists of depositing MFTs in thin lifts to dry and achieve the required strength under ambient conditions. The benefits of thin-lift drying are most marked when utilizing multi-lifts in order to reduce dedicated disposal area (DDA). However, this technology cannot be applied and related benefits cannot be realized if additions of the new lifts eliminate the developed strength of the underlying lifts. The multi-lift drying of MFTs involves very complex hydraulic (H; e.g., evaporation, fluid flow, suction) and mechanical (M; e.g., strength increase/decrease, deformation, cracking) processes which also strongly interact with each other. An understanding of these HM processes and the HM behavior of thin-lifts of MFTs is crucial for the successful application of the multi-lift or thin lift drying technology. To date, our understanding of the HM processes that occur in multi-lifts of MFTs and the HM behavior of the deposition of multiple lifts of MFTs under atmospheric drying is limited. Hence, the objective of this study is to assess the HM processes and behaviors of raw MFTs deposited in thin-lifts under atmospheric drying by conducting column experiments.

3.2 Experimental program

3.2.1 Material

3.2.1.1 Mature fine tailings (MFT)

Raw MFTs were taken from an oil sand tailings pond located in northern Alberta, Canada as the sample. The physical, mineralogical and chemical characteristics of the sampled tailings were determined by conducting various laboratory tests. Figure 3.1 depicts the grain size distribution curve of the MFTs used. The tested MFTs contain about 18% clay, 81% silt and 1% sand. The liquid limit (LL) and plastic limit (PL) of the MFTs are 51.2 and 37.2, respectively (Farkish and Fall, 2013). So, the plasticity index (PI) is equal to 14 and activity (A) is 1.16 which corresponds to a normal clay. According to the X-ray diffraction (XRD) results, the mineralogy of the clay

component is kaolinite and illite. The average specific gravity was measured to be 2.36, which is lower than that of the other types of clays. Bitumen is found in tailings in the forms of free and adsorbed bitumen. The specific gravity of bitumen is about 1.03 and results in a lower recorded specific gravity of the MFTs compared with other natural clay soils (Jeeravipoolvarn et al., 2009). Typical material characteristics of the raw MFTs used are listed in Table 3.1.

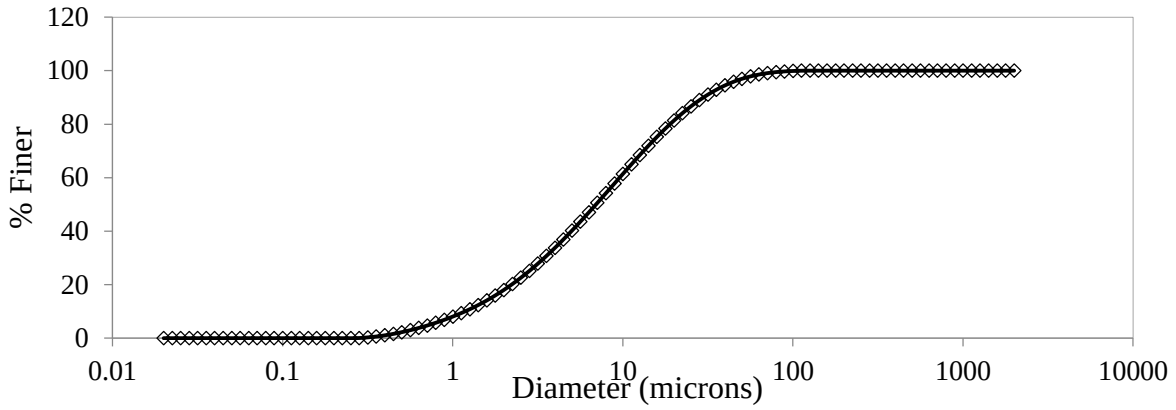

Figure 3.1, Grain size distribution of the used mature fine tailings

Table 3. 1, Physical properties of raw MFTs

Parameter	**Average value**
Initial solid content (%)	45
Initial water content (%)	121.7
Bitumen content (%)	18.37
Initial bulk density (g/cm^3)	1.31
Initial void ratio	3.44
Specific gravity	2.36
Liquid limit (%)	51.2
Plastic limit (%)	37.2
Plasticity index (%)	14.0

3.2.2 Developed experimental setup

Figure 3.2 presents a schematic diagram of the developed experimental setup of columns in this study. In total, four columns were manufactured, in which one column was for monitoring purposes and the last sampling after 30 days (column a) and the other three columns were for

sampling at different elapsed times of 5 days (column d, only one lift), 10 days (column c) and 20 days (column b) . The columns, made of Plexiglas with internal diameter of 25 cm and height of 55 cm, were used as the framework for analysis. A 3 cm layer of sand was used as the drainage layer at the bottom of the columns which was separated from the tailings with a perforated plate. Coarse filter paper covered the perforated plate in order to hold the tailings and prevent them from going into the drainage layer. The top of the columns remained open and was exposed to the environment. There was also a fan placed on top of each column in order to simulate the wind at the site. The placement of the fans could be adjusted so as to provide equal distance from the tailings surface after the addition of each lift.

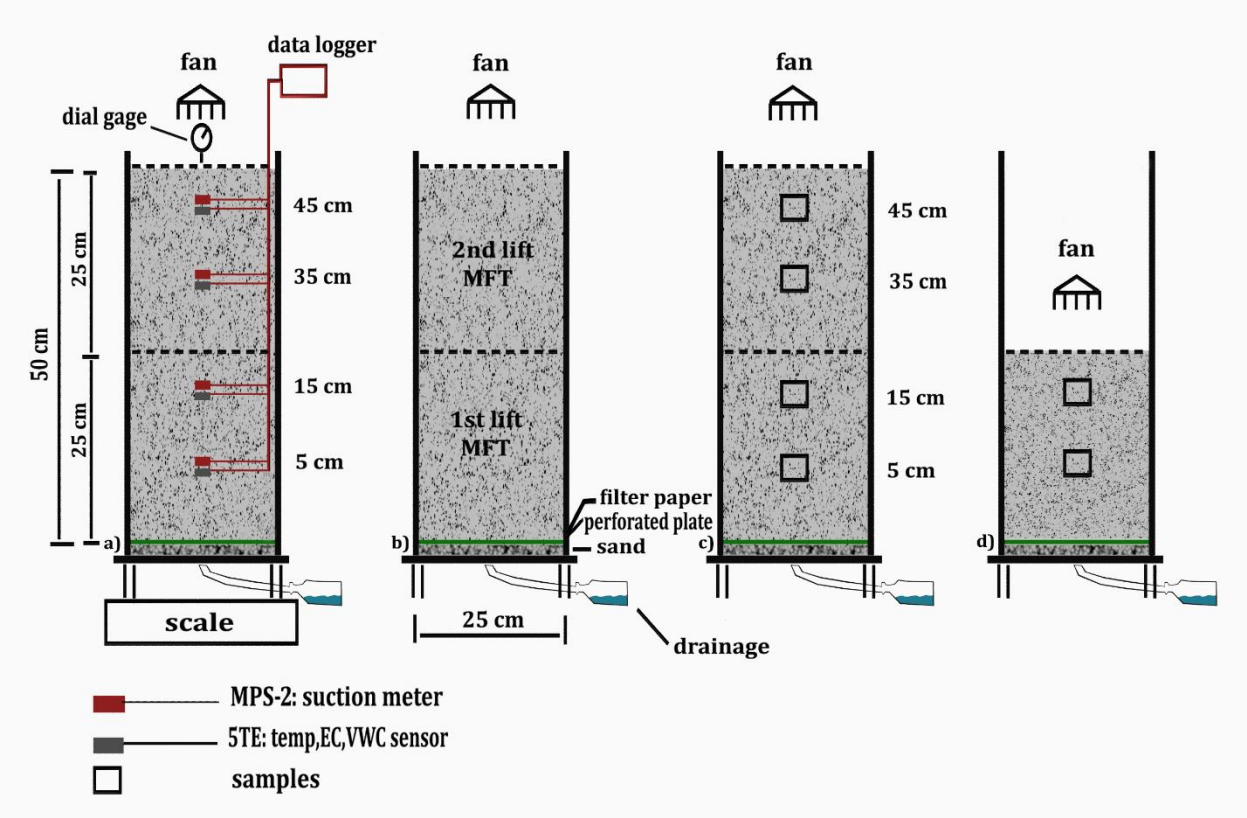

Figure 3.2, Schematic diagram of the experimental setup: arrangement of the sensors and dial gage, filling sequence and sampling locations

3.2.3 Column instrumentation and monitoring

The monitoring column was equipped with various sensors, including four MPS-2 sensors (Decagon Devices Inc.), four 5TE sensors (Decagon Devices Inc.), and a dial gage (3058S, Mitutoyo Co.) for measuring the settlement. MPS-2 is capable of measuring the soil water potential in the range of 0 to -500 kPa with an accuracy of ± 0.25 kPa and a resolution of 0.1 kPa. This sensor can also record the temperature in the range of -40℃ to 60℃ with an accuracy of ±1°C. The 5TE sensor measures electrical conductivity (EC) in the range of 0-23 dS/m with an accuracy of 10%. This sensor also measures the volumetric water content (VWC) in the range of 0-100%. In total, eight sensors were installed at heights of 5, 15, 35, and 45 cm from the bottom and connected to a data logger to record and collect the data. To measure the self-weight settlement as well as the drying shrinkage from drying due to evaporation, a dial gage was installed at the top immediately after casting the second lift. The filling strategy was carried out as follows: two stages of fillings with a thickness of 25 cm would be casted, with the first filling at the start of the experiment and five days later for the second filling. That is, five days after casting the first lift, the second lift was added. Each column was allocated to one specific period of elapsed time. After each elapsed time (5, 10, 20, and 30 days) the columns were dismantled and samples were taken from four different heights. The design locations of the sensors, filling sequence and location of obtained samples are illustrated in Figure 3.2.

The mass of water lost in each column by evaporation was obtained by measuring the mass of the column on an approximately daily basis using a scale (OHAUS Defender) with a readability of 0.01 kg. The initial mass of soil was recorded before evaporation was permitted. The mass of the container and tailings was measured and compared with the initial mass. The difference in mass was attributed to the mass of water lost by evaporation and drainage.

3.2.4 Experimental test program

In addition to the column monitoring program and procedure described above, extensive laboratory tests were conducted on MFTs samples extracted from different heights of the columns at different elapsed times. The extracted samples were subjected to mechanical tests (vane shear strength) and physical properties analysis. The gravimetric water content (ω), void ratio (e), porosity (n), degree

of saturation (S_r), solid content (%) and density dry/wet (γ_d/γ_b) were determined for all of the columns.

3.2.4.1 Mechanical tests

The miniature vane shear test was carried out with the insertion of a four bladed vane into an undisturbed MFTs sample at a minimum depth that was equal to twice the vane height to ensure that the top of the blade was embedded below the sample surface. The vane was then rotated at a constant rate which would determine the torque that was required to cause shearing of the cylindrical surface. For each height of the column, two samples were tested and the average was taken. This test was carried out in accordance with ASTM standard D4648. Vane shear that is a function of the vane blade and spring constants and deflection is gotten by Eqs. (3.1) and (3.2):

$$\tau = (\Delta)(b)/K \qquad (3.1)$$

Where:

τ = Undrained shear strength (Pa)

Δ = Deflection(°)

b = Spring constant (N/m)

$$K = \frac{\pi D^2 H}{2*10^9}\left[1 + \frac{D}{3H}\right] \qquad (3.2)$$

Where:

D = Measured diameter of the vane (mm)

H = Measured height of the vane (mm)

The spring and vane blade constants that apply to this study were 0.000942 N/m and $4.290 * 10^{-6}$ (m^3), respectively.

3.2.4.2 Determination of the physical properties

The gravimetric water content was measured in accordance with ASTM standard D4959 in which direct application of heat was carried out. The water content (expressed as a percentage) was determined by dividing the mass of the water by the dry mass of the tailings. The density was determined with ASTM standard D7263. Dry and bulk densities can be used to convert the water fraction of tailings from a mass to a volume basis and vice versa. When the particle density, that is, specific gravity (ASTM D854) is also known, dry density can be used to calculate porosity and void ratio.

3.3 Results and discussion

3.3.1 Evaporation, drainage and settlement behavior

3.3.1.1 Evaporation

The rate of evaporation over time from a soil surface generally has three phases (Wilson, 1994; Yanful and Choo, 1997). Initially, the rate of evaporation is limited by external factors. In a constant environmental condition, the water content gradually decreases until equilibrium with the atmospheric pressure is established. This stage is called phase I and external conditions control the evaporation rate (Wilson, 1994). In phase II, the soil hydraulic properties limit the maximum rate of evaporation, and decline in the rate of evaporation is the result of development of a drying zone (Wilson, 1994; Fisseha et al., 2010). In phase III, the evaporation rate gradually decreases to reach a residual value in which the liquid and vapor phases are discontinuous (Wilson, 1994; Yanful and Choo, 1997). A comparison of the potential rate of evaporation (PE) with the actual rates of evaporation (AE) for raw MFTs from the small scale (one lift) column is carried in this study (Figure 3.3). An evaporation pan with a known surface area was filled with water and placed adjacent to the columns to determine the PE. During this time, the average temperature and humidity were 24 °C and 26%, respectively. The average PE over 21 days was 16 mm/day.

The initial rate of evaporation in the columns was relatively high for the first two days but lower than the PE (Figure 3.3). This corresponds to Phase I as previously defined. After the first two days, the rate of evaporation decreased and became independent of the environmental conditions. Evaporation was limited by the water availability. The rapid decline in the rate of evaporation continued for about 17 days. This stage corresponds to Phase II. After approximately 17 days, the

onset of drying was observed, which corresponds to Phase III. The final AE was 0.076 mm/day. The continuation of the evaporation was due to the process of osmotic suction.

Understanding of evaporation in MFTs can help to predict the rate of strength that can be achieved. Evaporation also reduces the total volume of the tailings by increasing the density and reducing the void ratio (Fisseha et al., 2010). A series of tests are therefore conducted in this study to determine the AE from the deposition of multiple thin-lifts of raw MFTs. The moisture loss from the MFTs columns was measured for a period of 30 days. The results which include the rate of evaporation and accumulative water loss in the real scale columns (with two lifts) are shown in Figure 3.4. The evaporation rate depends on the temperature and relative humidity of the ambient air. The ambient temperature and humidity are plotted in Figure 3.5 as well. As discussed above, the test comprised the drying of an initial lift for 5 days before adding a second lift, and another 25 days of drying after the second load (monitoring column). The evaporation rate was approximately 1.14 kg/(h.m^2) immediately after casting the first load and reached 0.48 kg/(h.m^2) after 5 days (before loading the second lift). The evaporation rate gradually decreased and a relatively stable condition was finally reached after 30 days in the residual phase (around 0.13 kg/(h.m^2)). The accumulative water loss showed a sharp increase in the first 15 days of the second lift and then gradually decreased to reach the total water loss of around 13 kg on 30th day.

The decline in the rate of evaporation is related to the formation of a salt crust on top of the column which resisted against the water flow. According to Fujiyasu et al. (2000), the evaporation rate of saline tailings is lower than that of freshwater tailings. The salt crust with a concentration of 166 g/L showed a resistance of 3500 s/m for the slurry, and that with a concentration of 20 g/L was 500 s/m for the low salinity slurry.

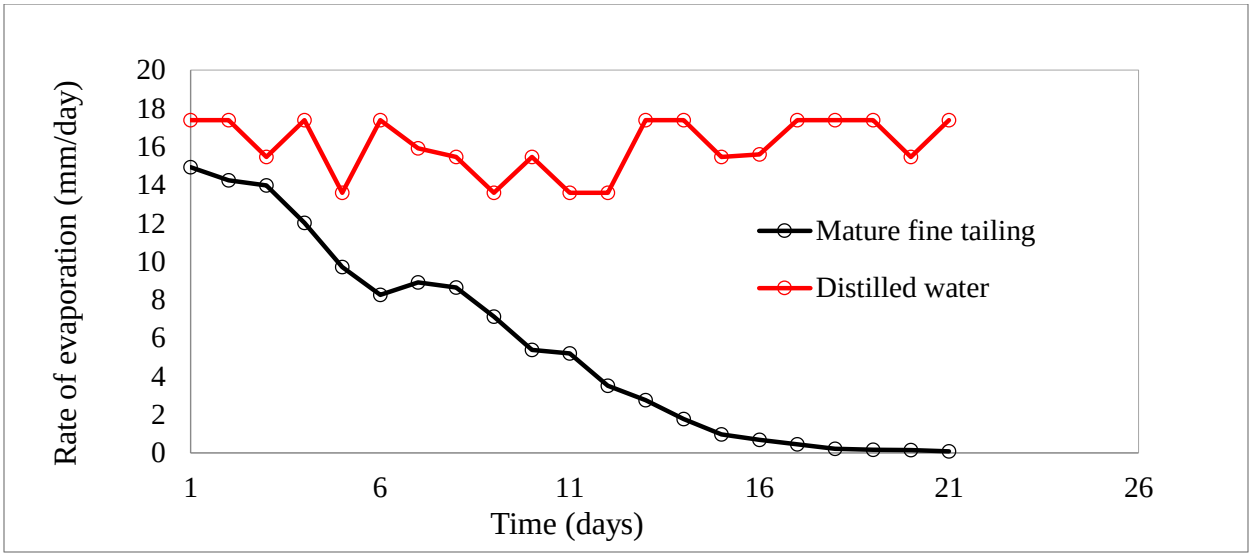

Figure 3.3, Actual and potential rate of evaporation from small scale column (one lift) in comparison with evaporation of distilled water from pan

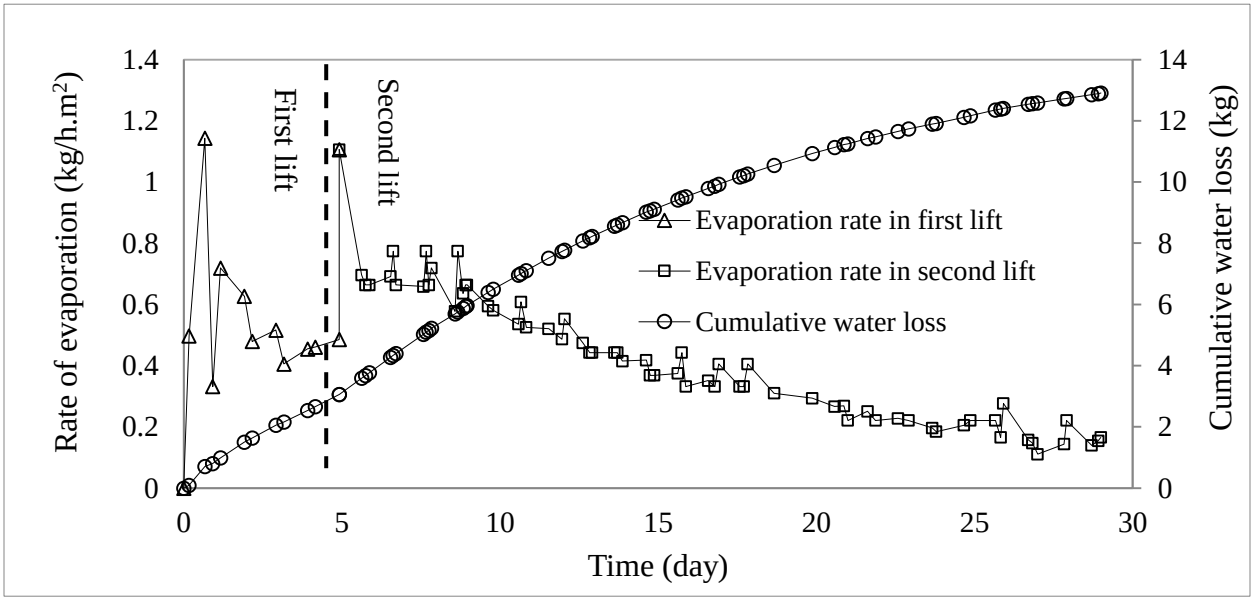

Figure 3.4, Actual rate of evaporation and cumulative water loss (by evaporation) for the first and second lifts

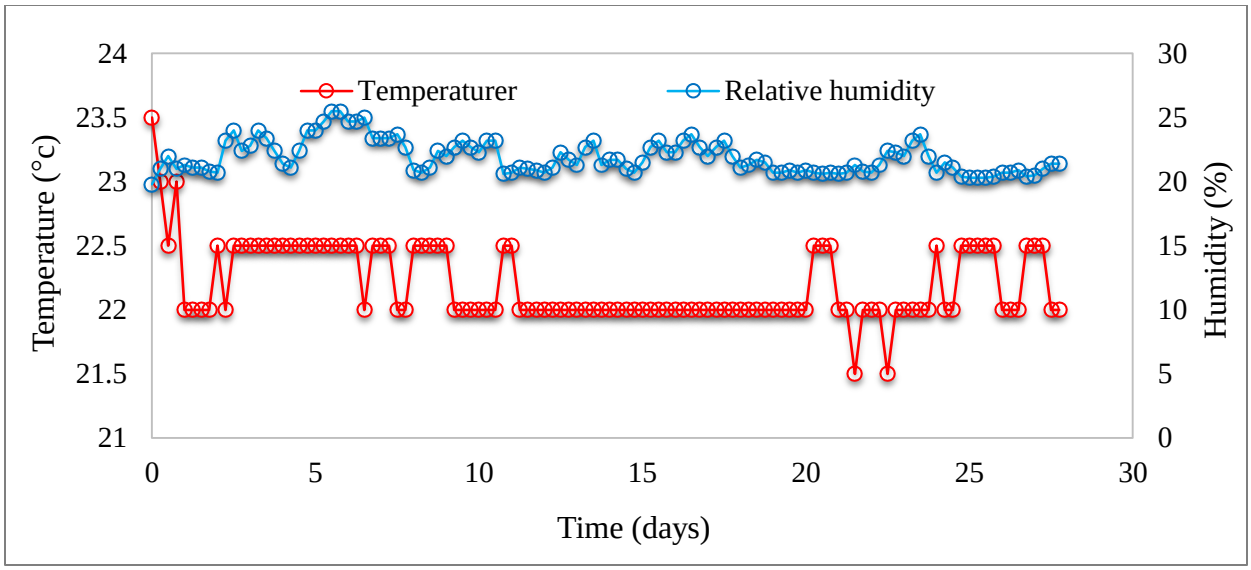

Figure 3.5, Room temperature and humidity

3.3.1.2 Drainage

Figure 3.6 depicts the results of the measured rate of drainage and accumulative drainage. The rate of drainage is greater in the first five days after each loading and then shows a slight increase and levels in the last 10 days. The accumulative drainage of water on the first day was around 160 gr and the maximum rate of drainage can be observed as well at a rate of around 12 gr/h. After loading the second lift, the rate of drainage decreased to 5 gr/h and then had a decreasing trend until the end of the testing period. Development of cracks after the first day of each load caused water molecules to move upward to the evaporation boundary layer rather than drainage taking place. These results indicate that regardless of the height of the tailings layer, evaporation is a major factor in removing water in comparison to drainage. Similar observations were made by Junqueira et al. (2011).

3.3.1.3 Settlement

Figure 3.7 illustrates the settlement behavior of the dewatered MFTs with time. During the 30 days, the settlement of the tailings reaches approximately 1.8 cm and has settled at the uniform rate during the last 20 days. The average solid content at the top of the columns (heights of 35 and 45 cm) increases from its initial 45% (void ratio of 2.8) to 98% (void ratio of 0.67). This settlement behavior is due to evaporation induced desiccation, drainage and self-weight pressure. These three processes can lead to high rate of vertical settlement at the very early stages (first 5 days after the

second load). In turn, mechanical properties begin to increase, for example, strength. When the evaporation rate, drainage and suction reach an almost constant value, vertical settlement reaches a constant value as well. Jeeravipoolvarn et al. (2009) measured a total settlement of 3.2 m for 10 m standpipe tests of oil sands tailings over a period of 26 years. Junqueira et al. (2011) reported settlement of around 14 cm for a lift of raw MFTs that was 100 cm in thickness induced by evaporation and drainage in a 60 days period of time. Settlement of the first lift (after 14 days) and second lift (after 12 days) of a flocculated MFTs (0.5 m each) were reported 3 cm and 4 cm, respectively (Fasking et al., 2011).

Cracking and lateral shrinkage away from the column walls were seen on Day 3. Cracks started to form again after 2 days of casting the new lift. It is interesting that cumulative settlement after 10 and 20 days of casting the second lift was approximately 6 cm and 9 cm, respectively. In the monitoring column, the instrumentation caused reinforcement which prevented the tailings from settling more than 1.8 cm.

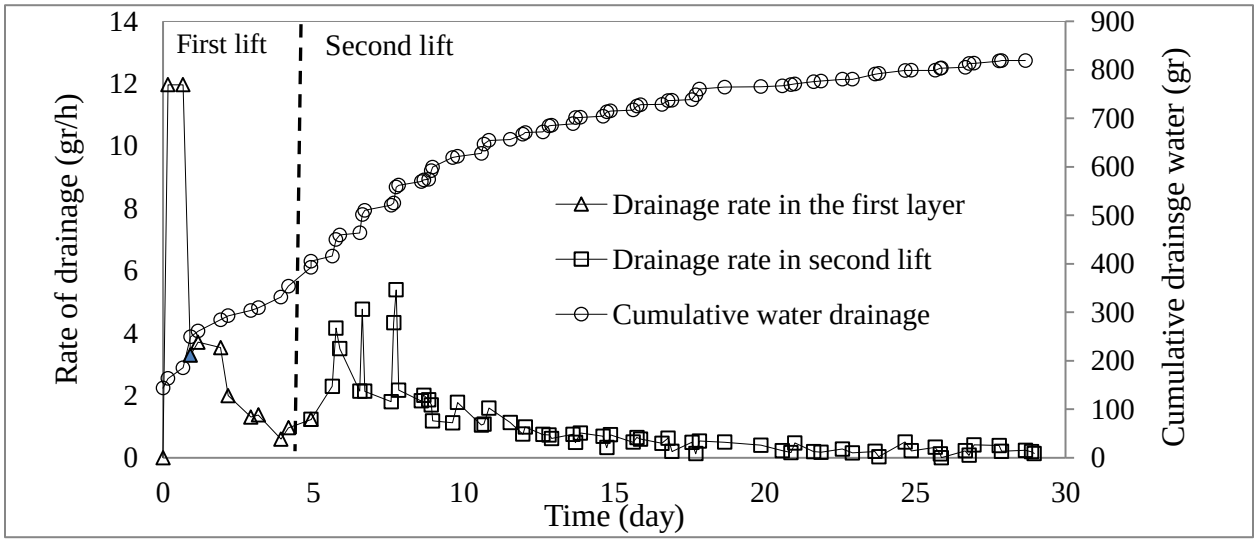

Figure 3.6, Rate of drainage and cumulative water loss (by drainage) for the first and second lift

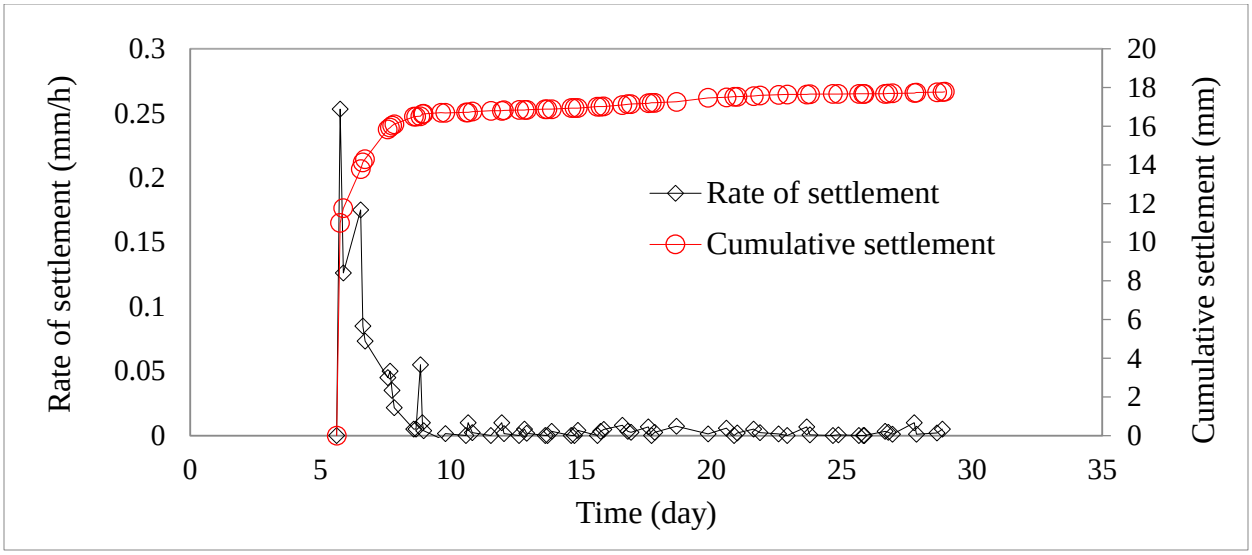

Figure 3.7, Rate of settlement and cumulative settlement

3.3.2 Changes in physical properties

The changes in the physical properties, such as void ratio (e), density (γ), water content (ω) and degree of saturation (S_r) with column height and time, were investigated. Figure 3.8a illustrates the variations in the void ratio in the columns for different elapsed times. Two different phenomena of the void ratio can be observed in the columns. The void ratio decreases in the higher parts of the columns due to the high rate of evaporation, settlement and shrinkage at the top. Water content is the main factor related to changes in the void ratio. The void ratios are relatively high at the bottom and middle of the columns. The void ratio is 2.38 at the bottom and around 0.67 at the top of the monitored column (after 30 days). The same trend was observed for porosity (Figure 3.8b). The porosity decreased from 0.7 at the bottom to 0.4 at the top of the column after 30 days. The void ratio and porosity in the first lift after 5 days (before placing the second lift) did not change. The increase in the void ratio after 20 days (in lower parts of the column) was due to downward flow of the pore water which caused a higher void ratio and porosity while the development of cracks and drainage after 30 days caused a steady decreasing trend in the void ratio and porosity. A high evaporation rate at the surface, which causes the development of shrinkage, resulted in very low degree of saturation in the 20 and 30 days columns. The degree of saturation ranged from 94% in the layer beneath the surface (45 cm) after 5 days to around 19% after 30 days. It is interesting to note that around 70% of the column height was affected by evaporation after 30 days. Figure 3.8c depicts the degree of saturation versus height. Figure 3.8d presents the variation in dry density.

The dry density ranges from 0.69 g/cm^3 after 5 days to around 0.78 g/cm^3 after 30 day at the bottom while at the top of the columns, the dry density increases to 1.54 g/cm^3 and 1.59 g/cm^3 after 20 days and 30 days, respectively. This increase is the result of evaporation on the surface.

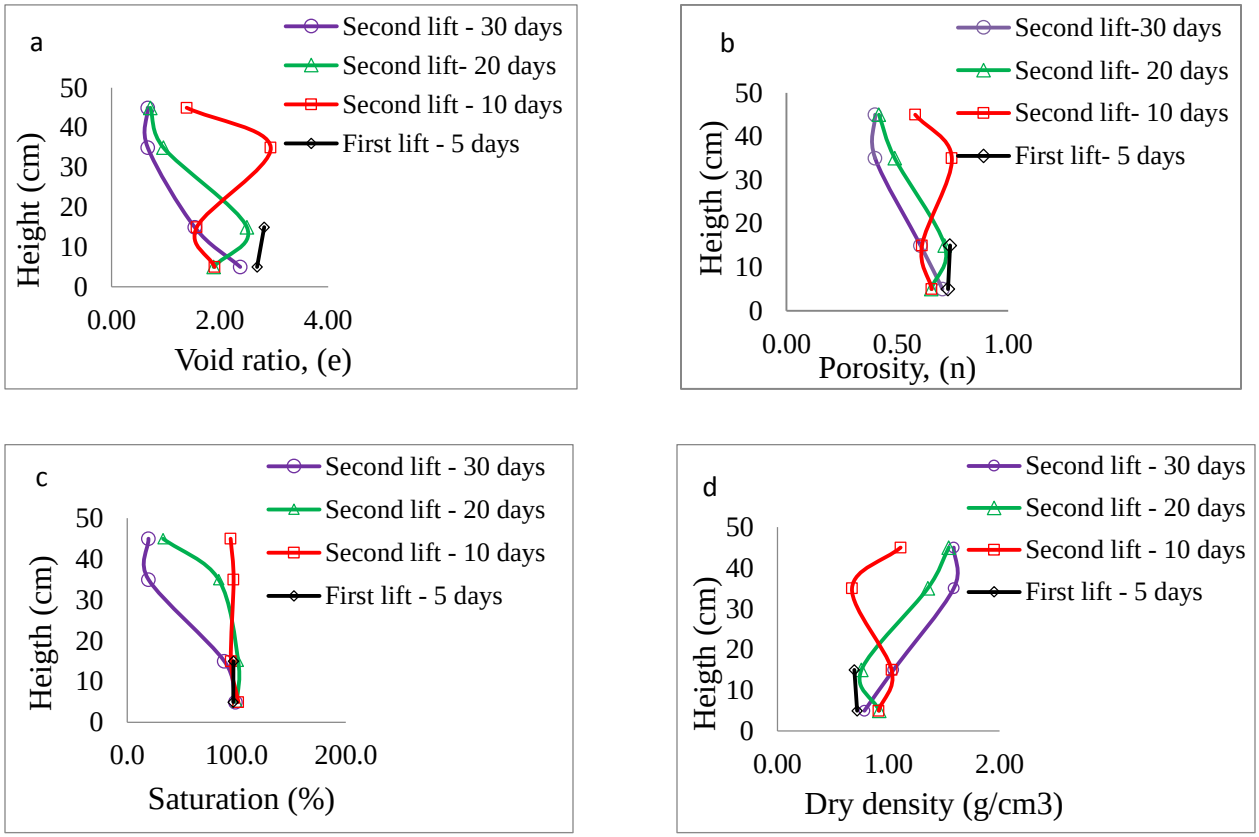

Figure 3.8, Physical properties of the soil: void ratio (a), porosity (b), saturation (c), dry density (d)

3.3.3 Suction changes

Figure 3.9 shows the variations in suction with time in the columns for the experimental period of 30 days. The suction is around 0 kPa at the early ages. The right side of Figure 3.9 shows that there are changes in suction for the first 10 days after column filling. Five days after filling the first lift (before the second lift is added), the suction is around 17 kPa at a column height of 15 cm. After the addition of the second lift, the developed suction at this column height showed a steady decreasing trend untill the last day when it reached almost the same suction on Day 30, at approximately 22 kPa. The reduction in suction after the second load is attributed to the drainage of water from the upper lift to the lower part of the columns, which recovered after 25 days. Due to the effect of evaporation, the highest amount of suction is found closer to the surface. The

suction at column heights of 35 and 45 cm significantly increases to over 500 kPa between Days 7 and 8 (or second and third days after the second lift is added) after 12 days and 17 days, respectivly. Afterwards, the sensors detected cavitation. In term of the suction development at a column height of 5 cm (bottom of the column), the installed suction meter showed the lowest suction values during the testing period. Increase in water content due to the drainage of water from the upper to the lower part of the columns caused a significant reduction in suction and thus the material gained strength. when the drying process started in Phase II, the rate of evaporation then became a function of the total suction and water content rather than attributed to environmental conditions (Wilson et al., 1997). Vapor flow is dominant in the dry zone while liquid flow is dominant in layers below.

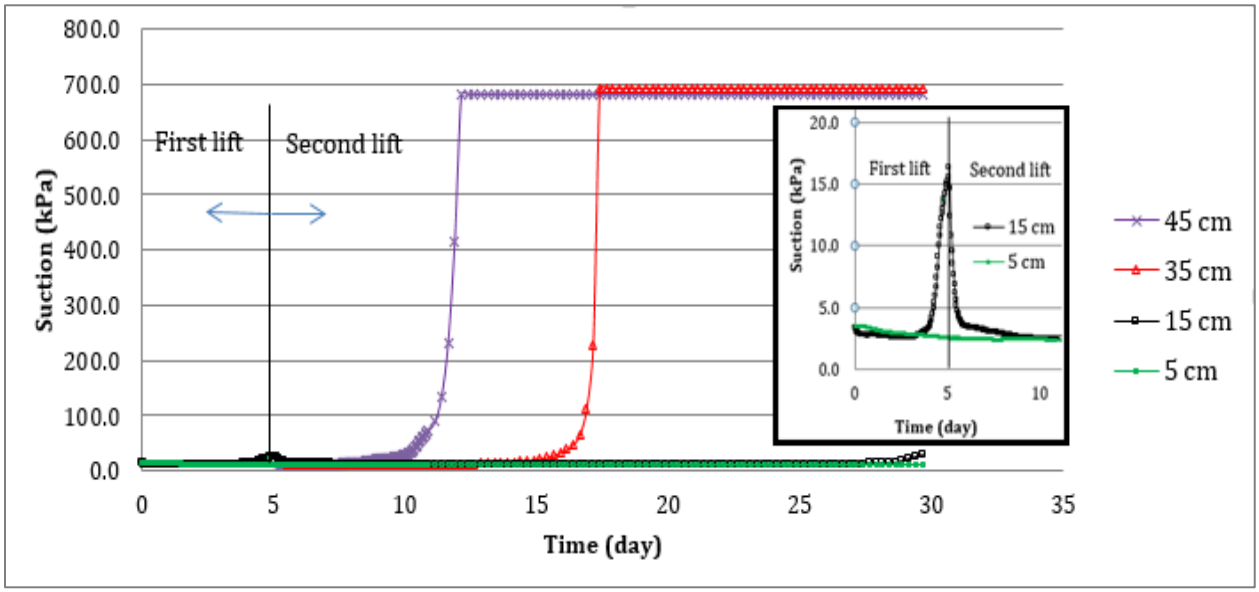

Figure 3.9, Evolution of suction with time and column height

3.3.4 Temperature profile

Figure 3.10 shows the temperature profile of the raw MFTs during drying with time in the columns. Lower tailings temperatures are evident near the surface of the columns where drying fronts are developing due to the consumption of energy from the latent heat of vaporization. The location of the drying fronts advanced in the columns. The data collected by the sensors of the first lift show a decreasing trend in tailings temperature. The lowest temperature point in the temperature profile after five days of casting the first load is 17.5 °C at a height of 15 cm (10 cm below the surface). The addition of the second lift covers the layer below and therefore, these sensors detect an

increasing trend in temperature. After the second lift is atmospherically exposed, the temperature decreases in the first 10-15 days and then when cracks develop and the rate of evaporation is reduced, the entire column is room temperature. The depth and width of the cracks are significant enough to expose the sensors (at heights of 35 cm and 45 cm) to the environment. The temperature is lower at the drying zone because of the latent heat required to transform the liquid water to the vapor phase (Wilson, 1994). The lower tailings temperature result in a slightly lower saturated vapor pressure at the surface of the columns (Beier et al., 2013). Yanful et al. (1997) observed a similar trend in columns with soil and clay due to evaporation.

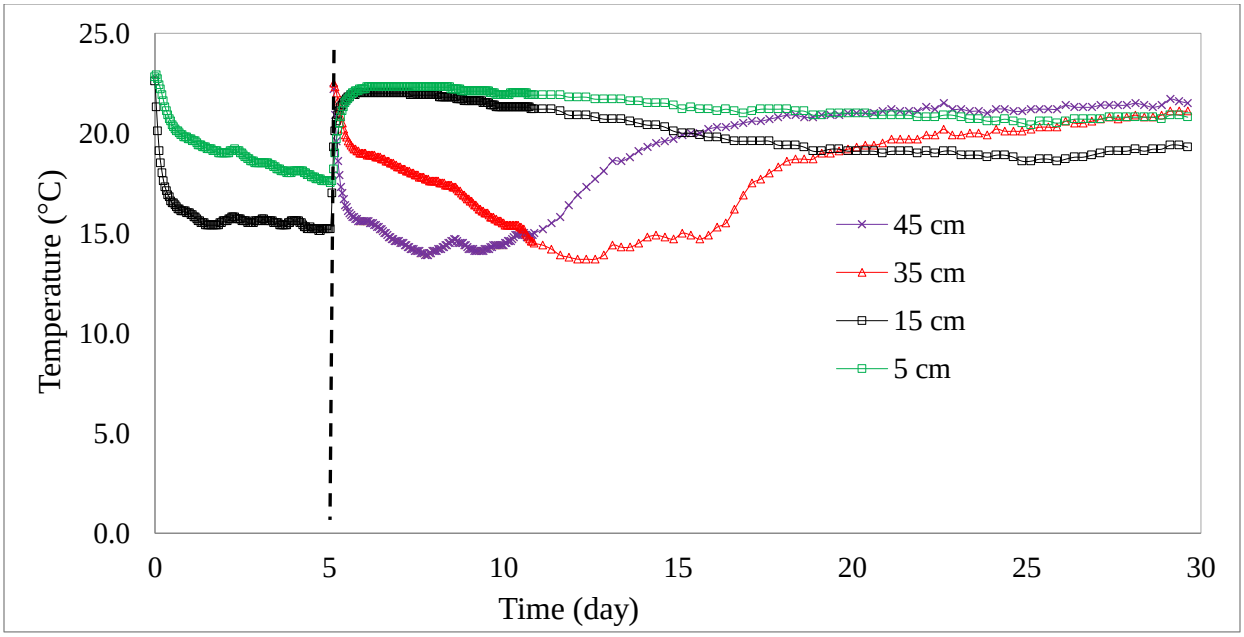

Figure 3.10, Evolution of tailings temperature with time and height

3.3.5 Undrained shear strength of mature fine tailings and solid content changes

Undrained vane shear strength testing was conducted on samples for different heights of the columns at defined elapsed times. Figure 3.11 presents the variation in strength against different heights after 5, 10, 20 and 30 days. It is evident that the strength increases with time. Evaporation leads to a dense matrix and increase in vane shear strength. In adittion, the impact of the void ratio on the strength and development of suction in the columns has a significant impact on the mechanical properties of the tailings (Ghirian and Fall, 2014). Figures 3.9 and 3.11 show the coupled HM relationship. It can be concuded that increase in suction increases strength.

In terms of the strength at the bottom of the columns, the samples showed minimum strenght for all of the elapsed times. Water drained from the second lift because of gravity into the lift below and accumulation of drained water resulted in lower suction values and lower stength gain at the bottom of the columns. significant strength increase for the samples taken from top of the columns were observed at different elapsed times (Figure 3.11). The vane shear strength of the upper part of the first lift after five days and before casting the second lift was around 10 kPa. The subsequent development of suction and strenght was due to evaporation in this layer. Suction was not able to develop well in the first lift within the first 5 days. Only the top layer (of 15 cm) reached a suction of around 10 kPa and the rest of the coulum that was not exposed to the environment had much lower strenght. After filling the column with the second lift, the strength decreased to around 1 kPa . This reduction is due to the water drainage from the fresh lift added which reduced the developed suction and caused a substantial reduction in strenght in the next 20 days. At the end of the testing period, or after 30 days, the cracks extended with depth and the developing suction (caused by evaporation) increased the vane shear strength at 15 cm to around 7 kPa. The suction that developed on Day 30 at 15 cm is provided in Figure 3.9. The strength of the top portion of the columns (35 cm and 45 cm) is over 2 MPa after 20 days.

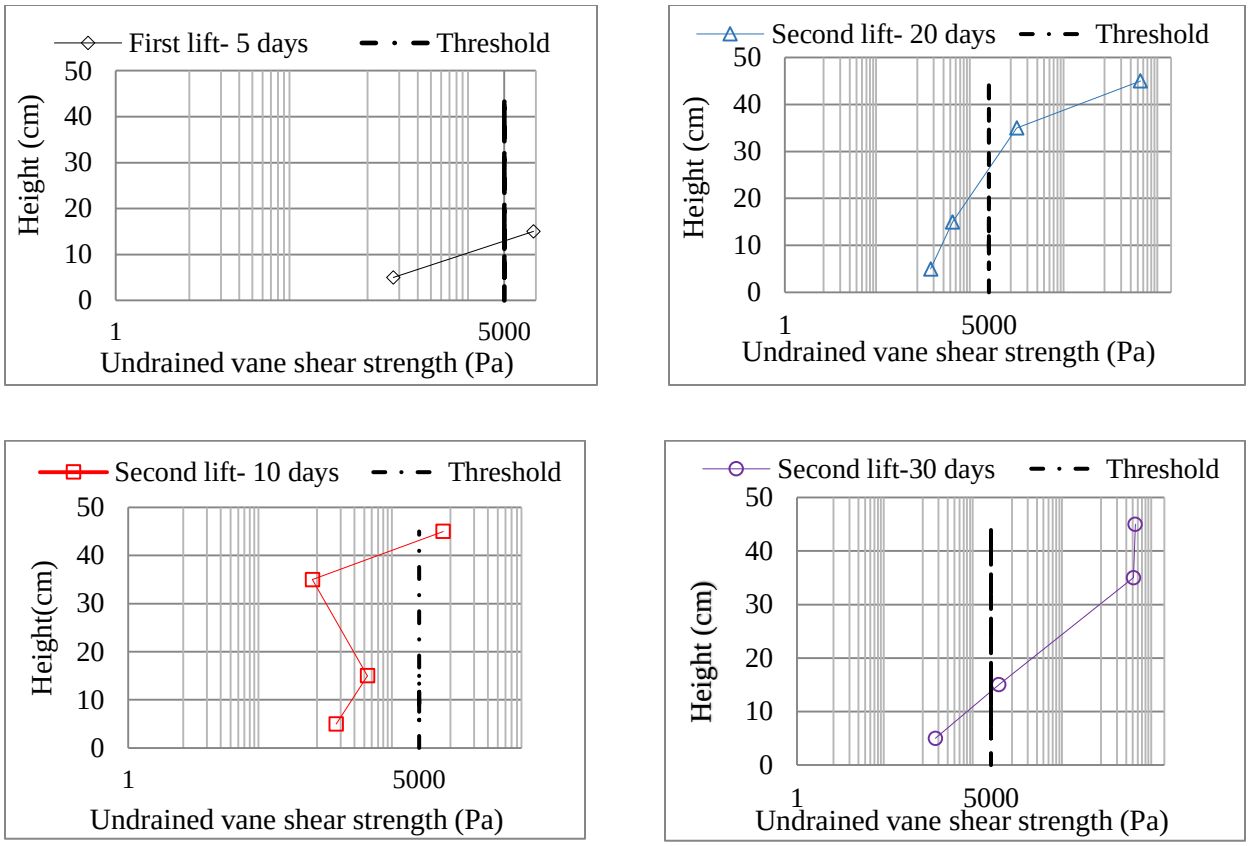

Figure 3.11, Changes in undrained vane shear strength for four different elapsed times

The regulations in Directive 074 dictate that sufficient water needs to be removed from tailings. Therefore, dewatering increases the solid content and consequently increases the strenght. The initial solid conten is approximately 45% (void ratio of 2.9-3.4). The solid content then increases from its initial value to around 58%, 72%, 98% and 99% after 30 days for column heights of 5, 15, 35 and 45 cm, respectively. The void ratio is reduced from 3.5 to 0.67 (see Figure 3.8a). Evaporation, drainage and self-weight consolidation are therefore the mechanisms that effectively contribute to these trends.

3.4 Conclusions

This paper presents the changes in mechanical, hydraulic and physical properties of raw MFTs and their interactions under atmospheric drying. Based on the result, vane shear strength as a mechanical property greatly varies with time and column height. The filling sequence has two negative effects on the developed strength in the first lift. Water drainage from the upper part of the column through the first lift which covers the exposed boundary layer and stops evaporation

process leads to a decrease in suction and strength in the first lift. However, this effect is not permanent; the strength and suction are recovered and exceed the previous values (prior to the addition of the second lift). According to the obtained data, a strong relation can be observed between the strength and void ratio. Also, strong coupled HM behavior shows that there is a coupled relationship between suction and strength in the column. The rate of evaporation and drainage show that evaporation is the dominant mechanism in the dewatering process and not drainage. The presence of cracks and propagation of micro cracks are primarily responsible for fluid mobility as opposed to the very low hydraulic conductivity (drainage) of the MFTs. In terms of physical properties, the solid content and density increase with time in the columns but the void ratio (porosity) is reduced. Evaporation, drainage, self-weight consolidation and crack development are the main mechanisms for this phenomenon. The rate of settlement shows that the MFTs undergo large changes in volume during atmospheric drying. This study thus reveals that the coupled HM behavior of the placement of multiple lifts of MFTs is important and needs to be taken into consideration for the effective management of MFTs in order to reduce DDAs and meet the requirements of Directive 074.

Acknowledgements

The authors would like to thank the University of Ottawa and the National Natural Sciences and Engineering Research Council of Canada (NSERC) for supporting this research.

3.5 References

Beier, N., Wilson, W., Dunmola, A., and Sego, D. (2013). Impact of flocculation-based dewatering on the shear strength of oil sands fine tailings. Canadian Geotechnical Journal, 50, 1001–1007.

BGC Engineering Inc. (2010). Oil sands tailings technology review. Oil Sands Research and Information Network, OSRIN Report No. TR-1.

Bhuiyan, I., Shahid, A., Shifullah, K., and Patrick, L. (2016). Geotechnical behavior of uranium mill tailings from Saskatchewan, Canada. International Journal of Mining Science and Technology, 26(3), 11-23.

Energy Resource and Conservation Board (ERCB), 2011. Government of Alberta.

Farkish, A., and Fall, M. (2013). Rapid dewatering of oil sand mature fine tailings using super absorbent polymer (SAP). Minerals Engineering, 50–51, 38–47.

Farkish, A., and Fall, M. (2014). Consolidation and hydraulic conductivity of oil sands mature fine tailings dewatered by using superabsorbebt polymer. Journal of Geotechnical and Geoenvironmental Engineering, 140 (7), 1-6.

Fasking, T., Dunmola, A., Mckay, D., Masala, S., and Langseth, J. (2011). Bench scale drying of multi-layered thickened TSRU tailings. Proceeding in International Tailings Conference, Edmonton, Alberta, Canada.

Junqueira. F., Sanin, M., Sedgwick, A., and Blum, J. (2011). Assessment of water removal from oil sands tailings by evaporation and under-drainage, and the Impact on tailings consolidation. Proceeding in International Conference of Tailings and Mine Waste, Vancouver, British Colombia, Canada.

Fisseha, B., Bryan, R., and Simms, P. (2010). Evaporation, unsaturated flow, and salt accumulation in multilayer deposits of " Paste " gold tailings. Journal of Geotechnical and Geoenvironmental Engineering, 136, 1703–1712.

Fujiyasu, Y., and Fahey, M. (2000). Experimental study of evaporation from saline tailings, Jornal of Geotechnical and Geoenvionmental Engineering, 126, 18-27.

Ghirian, A., and Fall, M. (2014). Coupled thermo-hydro-mechanical-chemical behavior of cemented paste backfill in column experiments. Part II: Mechanical, chemical and microstructural processes and characteristics. Intrenational Journal of Engineering Geology, 170, 11–23.

Jeeravipoolvarn, S., Scott, J. D., and Chalaturnyk, R. J. (2009). 10 M standpipe tests on oil sands tailings: Long-term experimental results and prediction. Canadian Geotechnical Journal, 46(8), 875–888.

Mikula, R., Kasperski, K., and Burns, R. (1996). Nature and fate of oil sands fine tailings. Journal of American Chemical Society, 251 (14), 677-723.

Pengyu, L., and Li, L. (2015). Investigation of the short-term stress distributions in stopes and drifts backfill with cemented paste backfill. International Journal of Mining Science and Technology, 25 (5), 721-728.

Wilson, G. (1994). Coupled soil-atmosphere modelling for soil evaporation. Canadian Geotechnical Journal, 31, 151-161.

Wilson, G., Fredlund, D., and Barbour, S. (1997). The effect of soil suction on evaporative fluxes from soil surfaces. Canadian Geotechnical Journal, 34, 145-155.

Yanful, E., and Choo, L. (1997). Measurement of evaporative fluxes from candidate cover soils, Canadian Geotechnical Journal, 34, 447–459.

4 Microstructural, hydraulic conductivity and geochemical changes of drying mature fine oil sand tailings in column experiments

Anis Roshani, Mamadou Fall, Kevin Kennedy.
Journal of Mining, Reclamation and Environment, http://dx.doi.org/10.1080/17480930.2017.1278658

ABSTRACT

This study offers new insights into two-lift deposition of mature fine tailings under atmospheric drying. The interaction of newly added lift and former lift(s) was evaluated using column experiments in terms of volumetric water content, electrical conductivity (EC), hydraulic conductivity, geochemistry and microstructure. Water content and EC followed the same trend and decreasing of water content appears to be responsible for significant reduction in EC. Evaporation on top of the column reduced the water content to almost zero. The obtained results support the coupling between the hydraulic and chemical processes that should be considered by active operators.

Keywords: Tailings; oil sand tailings; evaporation; environment; thin lift deposition; waste management.

4.1 Introduction

The oil sand extraction process to produce bitumen has been utilised in Alberta (Canada) over the last few decades. In this water-based process, hot water, steam and sodium hydroxide are added in order to wash the bitumen from the sand. The by-product stream of this process is a mixture of clay, silt and sand called the whole tailings. This stream is hydraulically transported and stored in surface tailing ponds where the coarse fraction segregates and settles quickly and where the fine fraction (clay and silt) remains in a floating layer called fluid fine tailings with a solid content of around 2%.

Here, thin fine tailings (TFT) will start to form immediately; it has the solid content of less than 30%. TFT consolidates and within approximately three-year period becomes mature fine tailings (MFTs) which is a mixture of sand, silt, clay, residual bitumen and water with solid content of around 30%. MFTs exhibits poor consolidation and water release characteristics (Chalaturnyk et al., 2002; Mikula et al., 1996). The great depth of the ponds and low hydraulic conductivity of the MFTs cause very slow densification, and the full consolidation of the MFTs can take several decades under natural conditions (Suthaker and Scott, 1997; Klein et al., 2013). The inevitable expansion of oil sand development has and will continue to have a huge impact on land, water resources, ambient air, wildlife and human health. Tailings ponds contain a variety of harmful chemicals from heavy metals to naphthenic acids, which are of concern due to their toxicity to aquatic organisms, birds and wildlife in general (Jordaan, 2012; Rogers et al., 2002). Therefore, tailings pond seepage is another significant risk of pollution (Timoney and Lee, 2009). In fact, the sediment arsenic concentration in Lake Athabasca increased over the period of 1970–1990 from 2 to 10 mg/kg (Chalaturnyk et al., 2002), while the interim fresh water guideline for protection of aquatic life is 5.9 mg arsenic/kg. In 2009, the Alberta Energy and Resources Conservation Board (ERCB) released new rules to regulate the reclamation of tailings, and oil sand operations were required to submit their management plans in accordance with Directive 074 entitled ‘Tailings Performance Criteria and Requirements for Oil Sand Mining Schemes’ (ERCB, 2009). The key purpose of Directive 074 is to regulate tailings in the oil sand industry and to reduce the volume of fluid fine tailings that are produced. The ERCB wants to hold mineable oil sand operators accountable for their produced tailings by setting timelines for the reduction in the amount of fluid tailings and creating a trafficable surface through different techniques of consolidation, drying,

drainage, etc. (BGC, 2010). According to Directive 074, material deposited in a dedicated disposal area (DDA) must achieve minimum undrained shear strength of 5 kPa within one year of deposition. If it does not meet this criterion, the material must be removed or remediated.

One of the main challenges in the oil sand industry is dewatering of tailings, particularly MFTs, in order to strengthen the deposit in the ponds that will lead to enhanced volume recovery. Moreover, tailings pond volume can be reclaimed, and water can be recycled back into the extraction process. Enhanced MFTs dewatering can help to minimise DDAs, as well as aid in the sequestration of toxic material.

Thin lift deposition is one of the management techniques that has been considered in recent years by active operators in this industry (ERCB, 2009; BGC, 2010). Thin lift involves tailings deposition in thin lifts (< 30 cm). Each lift is allowed to dry before deposition of the next lift. Multilayer deposition has a high impact on minimising the DDA. But there are some issues regarding this technique. Sequential lift acts as a cover for former lift to prevent evaporation. Drainage water that goes through the last layer (due to gravity) has a negative impact on the shear strength of the deposition. So, the thin lift deposit technique is not applicable if the developed strength in each lift is compromised by the freshly deposited layer. Moreover, the effectiveness of thin lift deposition is dependent on the availability of dry weather. This technique will not work properly in wet weather conditions. Thin lift deposition of oil sand tailings as a geotechnical system is subjected to strong coupled hydraulic (H) and chemical (C) processes. The interplays between these factors demand a comprehensive study to follow the behavior of the deposited tailings. Ions transformation, salt precipitation and shrinkage induced by evaporation (causes an increase in suction) lead to porosity or void ratio reduction (Simms et al., 2007; Lee et al., 2003). This means they lead to the evolution or change of the microstructural properties of the tailings material. This microstructural evolution impacts hydraulic properties. Therefore, there is a need to understand the effect of micro-structure, hydraulic conductivity and geochemical evolution on MFTs behavior when it is drying. Based on our literature review on MFTs studies (Suthaker and Scott, 1996; Jeeravipoolvarn et al., 2008; Beier et al., 2013; Yao et al., 2012; Junqueira et al., 2011; Fasking et al., 2011) the impacts of geochemical and microstructural properties on chemical and hydraulic behavior of MFTs in the multi-lift deposition have not been addressed. These gaps inspired the authors to conduct the current study to analyse the geochemical and microstructural evolution in a

multi-lift MFTs deposition by column experiment. The impacts of geochemical and microstructural properties on hydraulic behavior have been addressed as well. The findings of this research can provide a better understanding of multi-lift deposition and, thus, lead to a more cost-effective and applicable design for oil sand tailings containment.

4.2 Experimental program

4.2.1 Material

MFTs were delivered from Alberta and underwent different mineralogical tests. Figure 4.1 shows the grain size distribution by wet laser diffraction analysis. The tailings were composed of around 18% clay (≤ 2 μm), 81% silt (2 μm < Ø ≤ 75 μm) and less than 1% sand (75 μm < Ø ≤ 2.3 mm). Percentage of fines (< 44 μm) was around 95%. Initial solid content was measured around 45%, and organic content was around 18%. The average specific gravity of the tailings was around 2.37, and it is believed that the bitumen that has a specific gravity of about 1.03 is considered part of the fine solids and results in quite low specific gravity of the total solids, compared with other natural clay soils (Jeeravipoolvarn et al., 2009). The liquid limit (LL) and plastic limit (PL) of the MFTs are 51.2 and 37.2, respectively (Frakish and Fall, 2013). So, the plasticity index (PI) is equal to 14 and activity (A) is 0.77, which is considered as a normal clay. The X-ray diffraction analysis results of the MFTs sample indicated that the mineral content mainly consists of quartz, kaolinite and illite.

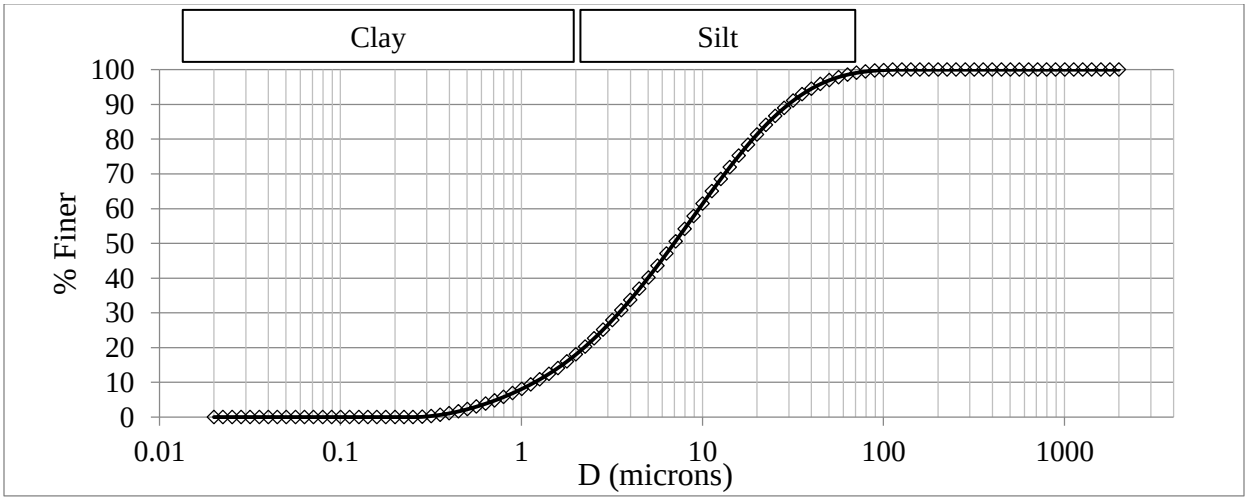

Figure 4.1, Grain size distribution of mature fine tailings

4.2.2 Developed experimental setup

A schematic diagram of the developed experimental setup is illustrated in Figure 4.2. The Plexiglass columns are 24 cm in diameter and 55 cm in height. The bottom of each column was filled with a layer of sand, and a perforated sheet covered by a filter paper holds the tailings and prevented them from going through the drainage pipe. The surface was exposed to ambient air, and room temperature and humidity were continuously measured (the average temperature and relative humidity were 24 °C and 26%, respectively). The distance between the MFTs'surface and the fan was controlled. Filling consisted of two separate stages (25 cm each).

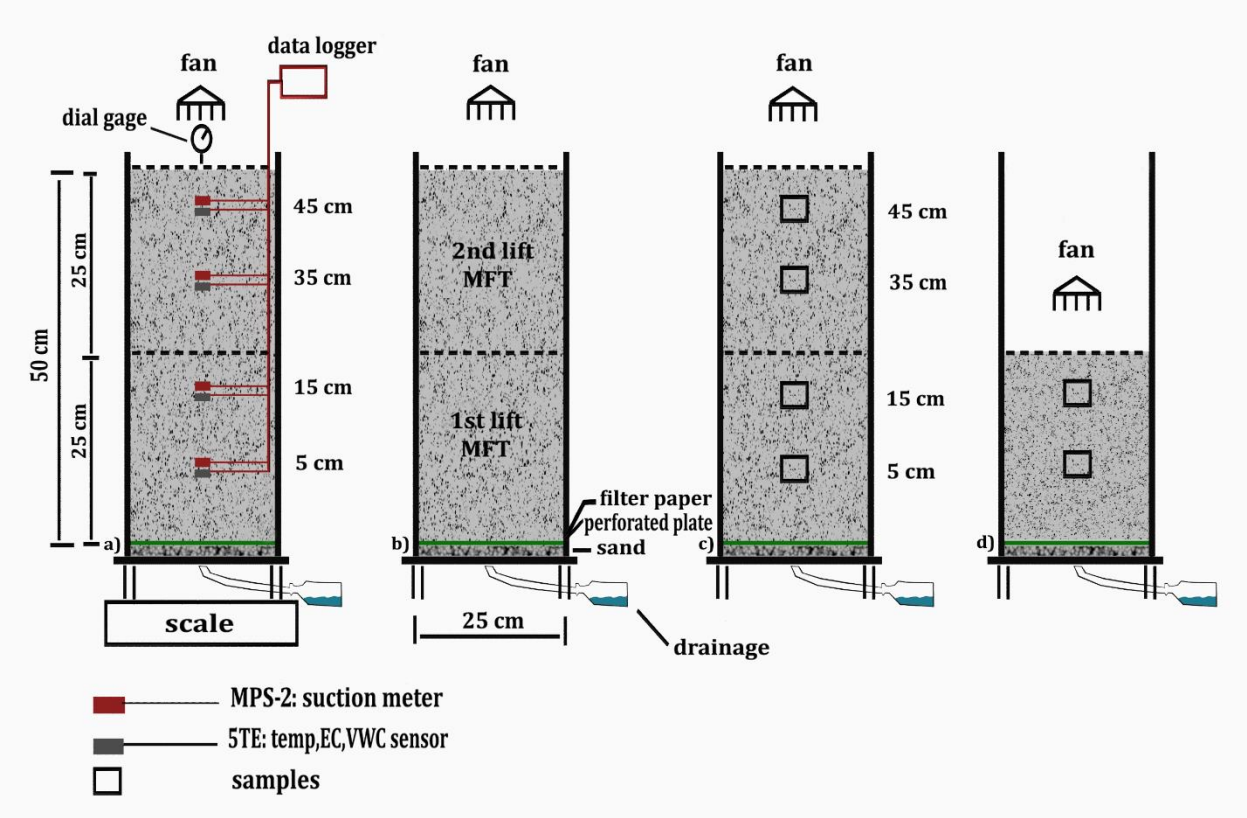

Figure 4.2, Schematic diagram of the experimental setup: (a) arrangement of the sensors and dial gage – second lift 30 days, (b) filling sequence – second lift 20 days, (c) sampling locations – second lift 10 days, (d) first lift 5 days

The first lift was added, and after five days (to expose the first lift to evaporation-induced dewatering), the second load was added. In total, four columns were manufactured in which one column was for instrumentation and monitoring for a period of 30 days and the other three columns were for sampling after 5, 10 and 20 days. Each column was dismantled at each defined elapsed

time, and samples were taken from different heights: 5, 15, 35 and 45 cm for the experimental testing programme.

4.2.3 Column instrumentation and monitoring

The monitoring column was equipped with two different kinds of sensors to monitor suction, temperature, electrical conductivity (EC) and volumetric water content that were all connected to a data logger. Four MPS-2 sensors (Decagon Devices Inc.) monitored the suction (in the range of 0 to 500 kPa with the accuracy of ±25%) and temperature (in the range of −40 to 60 °C with the accuracy of ± 1 °C). Furthermore, four 5TE sensors (Decagon Devices Inc.) were installed at four different heights. They could record EC in the range of 0–23 dS/m and volumetric water content in the range of 1–80%. All the sensors were at fixed elevations. A dial gauge (3058S, Mitutoyo Co.) installed on top of the column (immediately after adding the second lift), measured the settlement induced by evaporation shrinkage and self-weight pressure. There was a fan positioned on top of each column for simulation of wind. The wind was blowing on the tailings surface. The average wind speed generated by the fan was 7.5 m/s. Each fan placement was adjusted to give an equal distance from the tailing surface after the addition of each lift. Location of sensors, filling sequence and sampling heights are shown in Figure 4.2.

4.2.4 Hydraulic conductivity

A saturated hydraulic conductivity test was conducted using constant head TRI-FLEX in which a known constant hydraulic gradient was imposed across the sample and then inflow and outflow were measured. The related procedure is well described in ASTM D5084. A constant head test calculated the hydraulic conductivity, *k*, as follows:

$$k = \frac{\Delta Q.L}{A.\Delta H.\Delta t} \qquad (4.1)$$

Where:

k = hydraulic conductivity, m/s, ΔQ = quantity of flow for given time interval Δt, taken as the average of inflow and outflow, m^3, L = length of specimen, m, A = cross-sectional area of specimen, m^2, Δt = interval of time, s, over which the flow ΔQ occurs ($t_2 - t_1$), t_1 = time at start of permeation trial, t_2 = time at end of permeation trial, Δh = average head loss across the

permeameter/specimen, $((\Delta h1 + \Delta h2)/2)$, m of water, $\Delta h1$ = head loss across the specimen at t_1, m of water, and $\Delta h2$ = head loss across the specimen at t_2, m of water.

four values of hydraulic conductivity were obtained in which the ratio of outflow to inflow rate was between 0.75 and 1.25 which meant the hydraulic conductivity was steady. Four readings were done and an average was reported as saturated hydraulic conductivity. Each test was performed twice to ensure the repeatability of the results.

4.2.5 Microstructural analysis

Microstructural analysis was performed by mercury intrusion porosimetry (MIP) and scanning electron microscopy (SEM) observation. The SEM observation was done with a Hitachi 3500-N microscope. The samples were first dried in an oven at 45 °C (this drying temperature does not result in cracking) to achieve mass stabilisation. SEM can show particle size distribution and morphology of the samples. However, it is worth mentioning that the SEM analysis was conducted on dried samples and sample preparation may impact the SEM results. The SEM results therefore only provide qualitative results at best. MIP observation can help to evaluate pore size distribution and total porosity. MIP analyses were performed using a Micromeritics Auto-Pore III 9420 mercury porosimeter. In addition, extensive experiments were conducted to calculate water content and density for each sample by following the standards procedures of ASTM D854 and D7263, respectively. The total volume of wet soil (V), water content (w), and specific gravity (G_s) and the mass of dry soil (M_d), void ratio (e), porosity (n) and saturation (S) for the columns can be calculated as follows:

$$\left(n = \frac{V - M_d / G_s}{V} \times 100, e = \frac{n}{100 - n}, S = \frac{G_s w}{e}\right) \quad (4.2)$$

4.2.6 Chemical analyses

The samples were ashed at 500 °C for 24 h, and the ashed residue was ground to a fine powder with a mortar and pestle. A mixture of 0.5 ml of concentrated HNO_3 and 1.5 ml of concentrated HCl was added to 0.1 gr of ash in a Teflon vial and allowed to stand for 4-5 h. Then, the mixture was heated (lightly closed) on a hot plate at 100 °C for 5-6 h. The acid was evaporated to near dryness. Next, 0.5 ml of concentrated HNO_3 was added and heated for 1 h. The volume was

brought to about 3 ml of water and centrifuged. Supernatant was transferred to another vial. The residue was rinsed with another 3 ml portion of water and centrifuged for the second time. The solutions from the two centrifugations were merged, and the total mass was brought to 10 g for an accurate measurement by inductively coupled plasma emission spectrometry (ICP-ES) and inductively coupled plasma mass spectrometry (ICP-MS).

4.3 Results and discussion

4.3.1 Volumetric water content, suction and electrical conductivity evolution

EC is a good indicator for soil salinity. The factors that affect EC of a soil are divided into three main groups: bulk soil properties (e.g. porosity, water content), solid particle quantifier that is time invariable (e.g. particle size distribution, cation exchange capacity (CEC), wettability) and environmental factors that affect soil solution (e.g. temperature, cation composition (sodium adsorption ratio)) (Mikula et al., 1996). Soil solution, as the only conducting phase, has a major impact on EC (Friedman, 2005). The other component of EC is surface conductivity, which directly relates to CEC in the electrical double layer (Tabbagh and Cosenza, 2007). An increase in water content promotes the mobility of the ions that accumulate on the soil surface, and this leads to a higher EC (Miyamoto et al., 2009). Figures 4.3 , 4.4 and 4.5 show variation in water content and suction with respect to the time and height of the column. In the first five days, evaporation on the surface (15 cm) decreased the water content and increased the suction. By loading the second lift, developed suction in the former lift was eliminated temporarily, but suction developed on the evaporating surface (45 cm). Figure 4.6 shows EC evolution with respect to the time. The distribution of EC in pore water shows the same general trend as water content. Decreasing the volumetric water content causes a falling trend in EC. Initial EC in the first lift (before second load) at the top (15 cm) was measured around 2 mS/cm, and that fell to 0.4 mS/cm after five days, where the high rate of evaporation caused water content reduction from 0.47 m^3/m^3 to 0.28 m^3/m^3. By loading the second lift, water content in the first lift increased temporarily due to drainage from the freshly added layer. As a result, the 5TE sensor at the height of 15 cm showed a sharp increase in EC on day five. After adding the second lift, water content at the top (45 and 35 cm) decreased sharply due to the high rate of evaporation and developed suction. EC at the height of 35 and 45 cm reached to almost zero when the water content fell to 0.112 and 0.103 m^3/m^3, respectively. The water content and EC at the bottom exhibited a slight decrease. EC at the height of 5 cm was

initially 2.06 mS/cm and decreased to 1.84 mS/cm after 30 days, where the initial volumetric water content was measured at 0.463 m ^{3}/m^3 and fell to 0.437 m^3/m^3. Rewetting the lower layer by downward drainage after subsequent lift prevented water content and EC from being reduced at the bottom. Furthermore, the cracks could not extend at the bottom (5 cm), and consequently, suction did not develop. In the last five days, when the cracks affected the water content at the height of 15 cm, a decreasing trend of EC was observed in this part.

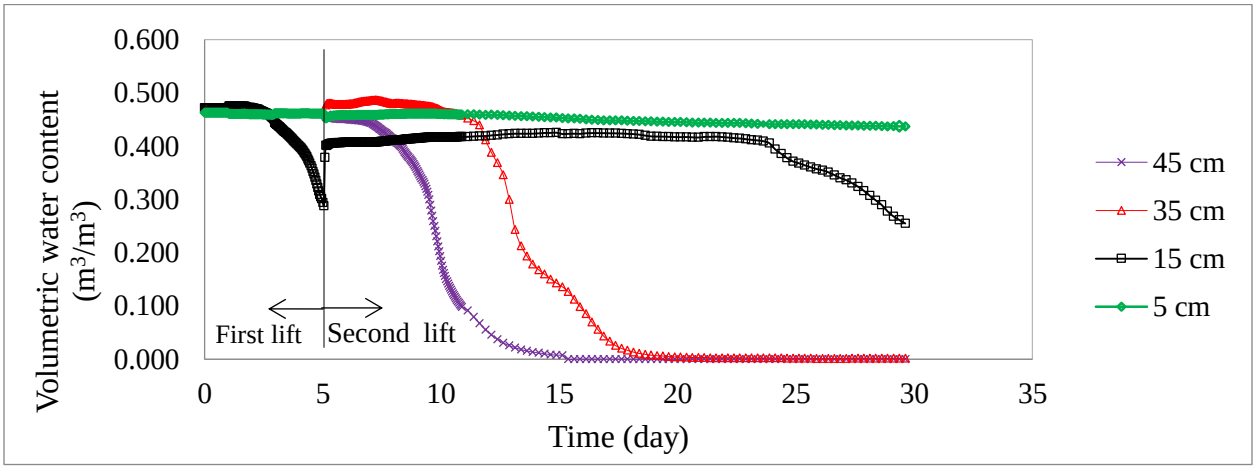

Figure 4.3, Evolution of the volumetric water content with time

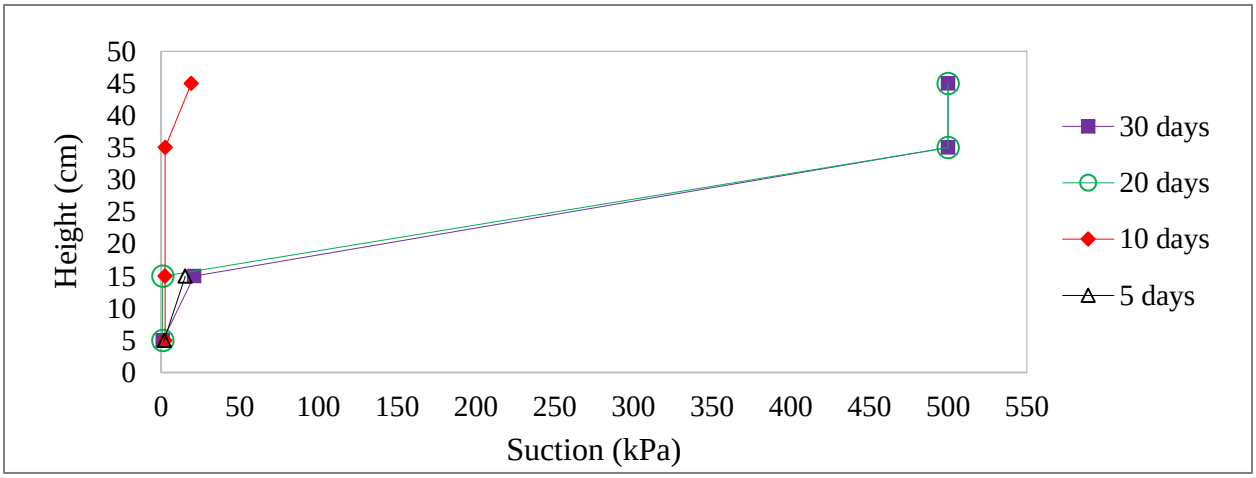

Figure 4.4, Suction development with respect to the elapsed time and column height

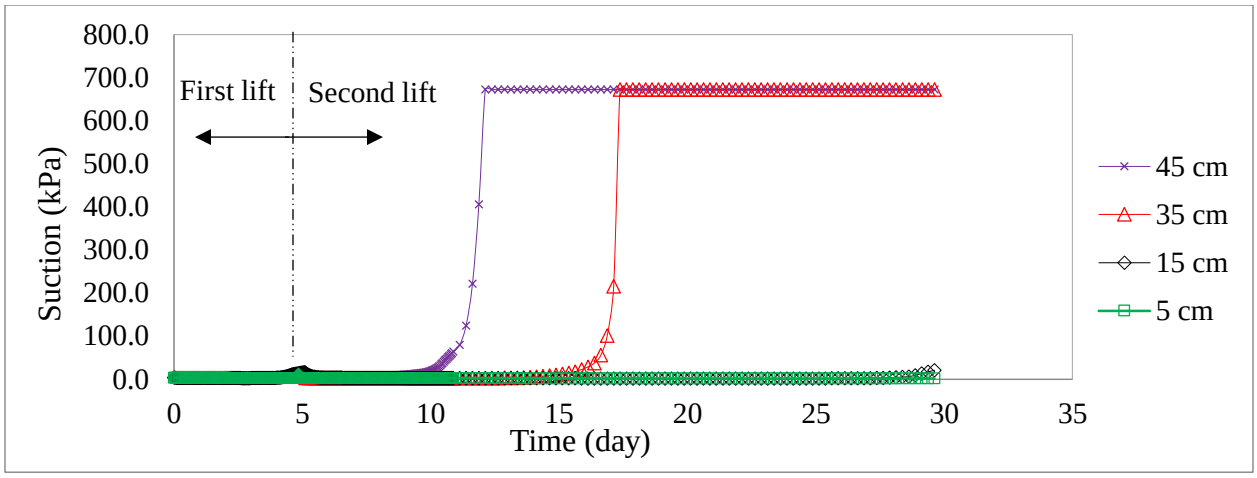

Figure 4.5, Suction development with respect to the time

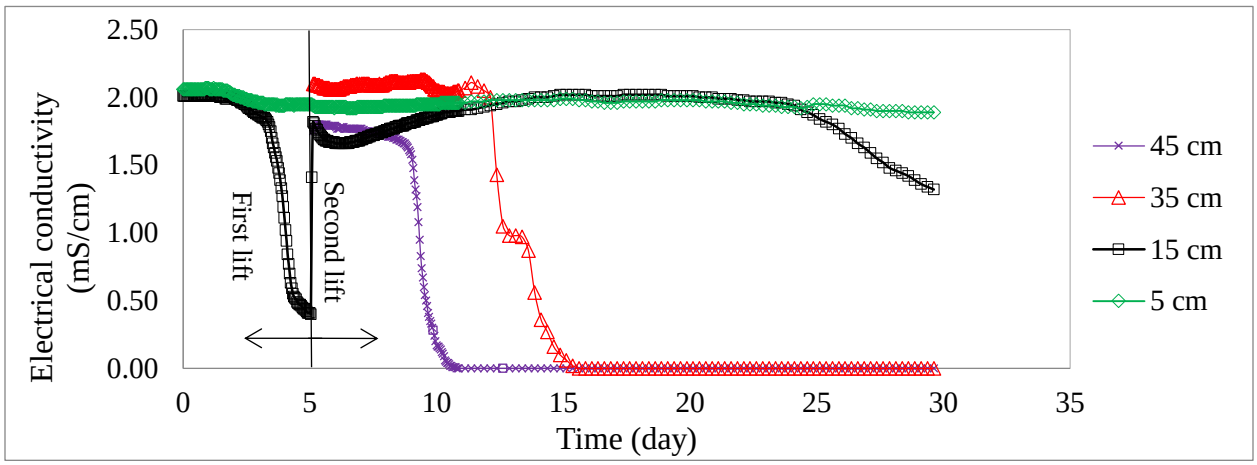

Figure 4.6, Evolution of the electrical conductivity with time

4.3.2 Solid content evolution

The solid content increases during desaturation was induced by sustained evaporation. An increase in density and consequent reduction in void ratio reduced the total volume of the deposition (Lee et al., 2003; Jeeravipoolvarn et al., 2008). Figure 4.7 shows the variation in solid content with respect to time and height of the columns. It was previously mentioned that solid content is defined as an oven dried sample divided by the total mass of the wet sample. The figure shows that after 10 days, the top portion of the column (45 cm) reached to a solid content of 77%. Since the cracks could not develop within the column (within 10 days), suction did not increase. After 20 days, by advancing the drying front and developing the cracks, suction increased in most parts of the column, and solid content increased up to 84% in the upper parts. Sensors reported the suction of around 680 kPa for the top 25 cm of the column. After 30 days, measured solid contents were 57,

72, 98 and 99% at heights of 5, 15, 35 and 45 cm, respectively. It has been noted that increases in solid content and dry density decrease the void ratio which, in turn, reduce the total volume of the tailings (Fisseha et al., 2010). To determine how the volume changes with respect to water content, void ratio should be studied. The fine tailings underwent volume changes as suction developed during the drying process. The void ratio of 0.67 at the top of the column related to the minimum volume that MFTs could attain after 30 days (upon drying to zero water content in atmospheric drying). The void ratio at the heights of 5 and 15 cm after 30 days were 2.3 and 1.5, respectively. Post-column experiment vane shear tests were conducted (according to ASTM D4648) on MFT samples to determine their shear strength. The measured vane shear strength (after 30 days) was around 500 Pa and 7 kPa for 5 and 15 cm, respectively, while the top portion of the columns showed a strength of more than 2 MPa. Increasing solid content that results in higher strength allows MFTs to achieve steeper deposition angles (Simms et al., 2007; Farkish and Fall, 2013).

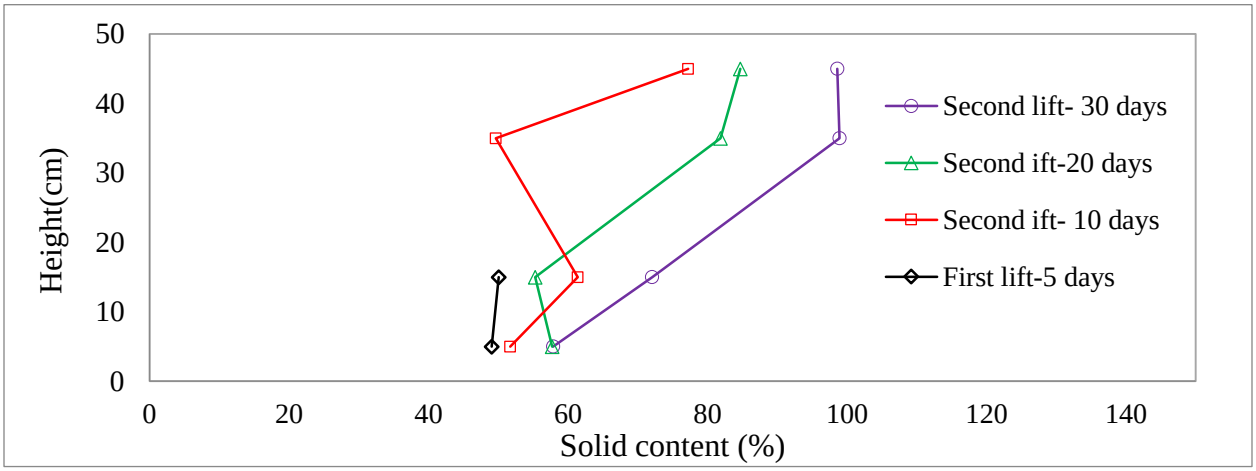

Figure 4.7, Evolution of solid content within the columns at different elapsed times

4.3.3 Geochemical evolution

Understanding geochemical evolution is helpful in meeting environmental compliance legislation by groundwater monitoring and seepage management techniques. Furthermore, ion precipitation at the evaporation surface can affect the evaporation rate through three phenomena: (1) salinity sup-presses vapour pressure at the soil surface because of the high osmotic suction; (2) albedo increases as the result of the increase in reflectivity of salt precipitation and (3) small pores are clogged with precipitated salts that act as a barrier against vapour transfer (Fisseha et al., 2010; Fujiyasu and Fahey, 2000; Fujimaki et al., 2006; Nachshon et al., 2011)). Assessment of major

cations (Na^+, K^+, Ca^{2+}, Fe^{3+}, Si and Al) and trace elements (Co, Ni, Cu, Zn, Sr and Ba) were examined in the current study in two different phases: in the liquid phase as process affected water and in the solid phase as a soil matrix. The concentrations of sodium, potassium, calcium, iron, silica and aluminium in pore water were measured and found to be 617.0, 14.10, 4.50, 0.85, 8.30 and 3.50 ppm, respectively.

Concentrations of nickel, copper and zinc in the liquid phase were 0.012, 0.002 and 0.007 ppm, respectively. These results of major and trace elements are in agreement with other studies (Mikula et al., 1996; Siwik et al., 2000). Figure 4.8 shows the concentration of ions in the dried soil matrix (ashed and then digested in acid) with respect to the time and column height. The higher concentrations of these cations were mainly observed in the older MFTs column (30 days) in which evaporation affected most of the column (50, 45, 35 and 15 cm). Precipitation of salts in the voids increased the salt concentrations and eventually reduced evaporation by increasing resistance to vapour diffusion. Table 4.1 represents the concentration of trace elements with respect to the elapsed times and heights. These data show that these concentrations did not have any special trend in terms of time and height. Low hydraulic conductivity of MFTs, in addition to the lower concentrations of these elements, caused the convection of trace elements not to develop towards the evaporating boundary.

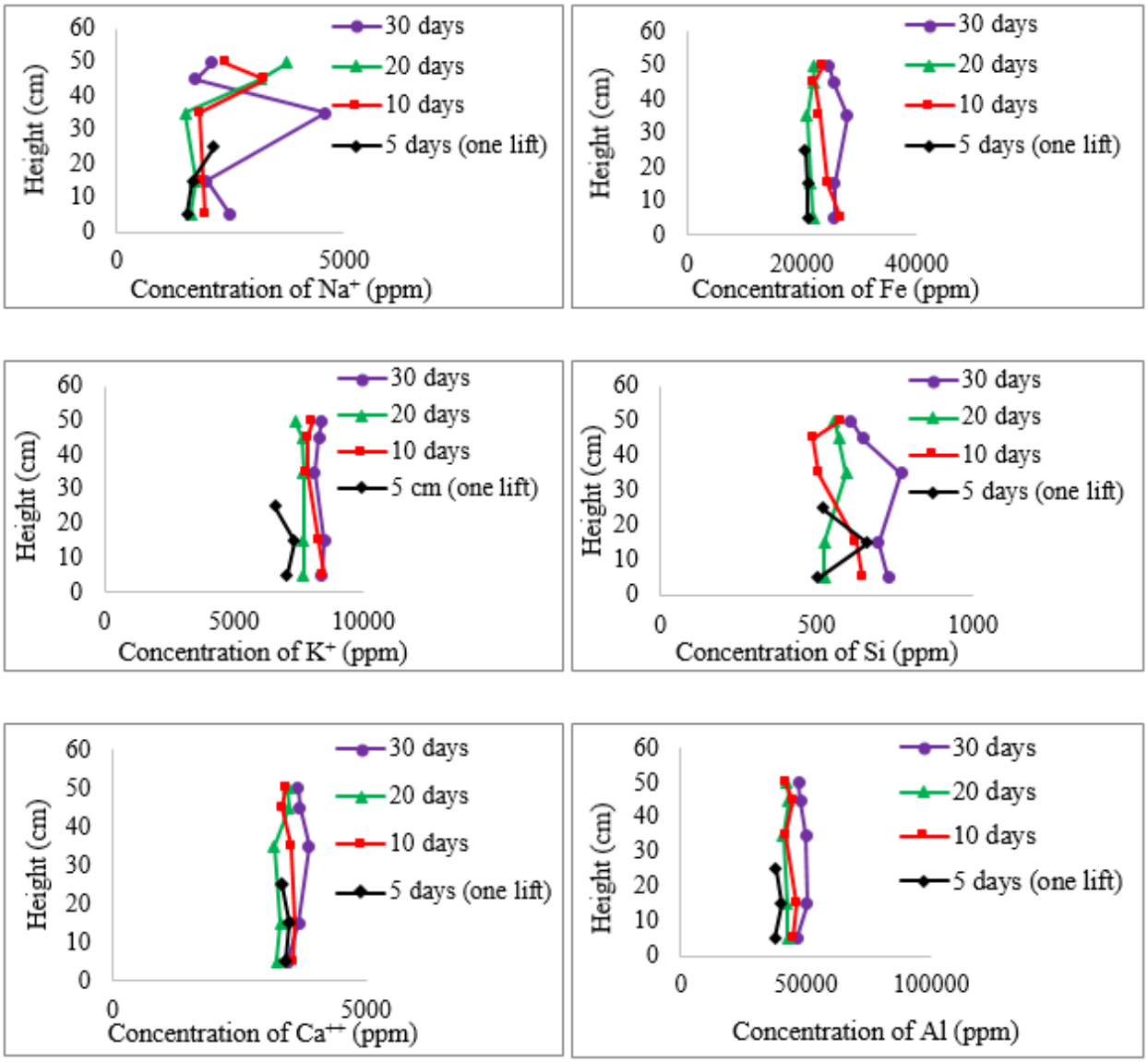

Figure 4.8, Evolution of ions concentration with respect to the height and time

4.3.4 Microstructural evolution

4.3.4.1 SEM images

Evaporation can affect the micro-fabric due to suction development (Rao and Revanasiddappa, 2005; Birle et al., 2008). Figure 4.9 shows SEM micrographs for four different samples obtained from 45 and 15 cm of the monitoring column (30 days) and 5 and 45 cm of the 10 day column. It can be observed that there is almost a card house structure in the image from the bottom of the 10 day column (Figure 4.9(a)) in which evaporation could not affect the tailings. Undeveloped suction

in this part of the column, as evidenced by Figures 4.3 ,4.4 and 4.5 kept the pores and voids in the original state and well-developed void spaces can be seen.

Table 4. 1, Evolution of trace elements concentration with respect to the height and time

	Co	**Ni**	**Cu**	**Zn**	**Sr**	**Ba**
	ppm	**ppm**	**ppm**	**ppm**	**ppm**	**ppm**
Limit of detection (ppm)	0.00109	0.00154	0.00074	0.01006	0.0011	0.00079
	Monitoring column (Two lifts 30 days)					
Surface (50 cm)	14.60	36.98	1.71	67.13	110.90	189.31
45 cm	14.79	37.99	1.79	61.32	105.21	181.09
35 cm	13.70	35.40	1.68	62.69	111.41	182.15
15 cm	14.46	37.25	1.70	65.18	110.76	188.00
5 cm	13.18	35.40	1.64	61.38	107.46	186.94
	Two lifts 20 days					
Surface (50 cm)	14.54	39.71	1.71	63.20	119.37	192.22
45 cm	15.16	40.58	1.78	66.13	124.91	203.48
35 cm	13.86	35.28	1.63	61.01	112.97	193.99
15 cm	14.15	36.84	1.78	67.04	117.43	216.03
5 cm	14.25	37.12	1.68	63.06	110.52	194.17
	Two lifts 10 days					
Surface (50 cm)	14.95	38.86	1.78	62.84	116.72	196.81
45 cm	15.42	40.08	1.83	64.82	116.94	194.98
35 cm	15.42	40.18	1.78	86.27	112.69	186.67
15 cm	15.06	38.58	1.67	63.00	113.87	199.05
5 cm	15.27	38.66	1.89	67.85	116.53	201.57
	One lift 5 days					
Surface (25 cm)	14.78	37.76	1.80	63.36	112.07	186.27
15 cm	15.02	38.63	1.74	66.11	116.95	202.83
5 cm	14.62	36.06	1.77	65.69	111.50	181.62

The calculated void ratio for this height was around 2, and connected voids provided channels for water flow and accounted for the higher hydraulic conductivity (Figure 4.13). Vane shear strength was measured at less than 500 Pa for samples taken from this height (5 cm). The transformation process from a slurry phase into a rigid solid phase can be understood by images 4.8b, 4.8c and 4.8d. Suction development (Figure 4.3) at upper parts of the column caused the voids to close, and in all cases, the edge to face card house fabric was altered to a compact, aggregated fabric. In

addition, salt precipitation contributed to closing or refining the voids. Precipitations (mostly sodium and calcium) can be seen in the SEM results as white spots. The void ratio in these conditions fell to 1.3 and 1.5, respectively, as indicated in Figures 4.9(b) and (c). The calculated void ratio for the top portion of the monitoring column was 0.67 which accounts for the solid content increase. Thus, vane shear strength reached to more than 2 MPa, while hydraulic conductivity decreased (Figure 4.13), as flow was further restricted. The results presented above indicate that the drying alters the microstructure of the MFTs which, in turn, affects its strength and hydraulic conductivity.

4.3.4.2 MIP results

A MIP test was carried out on four different samples: two samples taken from 45 cm and 15 cm of the monitoring column (30 days) and two samples from the top and bottom of the 10 day column (45 and 5 cm). This test allowed us to understand the effect of surface evaporation, salt precipitation and suction development on pore structure. The MIP results are presented in Figure 4.9 and Figures 4.10 and 4.11. By comparing the results of the samples taken from the bottom of the 10 day column (5 cm), a coarser pore structure can be observed. It can be seen that the sample at 45 cm of the monitoring column (4% water content) had the finest pore matrix of all the columns. This is due to surface evaporation which developed the suction and associated drying shrinkage and which, in turn, caused a reduction in porosity or void ratio. The water content of the sample at the top of the 10 day column and 15 cm of the monitoring column were 44 and 47%, respectively. By comparing the results from the MIP shown in Figures 4.11 and 4.12, it can be seen that around 60% of the pore distribution in the top part of the monitoring column (30 days) ranged from 0.1 to 0.3 of a micron. At the lower part of this column (15 cm), 55% of the pores had a diameter in the range of 0.1-0.3 of a micron, but around 10% of the pores had a diameter of more than 100 μm, which corresponded to a higher void ratio. In contrast, at the bottom of the 10 day column, where evaporation could not affect the tailings, only 10% of the pores were in the range of 0.1-0.3 of a micron, and around 60% of the pores had a 0.5-1 μm diameter.

In the MIP test, pore diameter related to the highest rate of mercury intrusion is called threshold diameter (TD), following a horizontal line of a cumulative intrusion graph, and this is a good indicator of the smallest pore diameters that are continuous within a sample.

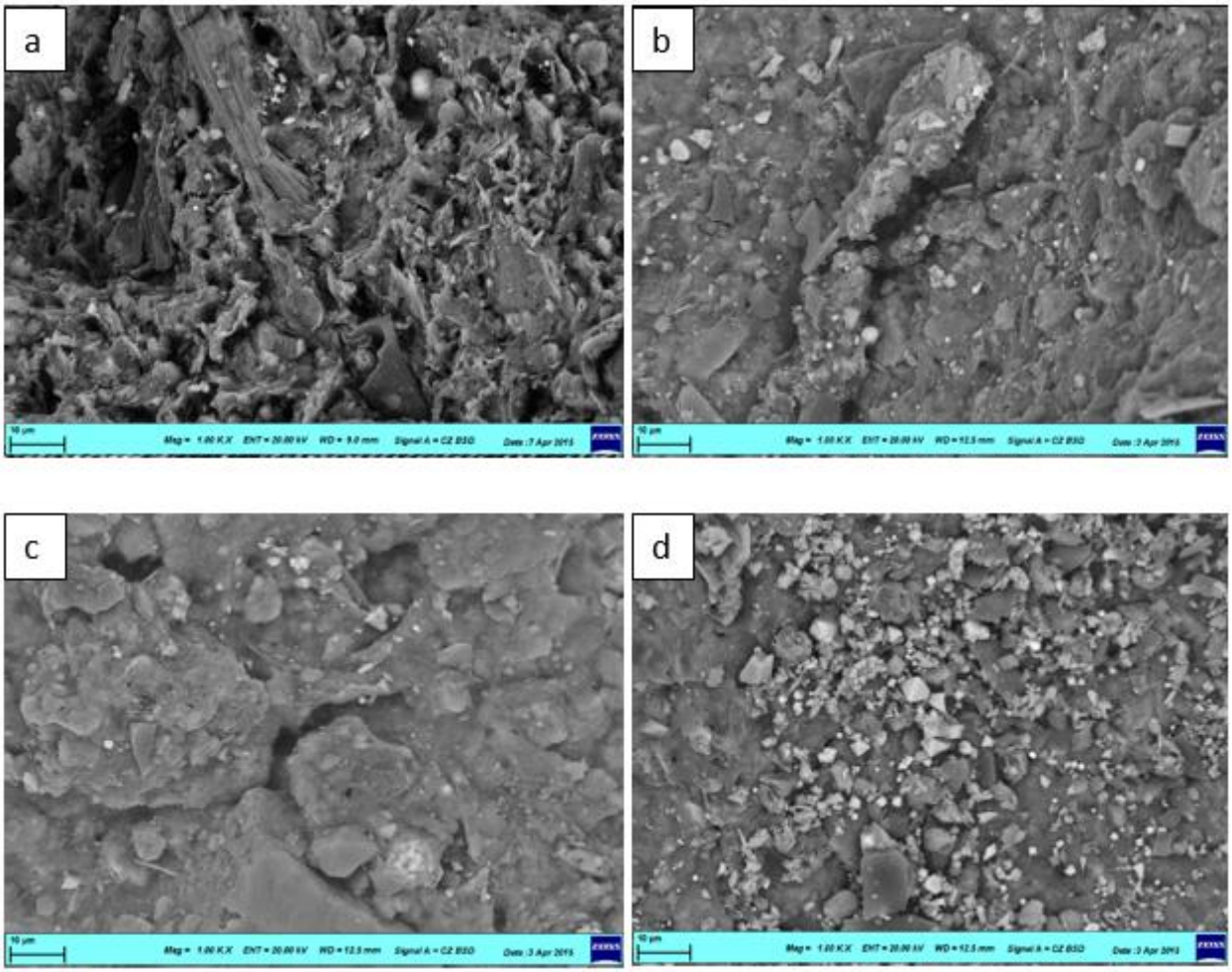

Figure 4.9, SEM images: (a) 5 cm height after 10 days (b) 45 height cm after 10 days (c) 15 cm height after 30 days (d) 45 cm height after 30 days

TD has an important influence on the permeability and diffusion of a porous medium (Cook and Hover, 1999; Ouellet et al., 2007). According to Fall et al. (Fall et al., 2005), an increase in fine particles leads to a reduction of threshold diameter. Based on MIP results, TDs of the samples from 45 cm and 15 cm heights of the monitoring column (30 days) were 0.4 of a micron and 0.5 of a micron, respectively, whereas the TD for the sample taken from the bottom of the 10 day column (5 cm) was around 3 μm. This difference in TD can be attributed to the high rate of evaporation, suction development and salt precipitation that made the pores finer; hence, the hydraulic conductivity of the MFTs decreased (Figure 4.13).

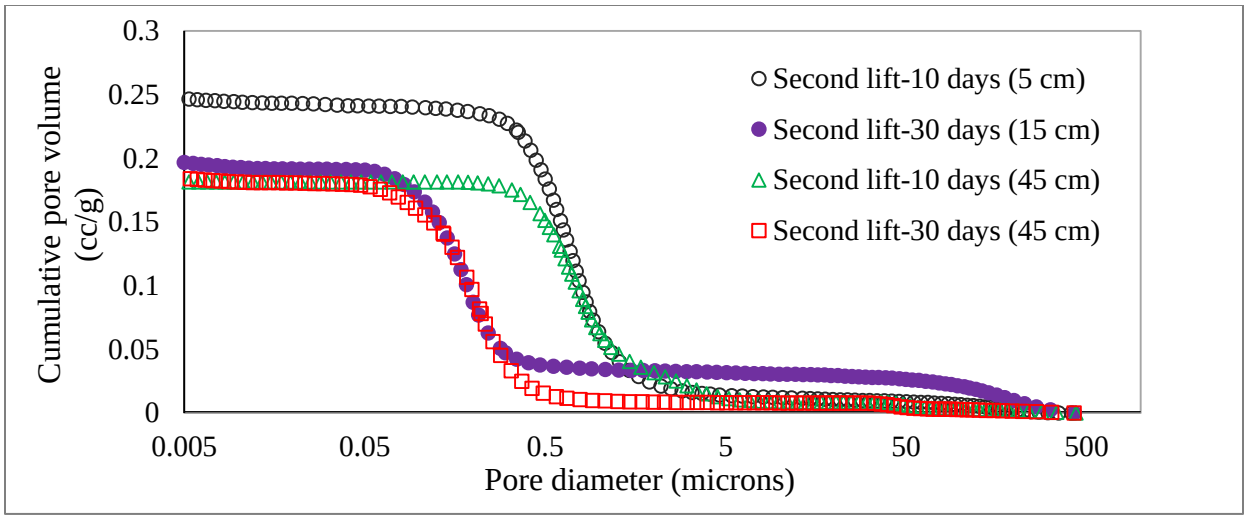

Figure 4.10, MIP test results for cumulative pore volume

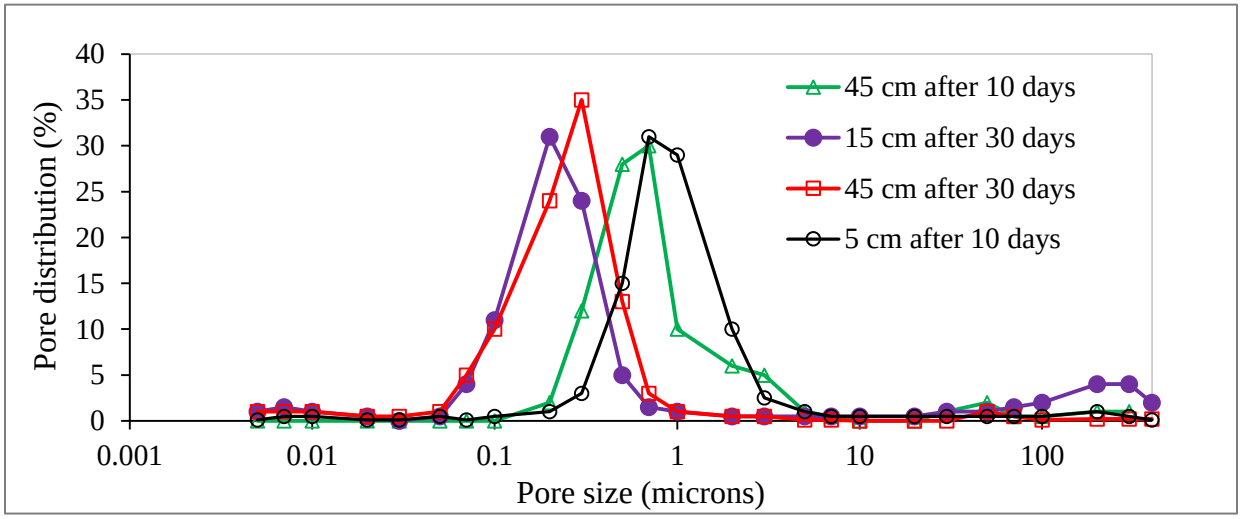

Figure 4.11, MIP test results for pore size distribution

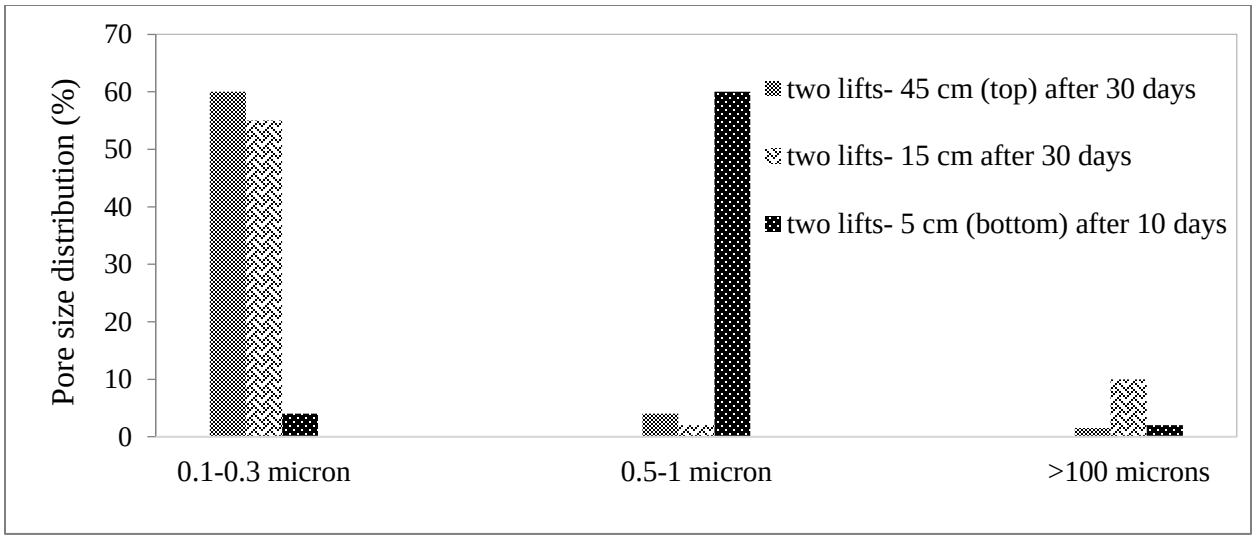

Figure 4.12, MIP test results for pore size distribution

4.3.5 Evolution of the hydraulic conductivity

The evolution of saturated hydraulic conductivity (k_{sat}) with column height is shown in Figure 4.13. Moreover, Figure 4.14 demonstrates the evolution of hydraulic conductivity for different void ratios within all the columns. From these figures, it can be seen that the values of k_{sat} decrease with void ratio reduction. This reduction in hydraulic conductivity can be attributed to the rearrangement of pores as a result of evaporation and suction development. At the top of the columns, by developing suction and increasing solid content, the soil matrix became dense and less permeable. Therefore, hydraulic conductivity dropped. While at the bottom, where the evaporation could not affect the suction, the connected void acted as a preferential channels for water to flow and caused a higher hydraulic conductivity. In Figure 4.13 it can be seen that the highest hydraulic conductivity was measured at the height of 35 cm after 10 days. Undeveloped suction at this height after 10 days (Figures 4.4 and 4.5) kept the voids connected for water flow. The measured void ratio for this height was 2.94, and that was the highest void ratio measured within all the samples. The inertia that must be overcome for changing the velocity from zero causes a time lag in reaching steady state inflow and outflow. This time lag has not been mentioned in this paper, and all the reported results are in a steady state condition. Hydraulic conductivity decreased from $2*10^{-7}$ cm/s at a void ratio of 2.94 to $4.1*10^{-9}$ cm/s at a void ratio of 0.67. This finding is in agreement with Suthaker and Scott (1996) who found that the hydraulic conductivity of MFTs decreases with decreasing void ratio.

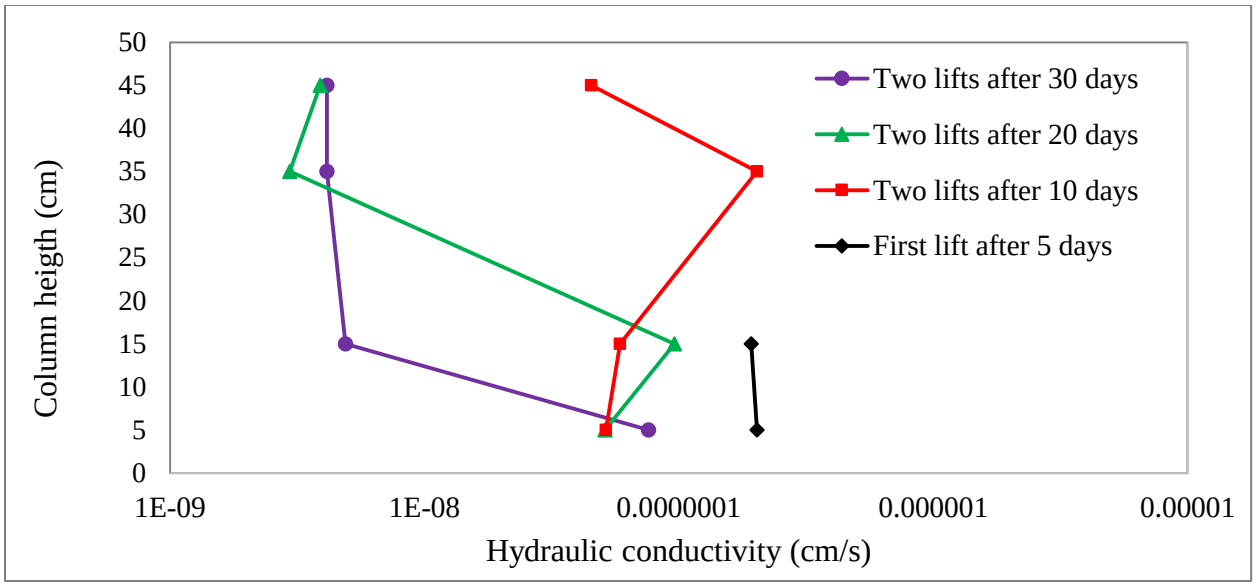

Figure 4.13, Saturated hydraulic conductivity with height

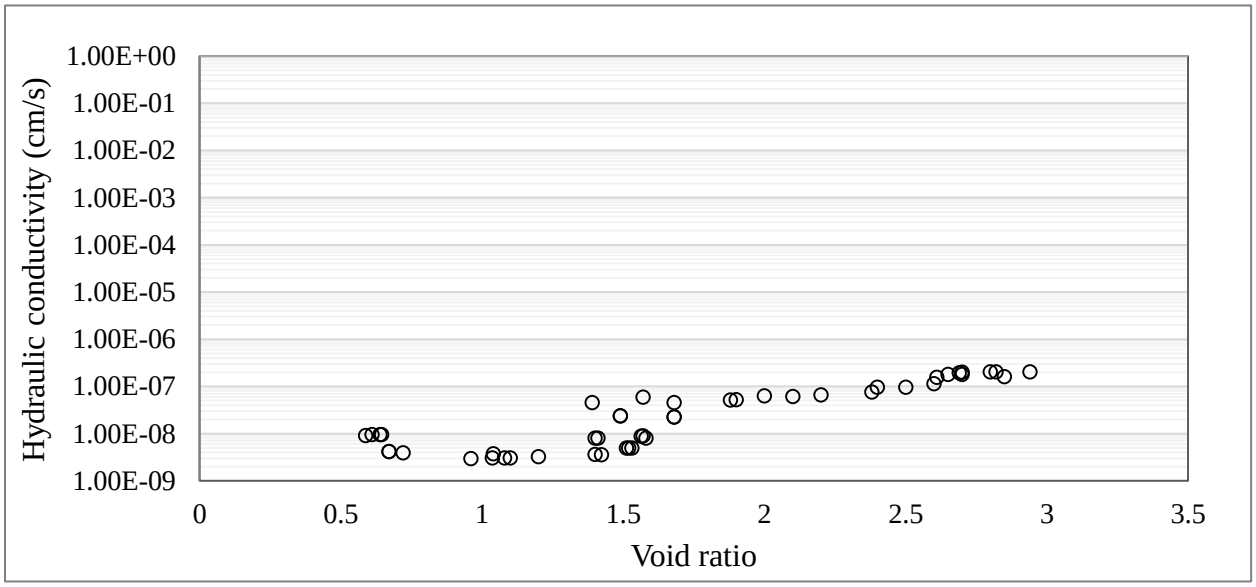

Figure 4.14, Evolution of the hydraulic conductivity with void ratio

4.3.6 Crack formation

Desiccation cracking results from induced stress by water loss through evaporation (Ayad et al., 1997; Tang et al., 2010; Tang et a;., 2011; Decarlo and Shokri, 2014). Hydrologically, desiccation cracks act as pathways for rapid water flow, and at higher plasticity indexes, excessive cracks may occur (Rayhani et al., 2007; Rayhani t al., 2008; Li and Zhang, 2011). Cracking and lateral shrinkage away from the walls were observed on day 3. Cracks again started to form after 2 days

of deposition of the second lift. The cracks were wide and deep enough to affect the water content of MFTs at height of 15 cm. To investigate the effect of evaporation on the morphology and length of cracks that are formed during the MFTs desiccation, imageJ was applied to segment the images into black and white (representing the crack and matrix, respectively). The extent of cracking was quantified by the crack intensity factor (CIF). CIF is defined as the time-dependent ratio of the crack area to the total surface area. Figure 4.15 shows the qualitative crack extension in the surface of the MFTs. As can be seen in Figure 4.15(a), suction in the top portion reached a level of 17 kPa at day 10 when the CIF was roughly calculated at 5%. After 20 days (Figure 4.15(b)), suction developed to around 500 kPa, and CIF was around 33%. After 30 days (Figure 4.15(c)), vertical settlement in half of the matrix was observed, and this made it impossible to calculate the crack surface with the software.

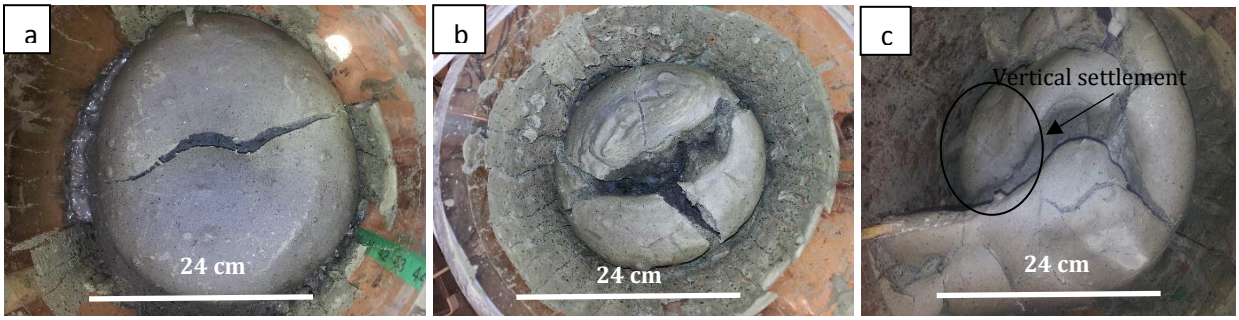

Figure 4.15, Crack formation a) after 10 days b) after 20 days c) after 30 days

4.4 Conclusions

The current paper presents hydraulic, chemical and microstructural properties of MFT in a two-lift deposition system under atmospheric drying as a long term disposal plan. After addition of the second lift, the water content of the first lift increased, and by elimination of the developed suction in the former lift, the strength decreased temporarily in the first layer. Crack extension, induced by sustained evaporation, developed suction in the second lift, along with the first lift (after 25 days). Precipitation of salt on the boundary surface formed a crust that restricted evaporation. With respect to the microstructural results, around 60% of the pore distribution at the top of the monitoring column ranged from 0.1 to 0.3 of a micron. In contrast, at the bottom of the 10 day columns, where evaporation could not affect the tailings, only 10% of the pores were in the range of 0.1 of a micron to 0.3 of a micron, and around 60% of the pores showed a 0.5–1 μm diameter.

Finer pores restricted the water flow, and consequently, hydraulic conductivity decreased. Hydraulic conductivity decreased from 2×10^{-7} cm/s at a void ratio of 2.94 to 4.1×10^{-9} cm/s at a void ratio of 0.67. In term of solid content, the height of 45 cm had a solid content of 99% after 30 days that resulted in the strength of 2 MPa whereas the solid content of the bottom (5 cm) was measured 57% with the strength of 500 Pa. The researchers believe that this study's findings indicate a highly effective process in the reclamation of DDAs which can provide industry-benefits. Despite the results obtained, it should be emphasised the effect of freeze-thaw, lift thickness, wind speed and wind direction should be addressed in future work.

Disclosure statement

No potential conflict of interest was reported by the authors.

4.5 References

Ayad, R., Konrad, J., and Soulie, M. (1997). Desiccation of a sensitive clay: application of the model CRACK. Canadian Geotechnical Journal, 34, 943–951.

Beier, N., Wilson, W., Dunmola, A., and Sego, D. (2013). Impact of flocculation-based dewatering on the shear strength of oil sands fine tailings. Canadian Geotechnical Journal, 50, 1001–1007.

BGC Engineering Inc. (2010). Oil sands tailings technology review. Oil Sands Research and Information Network, OSRIN Report No. TR-1.

Birle, E., Heyer, D., and Vogt, N. (2008). Influence of the initial water content and dry density on the soil-water retention curve and the shrinkage behavior of a compacted clay. Acta Geotechnical Journal, 3, 191–200.

Chalaturnyk, J., Scott, D., and Ozum, B. (2002). Mnagement of oil sands tailings. Journal of Petrolumn Science and Technology, 20(9-10), 1025-1046.

Cook, R., and Hover, K. (1999). Mercury porosimetry of hardened cement pastes. Cement and Concrete Research Journal, 29, 933–943.

Decarlo, K., and Shokri, N. (2014). Effects of substrate on cracking patterns and dynamics in desiccating clay layers. Journal of Water Resource Research, 50, 3039–3051.

Energy Resource and Conservation Board (ERCB), 2011. Government of Alberta.

Fall, M., Benzaazoua, M., and Ouellet, S. (2005). Experomental characterizaton of ther influence of tailings fineness and density on the quality of cemented paste backfill. Journal of Minerals Enginering, 18, 41- 44.

Farkish, A., and Fall, M. (2013). Rapid dewatering of oil sand mature fine tailings using super absorbent polymer (SAP). Journal of Minerals Engineering, 50–51, 38–47.

Fasking, T., Dunmola, A., Mckay, D., Masala, S., and Langseth, J. (2011). Bench scale drying of multi-layered thickened TSRU tailings. Proceeding in International Conference on Tailings, Edmonton, Canada, 2011.

Fisseha, B., Bryan, R., and Simms, P. (2010). Evaporation, unsaturated flow, and salt accumulation in multilayer deposits of "Paste" gold tailings. Journal of Geotechnical and Geoenvironmental Engineering, 136, 1703–1712.

Friedman, S. (2005). Soil properties influencing apparent electrical conductivity: a review. Journal of Computers and Electronics in Agriculture, 46, 45–70.

Fujimaki, H., Shimano, T., Inoue, M., and Nakane, K. (2006). Effect of a salt crust on evaporation from a bare saline soil. Vadose Zone Journal, 5, 1246-1256.

Fujiyasu, Y., and Fahey, M. (2000). Experimental study of evaporation from saline tailings. Jornal of Geotechnical and Geoenvionmental Engineering, 126, 18-27.

Jeeravipoolvarn, S. (2008). Sedimentation and consolidation of in-line thickened fine tailings. Proceedings in International Oil Sands Tailings Conference, Edmonton, AB, Canada, 1-14.

Jeeravipoolvarn, S., Scott, J. D., and Chalaturnyk, R. J. (2009). 10 M standpipe tests on oil sands tailings: Long-term experimental results and prediction. Canadian Geotechnical Journal, 46(8), 875–888.

Jordaan, S. (2012). Land and water impacts of oil sands production in Alberta. Journal of Environmental Science and Technology, 46, 3611–3617.

Junqueira, F., Sanin, M., Sedgwick, A., and Blum, J. (2011). Assessment of Water Removal from Oil Sands Tailings by Evaporation and Under-drainage, and the Impact on Tailings Consolidation. Proceedings in International Conference on Tailings and Mine Waste, Vancouver, BC, Canada.

Klein, C., Harbottle, D., Alagha, L., and Xu, Z. (2013). Impact of fugitive bitumen on polymer-based flocculation of mature fine tailings. Canadian Journal of Chemical Engineering, 91, 1427–1432.

Lee, I., Lee, H., Cheon, J., and Reddi, L. (2003). Evaporation Theory for Deformable Soils. Journal of Geotechnical and Geo-environmental Engineering, 129, 1020–1027.

Li, J., and Zhang, L. (2011). Study of desiccation crack initiation and development at ground surface. Journal of Engineering Geology, 123, 347–358.

Mikula, R., Kasperski, K., and Burns, R. (1996). Nature and fate of oil sands fine tailings. Journal of American Chemical Society. 677-723.

Miyamoto, H., Chikushi, J., and Kanayama, M. (2009). Coupled measurements of water content and electrical conductivity in dielectrically Lossy clay slurry using a coated TDR probe. Journal of Soils and Foundations, 49, 175–180.

Nachshon, U., Weisbrod, N., Dragila, M., and Grader, A. (2011). Combined evaporation and salt precipitation in homogeneous and heterogeneous porous media. Journal of Water Resources Research, 47, 1–16.

Ouellet, S., Bussière, B., Aubertin, M., and Benzaazoua, M. (2007). Microstructural evolution of cemented paste backfill: Mercury intrusion porosimetry test results. Cement and Concrete Research Journal, 37, 1654–1665.

Rao, S., and Revanasiddappa, K. (2005). Role of microfabric in matrix suction of residual soils. Journal of Engineering Geology, 80, 60–70.

Rayhani, M., Yanful, E., and Fakher, A. (2007). Desiccation-induced cracking and its effect on the hydraulic conductivity of clayey soils from Iran. Canadian Geotechnical Journal, 44, 276–283.

Rayhani, M., Yanful, E., and Fakher, A. (2008). Physical modeling of desiccation cracking in plastic soils. Journal of Engineering Geology, 97, 25–31.

Rogers, V, Wickstrom, M., Liber, K., and MacKinnon, M. (2002). Acute and subchronic mammalian toxicity of naphthenic acids from oil sands tailings. Journal of Toxicological Science, 66, 347–355.

Simms, P., Grabinsky, M., and Zhan, G. (2007). Modelling evaporation of paste tailings from the Bulyanhulu mine. Canadian Geotechnical Journal, 44, 1417–1432.

Siwik, P., Van Meer, T., MacKinnon, M., and Paszkowski, C. (2000). Growth of fathead minnows in oil sand processed wastewater in laboratory and field. Journal of Environmental Toxicology and Chemistry, 19, 1837–1845.

Suthaker, N., and Scott, J. (1996). Measurement of hydraulic conductivity in oil sand tailings slurries. Canadian Geotechnical Journal, 33, 642–653.

Suthaker, N., and Scott, J. (1997). Thixotropic strength measurement of oil sand fine tailings. Canadian Geotechnical Journal. 34, 974–984.

Tabbagh, A., and Cosenza, P. (2007). Effect of microstructure on the electrical conductivity of clay-rich systems. Journal of Physics and Chemistry of the Earth, 32, 154–160.

Tang, C., Cui, Y., Tang, A., and Shi, B. (2010). Experiment evidence on the temperature dependence of desiccation cracking behavior of clayey soils. Journal of Engineering Geology, 114, 261–266.

Tang, C., Cui, Y., Shi, B., Tang, A., and Liu, C. (2011). Desiccation and cracking behavior of clay layer from slurry state under wetting-drying cycles. Journal of Geoderma, 166, 111–118.

Timoney, K., and Lee, P. (2009). Does the Alberta tar sands industry polute? The scientific evidence. Journal of Open Conservation Biology, 3, 65-81.

Yao, Y., Tol, F., and Paassen, L. (2012). The effect of flocculant on the geotechnical properties of mature fine tailings: an experimental study. Proceeding in the 3rd International Oil Sand Tailings Conefernce, Edmonton, Canada, 391–398.

5 Drying behavior of mature fine tailings pre-dewatered with superabsorbent polymer (SAP): Column experiments

Anis Roshani, Mamadou Fall, Kevin Kennedy
Geotechnical Testing Journal 40(2): 210-220**.**

ABSTRACT

Laboratory column experiments were conducted to investigate the effect of superabsorbent polymer (SAP) on the drying behavior (dewatering, strength, suction, settlement) of mature fine tailings (MFTs). Four experimental columns, filled in two stages with dewatered MFTs of 1% (wt) SAP, were atmospherically dried, as were four additional columns (controls) filled with raw MFTs (not pre-dewatered with SAP). The rate of evaporation, drainage, settlement and evolution of suction, strength, and void ratio were monitored over 30 days. The results show that the rate of evaporation for SAP from pre-dewatered samples was lower than that of raw MFTs. Cumulative water lost via evaporation decreased from 13 kg for raw MFTs to 7.2 kg for pre-dewatered MFTs, due to the latter's lower water content. Water drainage for pre-dewatered MFTs showed an 82% reduction in comparison with raw MFTs, suggesting that the use of the SAP pre-dewatered method could considerably reduce seepage of toxic water from tailings and MFTs impoundments. Suction developed in the first lift showed a sharp reduction when loading the second lift due to redistribution of pore water, but this was temporary and suction in the second lift gained strength. Vane shear strength of pre-dewatered MFTs after 30 days was around 3.6 kPa and 7.3 kPa for 5 cm (bottom) and 15 cm heights respectively, and the upper parts' strength reached 2.3 MPa. SAP pre-dewatered MFTs had a much higher strength increase rate at early stages than raw MFTs. After 10 days drying, the undrained shear strength at all column depths exceeded or closely matched the one-year value (5 kPa) required by environmental regulations (ERCB). This could have significant practical implications with respect to acceleration of the dewatering process and consolidation of MFTs, increasing the pace of reclamation and reducing the cost of tailings management and heavy oil operations' environmental footprint.

Keywords: Mature fine tailings; Environment; Superabsorbent polymer; Contamination; Dewatering.

5.1 Introduction

The 1760s saw the first discovery of oil sand in Fort McMurray, northern Alberta. The high consumption of fossil fuel and requirement for different forms of energy have prompted the expansion of this industry throughout the state. To extract the oil sand, a process called the Clark Hot Water Process (CHWP) is applied, in which hot water is added to the sand to wash off the bitumen (Clark and Pasternack, 1932). Oil extraction and upgrading lead to the production of large volumes of liquid and solid waste materials (known as "whole tailings"), consisting of water, sand, silt, clay, and residual bitumen. This is discharged into an engineering dam as a settling basin or storage container known as a tailings pond, where it undergoes segregation. Sand fractions form beaches, with around 50% of the total mass of fine particles becoming trapped within the sand matrix. The dispersive nature of the oil sand extraction process affects the settling properties of the remaining particles, which are referred to as mature fine tailings (MFT), and over the course of a few years, the solid content of MFTs reaches around 30%-35%; full consolidation takes thousands of years (Mikula et al., 1996). Toxicity, risk of seepage, and uncertainties over their lifespan are controversial environmental impacts associated with oil sand tailings ponds (Jordaan, 2012). The nature and quality of the produced waste materials therefore call for the development of acceptable reclamation options.

Operators are actively considering thin-lift drying as a tailings management approach. In this method, the successive deposition of oil-sand tailings in thin lifts can maximize the influence of evaporation on the dewatering process, as well as accelerating the reclamation of land. However, the placement of new lifts redistributes water into lower layers and acts as a barrier to cut off the evaporation from previous lifts. Accordingly, thin-lift placement cannot be applicable if the addition of a new layer causes a reduction in the strength of underlying lifts. Various studies have addressed the combined effect of chemical processes (such as coagulation and flocculation) and natural processes (such as evaporation and freeze-thaw) to increase the strength of MFTs (Beier et al., 2013; Fasking et al., 2011; Yuan and Shaw, 2007; Jeeravipoolvarn, 2008). As a chemical amendment, the application of a novel dewatering technique using superabsorbent polymer (SAP) in the oil sand industry was investigated in 2013, and it was found that rapid dewatering and densification of MFTs was achieved and a significant strength increase was obtained (Farkish and Fall, 2013).

Hydrophilic gel, which consists of a network of polymer chains, exhibits the ability to swell in contact with solution and retains the solution within its structure. There is a special hydrogel called superabsorbent polymer (SAP), whose application in hygiene products is well known (Zohuriaan-mehr and Kabiri, 2008; Pó, 1994). In addition, its excellent water-absorbing properties and water retention capability have underpinned its use in a wide range of applications. SAP is used in many other areas, including agriculture, toys, tools, building, interior decoration, cryogenic gels, food and meat packaging, concrete strengthening, and reduction of ground resistance in the electrical industry (Zohuriaan-mehr and Kabiri, 2008; Pó, 1994; Schröfl et al., 2012). Masuda and Iwata (1990) applied highly water-absorbent polymer to the dewatering of coal, activated sludge, metal plating sludge, and clay. They found that the final water content for all of these materials was lower than that achieved by centrifugal treatment. Meanwhile, Kuai (1999) studied the effect of SAP on the drying of primary domestic sludge. In this study, mixing 1% of polymer with the sludge reduced the water content from 96% to 8.5% after less than a week, while for the control sample (without SAP) it took much longer. Elsewhere, Dzinomwa et al. (1996) proved that moisture content reduction of fine coal from 29% to around 12% can be achieved by mixing 1% of SAP within a contact time of four hours. In a similar study by Peer and Venter (2003), a 70% water reduction of fine coal was achieved by using SAP. Another team, Fall et al. (2010) investigated the potential use of densified polymer-pastefill (PP) mixture as waste containment barrier materials and showed that the hydraulic conductivity of PP decreases as the content of SAP increases. In addition, the absorption capacity of SAP for MFTs water was confirmed by Farkish and Fall (2013, 2014). These authors applied SAP to produce a dense MFTs with high shear strength, finding that mixing MFTs with 1% SAP can increase solid content from 40% to 70% in seven days. In this process, shear strength rose to around 2.5 kPa. However, the first study by Farkish and Fall (2013) considered only MFTs samples of small size, with multi-layer deposition of MFTs excluded. To date, no study has tackled the combined effect of atmospheric drying and SAP in multi-layer deposition of MFTs. This inspired the current authors to conduct the research at hand, using column experiments to study the evolution of the physical, mechanical, and hydraulic properties of dewatered MFTs with SAP in two-lift deposition. The findings may lead to a better understanding of the behavior of MFTs when pre-dewatered with SAP in order to achieve the sustainable development of the oil sand industry while meeting the Directive 074 (environmental) requirements.

5.2 Experimental program

5.2.1 Material

5.2.1.1 Tailings (MFT)

Mature fine tailings was delivered from an Alberta oil sand company and subjected to a range of mineralogical and physical tests. The tailings was composed of around 18% clay (≤ 2 micron), 81% silt (2 micron < Ø ≤ 75 micron), and less than 1% sand (75 micron < Ø ≤ 2.3mm). The proportion of fines (< 44 micron) was 95%. Initial solid content was measured at around 45%, while organic content accounted for 18%. The average specific gravity of the tailings was 2.37; bitumen with a specific gravity of about 1.03 is considered part of the fine solids, and results in a fairly low specific gravity of the total solids compared with other natural clay soils (Jeeravipoolvarn et al., 2009). The liquid limit (LL) and plastic limit (PL) of the MFTs were 51.2 and 37.2, respectively (Farkish and Fall, 2013). Accordingly, the plasticity index (PI) was equal to 14 and activity (A) was 0.77 (considered as normal clay). The mineralogy of the clay component was 33.6% quartz, 31.3% kaolinite, and 21.8 % muscovite (Farkish and Fall, 2013). Among the clay minerals, montmorillonite has the highest affinity to water and swells when hydrated, while illite has poor affinity to water and kaolinite has none, and minimal swelling characteristics (Chalaturnyk et al., 2002).

5.2.1.2 Superabsorbent polymers

A superabsorbent polymer (SAP) is a high molecular weight, cross-linked hydrophilic network that can absorb and retain huge amounts of water or aqueous solutions as high as 10-1000 grams per gram of polymer. Traditional absorbent materials (such as tissue papers and polyurethane foams), unlike SAPs, will lose most of their absorbed water when squeezed under pressure. This is not the case for SAP, because the water-imbibing mechanism of these polymers entails the physical entrapment of water via capillary forces in their macro-porous structure and the hydration of functional groups (Zohuriaan-mehr and Kabiri, 2008). When the powder is dry, the polymer chains are coiled. When hydrated, the sodium ion detaches so that the carboxyl groups (CO_2H) become negatively charged and repel one another to uncoil the polymer chain, allowing a greater amount of water to associate with more carboxyl groups or sodium atoms (Hu et al., 2004) and polymer inflates. Acrylic acid (AA) and its sodium or potassium salts and acrylamide (AM) are most frequently used for SAPs in industrial production. The commercially available Aqua Sorb

polymer, which is granularly cross-linked to insoluble sodium poly-acrylates with a free swell capacity of 250 g/g in deionized water, was used in this study. According to Farkish and Fall (2013, 2014), who used the same polymer in their studies, 1 gram of SAP can absorb 107 g of MFTs water. After hydration, transparent gel-like millimetre-sized crumbs are formed. The hydration of the polymer is fully reversible.

5.2.2 SAP preparation and mix proportions

The requisite amount of SAP (1% weight of MFTs) was mingled with MFTs in a mixer. A water-permeable cloth was used to prepare the bags that would hold the SAP. Each bag contained 10 g of SAP, and these sachets could draw out the water from the tailings and swell several times in size. Use of the sachets solved the problem of separation of the polymer from the MFTs. The MFTs slurry was combined with the SAP sachets using a mixer for 30 minutes per day over a six-day period. The solid content and vane shear strength were measured daily, and it was found that the solid content reached around 63% (vane shear strength of 2.5 kPa) after six days. Therefore, after this point, the SAP sachets were removed and the pre-dewatered MFTs with SAP was loaded in the columns (as the first or second lift) to continue the drying process under atmospheric conditions.

5.2.3 Developed experimental setup

Figure 5.1 presents a schematic diagram of the developed experimental setup of the columns, which had an inner diameter of 25 cm and height of 55 cm. At the bottom of each column, a thin layer of sand was placed for drainage. This layer was separated from the MFTs deposit by a perforated plate covered by a coarse filter paper. In total, four columns were run over the elapsed times of 5, 10, 20, and 30 days. According to Figure 5.1, the first lift (25 cm) was added to all four columns. After 5 days, column d was ready to take samples from two different depths of 5 cm and 15 cm; at the same time, the second lift was added to the other three columns (25 cm). Five days later (5 days after loading the second lift or 10 days from the beginning), column c was dismantled to take samples at 5 cm, 15 cm, 35 cm, and 45 cm. After 15 days (15 days after loading the second lift or 20 days from the beginning of the test), samples were taken from different heights of column b. In the final stage (after 30 days), column a (the monitoring column) was stopped to take samples. The tops of the columns remained open and exposed to the environment. A fan was placed on top of

each column to simulate wind on the site. Each fan was positioned to provide an equal distance from the tailings surface after the addition of each lift.

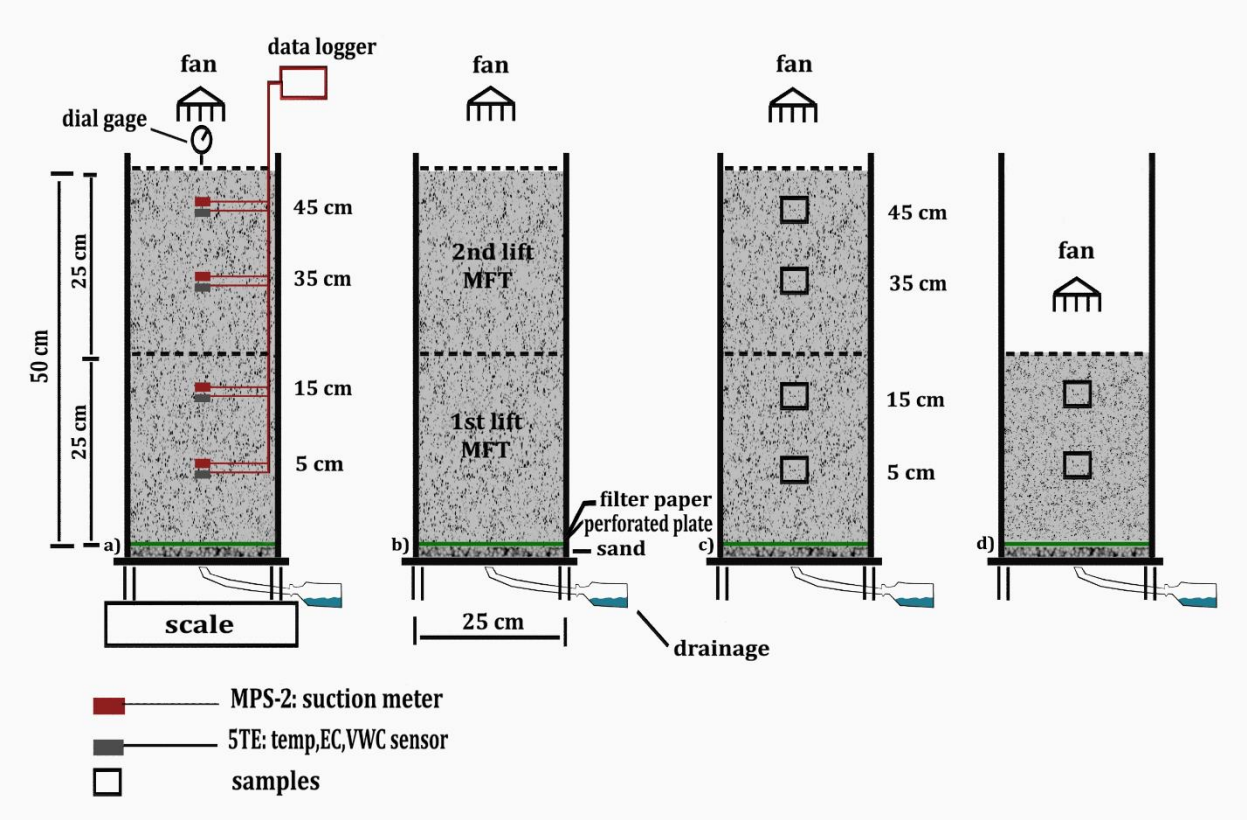

Figure 5.1, Schematic diagram of the experimental setup: (a) arrangement of the sensors and dial gauge – second lift 30 days, (b) filling sequence – second lift 20 days, (c) sampling locations – second lift 10 days, (d) first lift 5 days

The monitoring column was equipped with various sensors. It contained four MPS-6 sensors (Decagon Devices Inc.), four 5TE sensors (Decagon Devices Inc.), and a dial gauge (3062S-19, Mitutoyo Co.) for measuring the settlement. MPS-6 sensors measure suction (negative pore water pressure) and temperature. This sensor is able to measure suction in the range of 10 to 100,000 kPa with an accuracy of $\pm$0.25 kPa, and can record temperature in the range of -40℃ to 60℃ with an accuracy of $\pm$1℃. It is composed of a moisture content sensor and a porous substrate with a known moisture release curve. After the porous material has equilibrated with the surrounding soil (MFTs), the moisture sensor measures the former's water content and uses the moisture release curve to translate moisture content into water potential. The 5TE sensor, meanwhile, measures electrical conductivity (EC) in the range of 0-23 dS/m with an accuracy of $\pm$0.1. This sensor also

measures volumetric water content (VWC) in the range of 0-80% with an accuracy of ± 0.01 from 1-40% and an accuracy of ± 0.15 from 40-80%. In total, eight sensors were installed at heights of 5, 15, 35, and 45 cm, and were connected to a data logger to record and collect the data. To measure the self-weight settlement as well as drying shrinkage due to evaporation, a dial gauge was installed at the top immediately after casting the second layer. The assumed filling strategy was two stages of filling (25 cm each). Five days after casting the first layer, the second lift was added. Each column was allocated to one elapsed time. After each time period had elapsed: 5 days (column d), 10 days (column c), 20 days (column b), and 30 days (column a), the relevant column was dismantled and samples were taken from four different depths to conduct the tests. Design locations of the sensors and the location of obtained samples are illustrated in Figure 5.1.

The monitoring column was mounted on the scale. The mass of water lost in the monitoring column by evaporation and drainage was obtained by measuring the mass of the column on an approximately daily basis using the scale OHAUS Defender, with readability of 0.01 kg. The initial mass of soil was recorded before evaporation and drainage were permitted. The mass of the container and tailings was measured regularly over the 30-day period and compared with the initial mass.

5.2.4 Mechanical test

A vane shear test was conducted to determine the strength of the MFTs samples according to ASTM D4648. The concept underpinning the test was to measure the torque required to shear the sample by the vane. The required turning moment to shear the soil was as follows:

$$T = \tau \times K \qquad (5.1)$$

Where:

T = torque (N.m)

τ = undrained shear strength (Pa)

K = vane blade constant (m^3),

$$K = \frac{\pi D^2 H}{2\times 10^9}\left[1+\frac{D}{3H}\right] \qquad (5.2)$$

Where:

D = measured diameter of the vane (mm)

H = measured height of the vane (mm)

The vane shear test was performed on MFT specimens sampled from the columns. Undisturbed cylindrical specimens were taken from four different heights of each column. These had a sufficient diameter to allow clearance of at least two blade diameters between all points on the circumference of the shearing surface and the outer edge of the sample.

5.3 Results and discussion

5.3.1 Evaporation, drainage, and settlement behavior

5.3.1.1 Evaporation

The water removal process for oil sand tailings was controlled by evaporation rather than drainage (Junqueira et al., 2011). In general, evaporation from a soil surface occurs in three stages (Wilson, 1994). Initially, water is freely available on the soil surface and the rate of evaporation is limited by environmental factors. When the surface becomes unsaturated, the water supply to the surface becomes increasingly restricted and the rate of evaporation therefore begins to decline as an indicator of the onset of the second stage of evaporation. Eventually, the decreasing trend of the evaporation rate reaches a low residual value; this is the third stage of evaporation. Figure 5.2 shows a comparison between the evaporation processes of raw MFTs and MFTs pre-dewatered with SAP. The initial rate of evaporation for both was almost the same, and equal to around 0.055 kg/hr. A decreasing trend of evaporation was observed in the first five days after placing the first lift, due to the start of the second stage in which the conductive properties of the soil (MFTs) prevented the flow of sufficient water to the surface. Before loading the second lift, the evaporation rate fell to 0.012 kg/hr and 0.02 kg/hr for de-watered and non-dewatered MFTs, respectively. By adding the second lift, the evaporation rate for both samples reached an initial value of 0.05 kg/hr. Initial water content for pre-dewatered MFTs was around 57%, while for raw MFTs it was around 130%. Fluctuations in the rate of evaporation, particularly in the first four to five days of each lift, were a result of cracks that developed, exposing more evaporating surfaces. The value for residual evaporation rate for raw and pre-dewatered MFTs was measured as 0.007 kg/hr and 0.005 kg/hr, respectively. Cumulative water loss due to evaporation, for MFTs pre-dewatered with SAP,

showed a 56% reduction in comparison with raw tailings, from a 12.9 kg water loss in raw MFTs to around 7.2 kg in pre-dewatered MFTs. This decrease is due to the lower initial water content of pre-dewatered MFTs and its lower extended cracks, which reduce the flow ability of pore water toward the evaporating front.

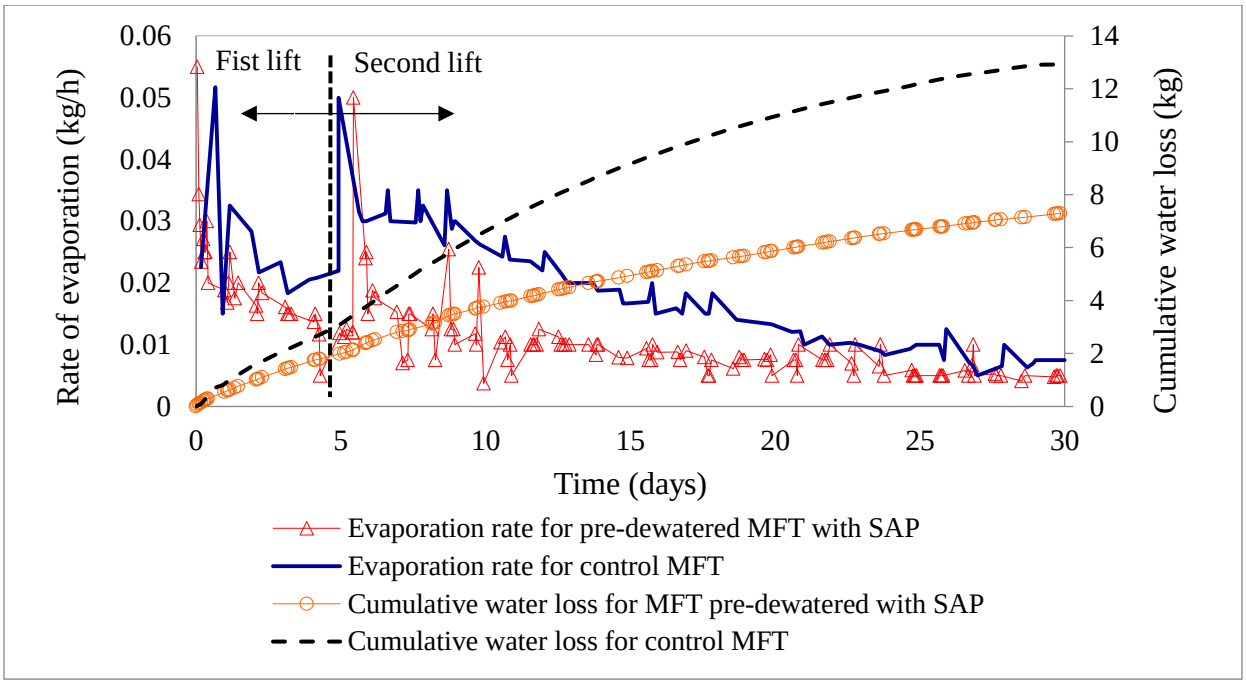

Figure 5.2, Rate of evaporation and cumulative water loss for pre-dewatered MFTs with SAP and raw MFTs

5.3.1.2 Drainage

Tailings pond seepage is one of the main concerns of this industry, due to the proximity of the ponds to key water bodies, notably the Athabasca river. A seepage rate of 11 million L/day has been publicly reported (Environment Defence, 2008), while increased levels of polycyclic aromatic hydrocarbons (PAHs) and pore water metal in the Athabasca are indicators of tailings pond seepage (Timoney and Lee, 2009). Figure 5.3 shows the drainage rate and cumulative drainage for the two-lift MFTs deposition in our study, with and without SAP. A maximum rate of 12 gr/h was measured in the first lift before placement of the second for the raw MFTs (initial water content of 130%), whereas the rate of drainage for pre-dewatered MFTs deposition (initial water content of 50%) was almost zero in the first five days. The addition of the second lift of raw MFTs increased the water content of the first lift; in particular, the dry top portion of the former

lift. Therefore, the rate of drainage was less than that for the first five days. From day 20 to the end of the test period, no drainage was observed for pre-dewatered MFT with SAP. Cumulative water loss through drainage was 820 gr for raw MFTs, while total drainage for pre-dewatered MFTs was measured at 150 gr, denoting an 82% reduction in total drainage. These findings point to the ability of SAP to absorb and retain MFTs-processed water, and thus to significantly reduce drainage water, suggesting that the use of the SAP pre-dewatered method could considerably mitigate the seepage of water from tailings and MFTs impoundments and remediate the associated environmental issues mentioned above.

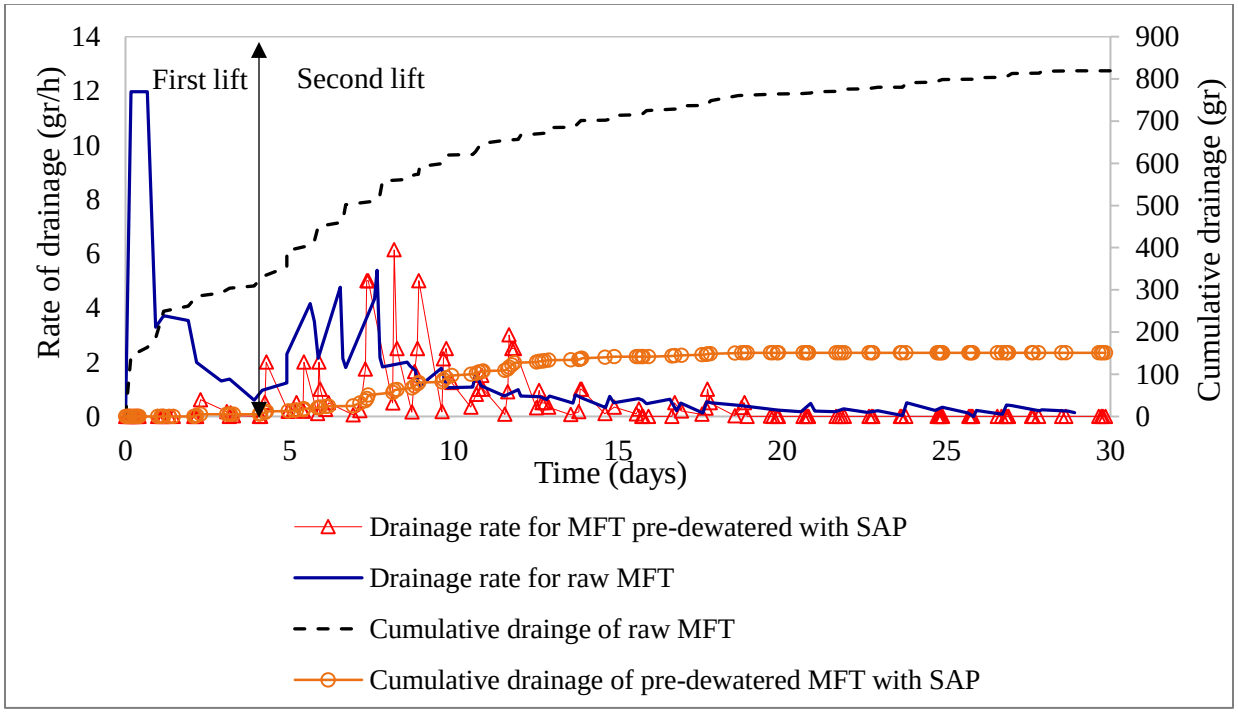

Figure 5.3, Drainage rate and cumulative drainage for the first and second lift

5.3.1.3 Settlement

Water loss from the surface of the MFTs resulted in volume shrinkage, which induced its vertical settlement and the generation of vertical cracks in its upper layer. After these cracks were initiated, they propagated downward, forming cracked MFTs columns. Figure 5.4 shows the evolution of the settlement of MFTs dewatered with SAP. According to the presented results, the maximum rate of settlement was observed in the first four to five days after loading the second lift, where the suction developed and attained more than 500 kPa (Figure 5.5). Cumulative vertical settlement was measured at around 3.5 cm after 30 days, while total settlement after 10 and 20 days was about 2.4

and 3.3 cm, respectively. Most of the crack formation and expansion occurred in the first five days, and after this time, the reduction in thickness decelerated. The generation of the observed vertical cracks can be explained by the fact that the desiccation-induced shrinkage of the surface layer of the MFTs caused an increment of horizontal tensile stress. The MFTs cracks when the tensile stress that develops within it exceeds its tensile strength. Similar observations have been made for other types of soils in several previous studies (Rayhani et al., 2007; Rayhani et al., 2008; Peron et al., 2009; Fisseha et al., 2010; Li and Zhang, 2011; Tang et al., 2011; Shokri et al., 2015). For example, Peron et al. (2009) found that moisture content gradient builds up tensile stress, until by sustained water loss at a critical point, the tensile strength is reached. By setting up the tensile strength induced by suction development, cracking occurs on the upper soil layer (Peron et al., 2009; Shokri et al., 2015).

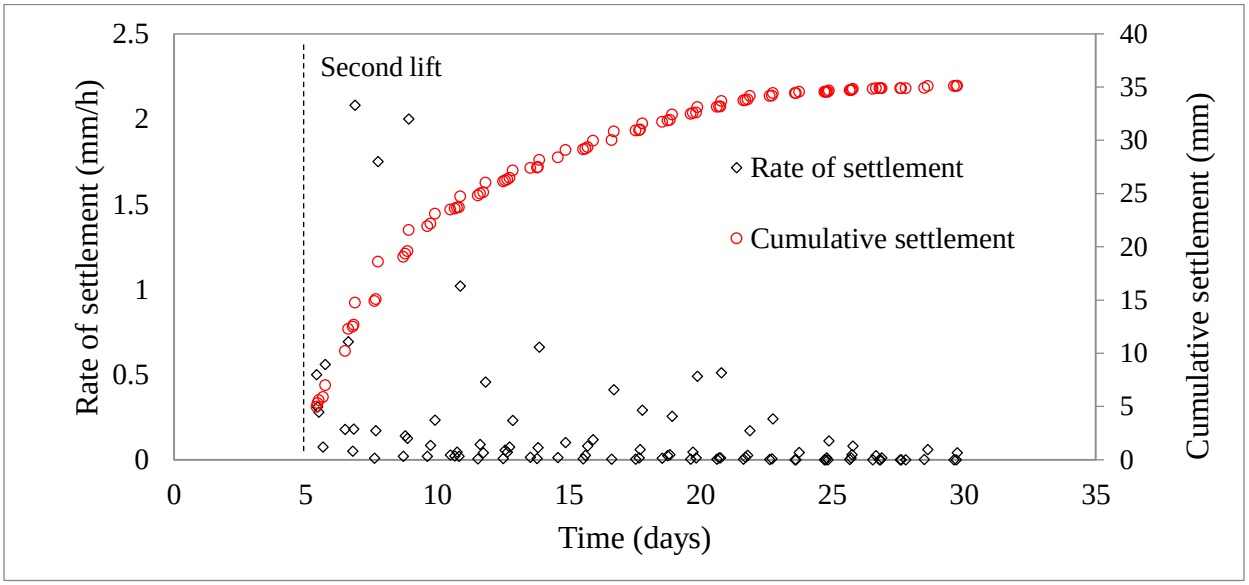

Figure 5.4, Rate of settlement and cumulative settlement of MFTs pre-dewatered with SAP after loading the second lift

5.3.2 Suction evolution

Figure 5.5 shows the suction versus height and time for two different columns filled with MFTs pre-dewatered with SAP and raw MFTs. For a better understanding of the developed suction in the first lift of both the pre-dewatered and raw MFTs columns (due to lower values), Figure 5.6 illustrates the evolution of the suction in the first lifts without considering the second lifts. Continual evaporation within the first five days (before casting the second lift) increased the

effective stress in the MFTs' matrices. Consequently, the suction on the top portion of the first lift (15 cm) for the MFTs pre-dewatered with SAP (initial water content of 50%) reached around 25 kPa, while the maximum developed suction in the raw MFTs (initial water content of 130%) for this time period was around 16 kPa. After adding the second lift, a sharp reduction in suction was observed, due to the drainage of pore water from the freshly added layer to the layer beneath. At the end of the test period, extended cracks in the raw MFTs' deposition, which penetrated deeply within the second lift, affected the top part of the first lift (15 cm) and suction increased to around 20 kPa at this height. Suction on the top of the pre-dewatered MFTs column (45 cm) increased sharply to more than 500 kPa within four days after loading the second lift, but at the height of 35 cm, the cracks grew more rapidly in raw MFTs, causing faster suction development at this height in comparison with pre-dewatered MFTs. The less extensive generation of cracks in pre-dewatered MFTs is mainly due to two factors. First, geochemical analyses performed on samples extracted from the upper layers of the desiccated pre-dewatered and raw MFTs revealed that a higher concentration of salt accumulated on the surface of the pre-dewatered MFTs in comparison with its raw counterpart. For example, the concentration of Na^+ for pre-dewatered MFTs at the surface after 30 days was around 3,600 ppm, while for the raw variety it was equal to 2,083 ppm. Concentrations of Mg^{2+} and K^+ for pre-dewatered MFTs after 30 days' drying were measured at 6,72 ppm and 12,85 ppm respectively, whereas raw MFTs had lower concentrations of both Mg^{2+} (4,71 ppm) and K^+ (8,39 ppm). A higher salt concentration decreases the rate of evaporation by reducing the driving force that downgrades the crack expansion (Fisseha et al., 2010; Shokri et al., 2015). Additionally, the much higher initial vane shear strength (2.5 kPa) of pre-dewatered MFTs results in a higher tensile strength and, consequently, a greater resistance to cracking.

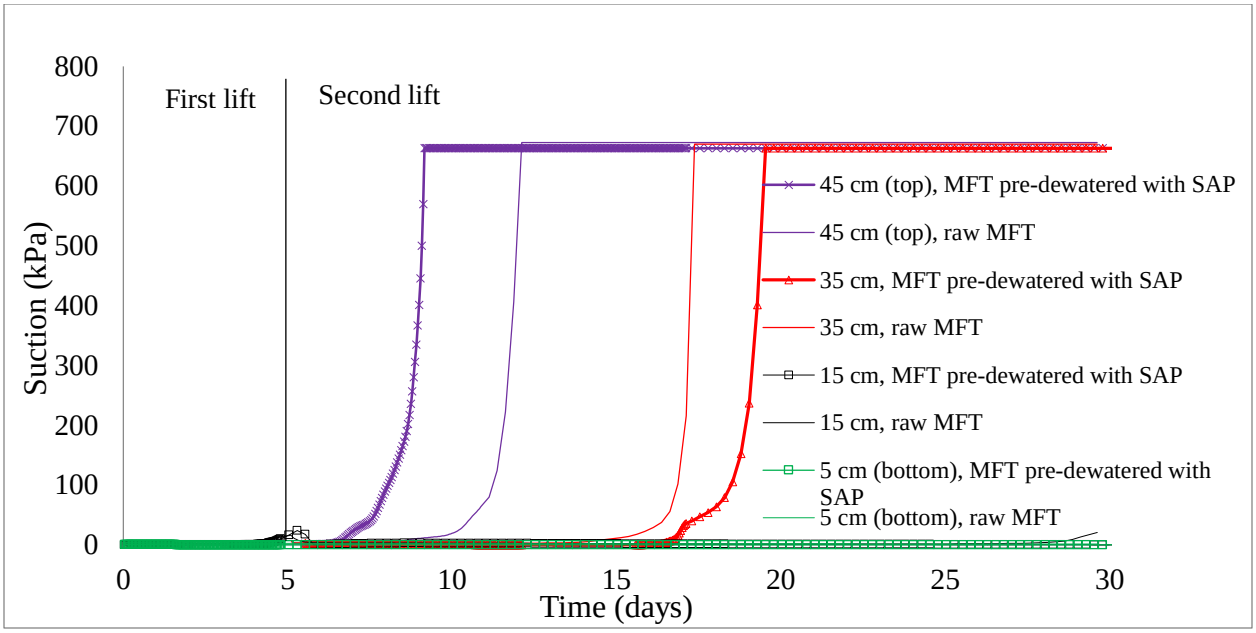

Figure 5.5, Suction evolution with respect to time and height

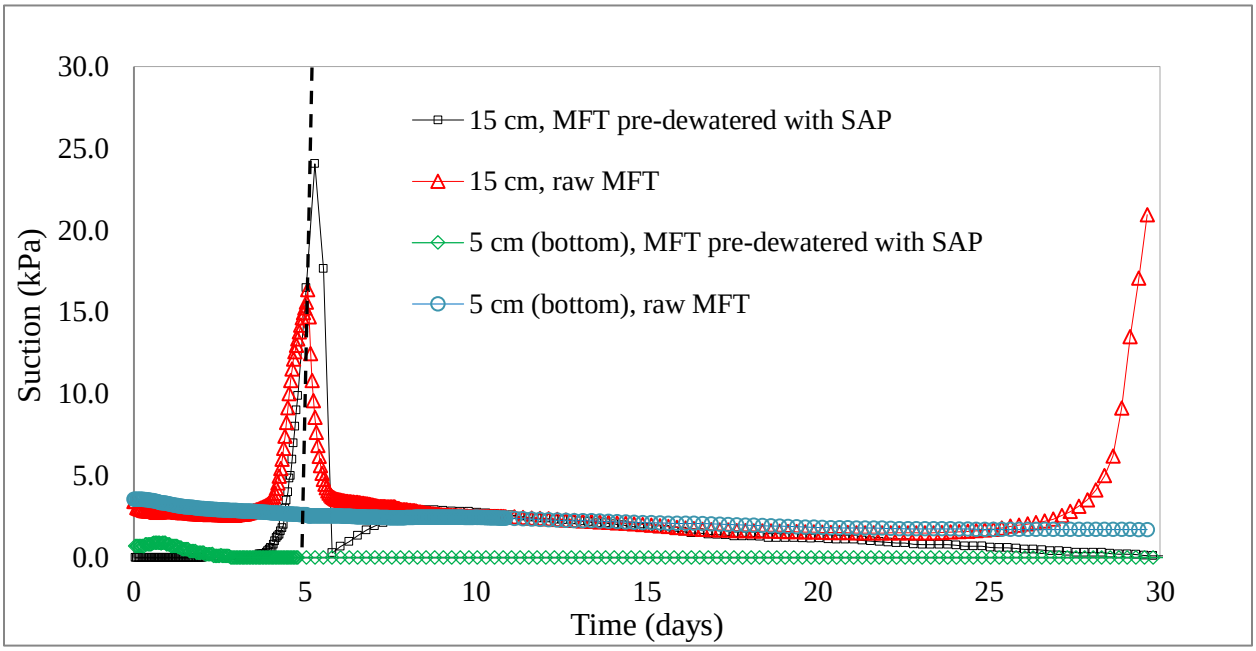

Figure 5.6, Total suction for the first lift of SAP for pre-dewatered and raw MFTs

5.3.3 Shear strength evolution

In order to meet directive 074 set by the ERCB, it is necessary to remove sufficient water from oil sand tailings to increase its solid content and, consequently, its strength. To illustrate the impact of pre-dewatering by SAP on MFTs strength, vane shear strength of pre-dewatered and raw MFTs

are compared in Figure 5.7 (a, b, and c). Raw MFTs exhibits very low initial strength (in the range of Pascal) at a solid content range of around 40-45%, while MFTs pre-dewatered by SAP with solid content of around 60-65% showed an initial strength of 2.5-2.8 kPa. According to Figure 5.7a, by loading the pre-dewatered MFTs into the column, atmospheric drying on top (45 cm) caused a higher increase in strength while MFTs unaffected by evaporation showed a negligible such increase in comparison, with an initial value of 2.5 kPa. The strength was measured as 3,100 Pa at the bottom (5 cm) and 3,700 Pa at a height of 35 cm. This slight increase may be due to self-weight and drainage. After 20 days (Figure 5.7b), the strength at heights of 45 cm, 35 cm, 15 cm, and 5 cm reached 2.3 MPa, 48 kPa, 6.3 kPa, and 3.3 kPa respectively. At this point, raw MFTs had a much lower strength. For example, at the height of 5 cm it had 400 Pa strength, while at a depth of 15 cm it was measured as 1,100 Pa. After 30 days (Figure 5.7c), because of suction development (Figures 5.5 and 5.8) and void ratio reduction, around 90% of both the pre-dewatered and raw columns showed a strength of more than 7 kPa. Vane shear strength of the lower part (5 cm) of the column filled with pre-dewatered MFTs attained 3.6 kPa, whereas the strength of raw MFTs was measured as only 400 Pa for the same height. Figure 5.8 shows the variation in strength with respect to the suction development for two different depths of 35 cm and 45 cm. As can be seen, by increasing suction, pore water pressure decreases and effective stress builds up; consequently, strength in the upper heights of the column increases (Vanapali et al., 1996; Tekinsoy et al., 2004; Kayadelen et al., 2007; Nasir and Fall, 2010).

MFTs pre-dewatered with SAP had a much higher strength increase rate at early stages. It can be observed from Figure 5.7a that after 10 days of drying, the undrained shear strength at all column depths exceeds or is close to the one-year value required by the ERCB (5 kPa). This may have significant practical implications with respect to accelerating the dewatering process and consolidation of MFTs, thereby increasing the pace of reclamation and reducing the cost of tailings management.

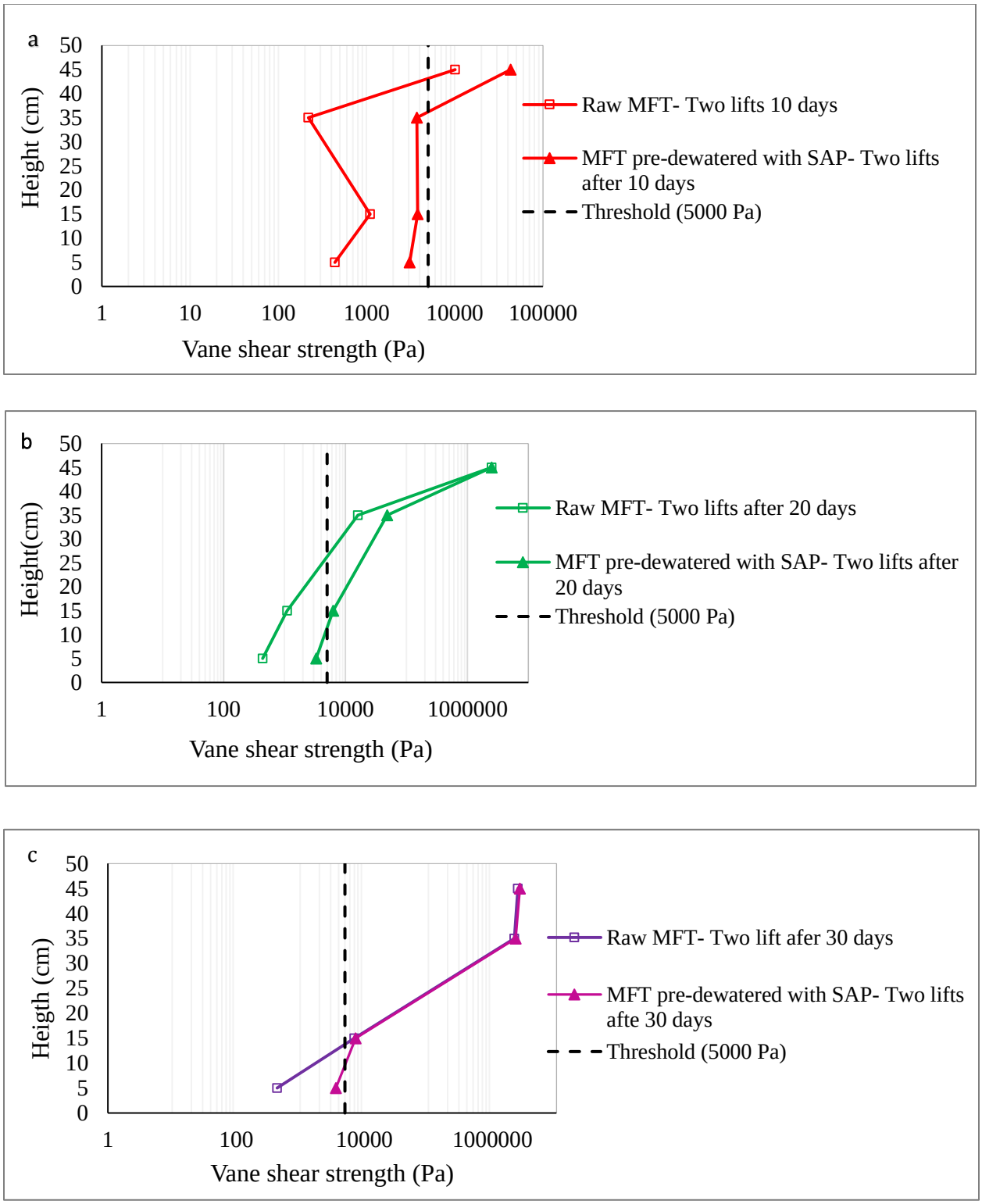

Figure 5.7, Evolution of strength for MFTs pre-dewatered with SAP with respect to the height and time

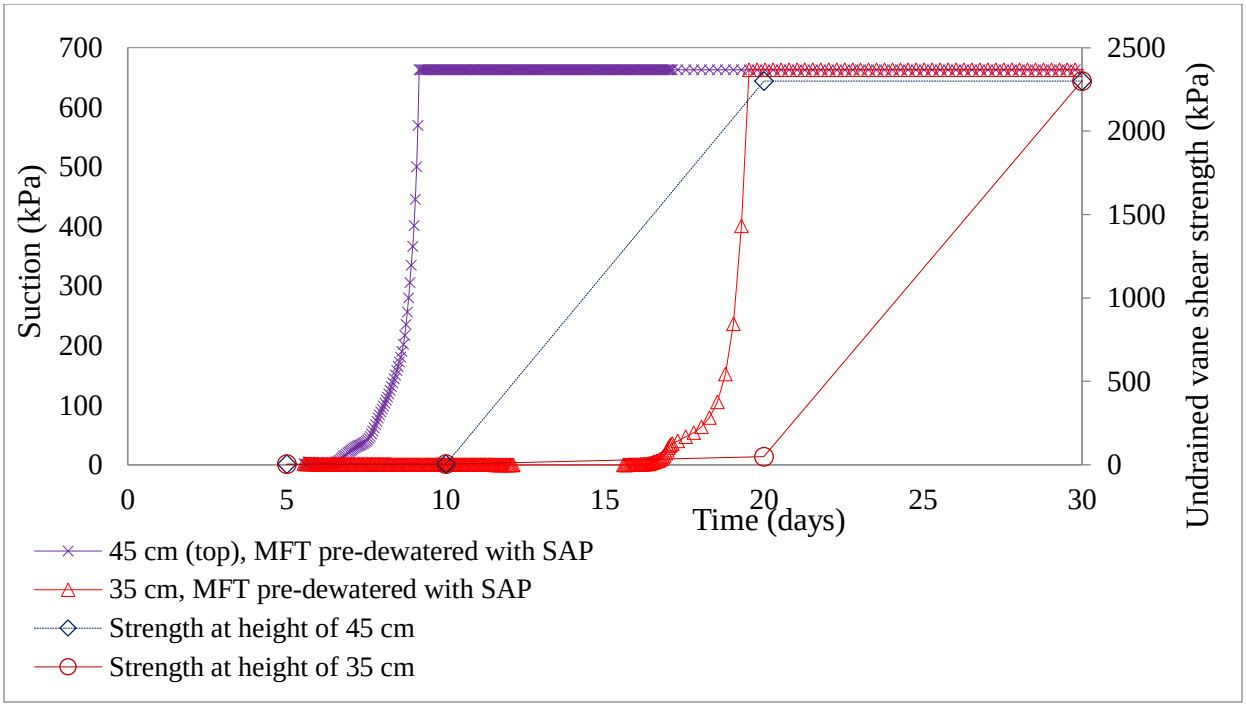

Figure 5.8, Evolution of strength in upper heights of the column with respect to the suction

5.3.4 Shrinkage curve

Upon drying, the evaporation causes volume shrinkage. The variation in bulk volume as a response to changes in the water content is described by the soil shrinkage curve. Particle size distribution and stress are the main factors that control shrinkage behavior (Fredlund et al., 2002). Three shrinkage behaviors that MFTs slurry can exhibit are shown in Figure 5.9. In the first stage, termed normal or basic shrinkage, a decrease in water content causes an equal void ratio reduction (Sposito and Giráldez, 1976; Cornelis et al., 2006). In the second stage, or residual shrinkage, further drying exceeds the volume changes but the slope of the curve is decreased. Finally, in the third stage, referred to as zero shrinkage, the soil particles reach a minimum void ratio that corresponds to the minimum volume that MFTs can gain upon further decrease in water content. The water content related to zero shrinkage is termed the shrinkage limit (SL). At the SL, by increasing the suction, no further volume changes occur and clay particles attain their densest configuration. In our study, the minimum void ratio as a result of the suction development was measured at around 0.58, corresponding to an SL of about 13%.

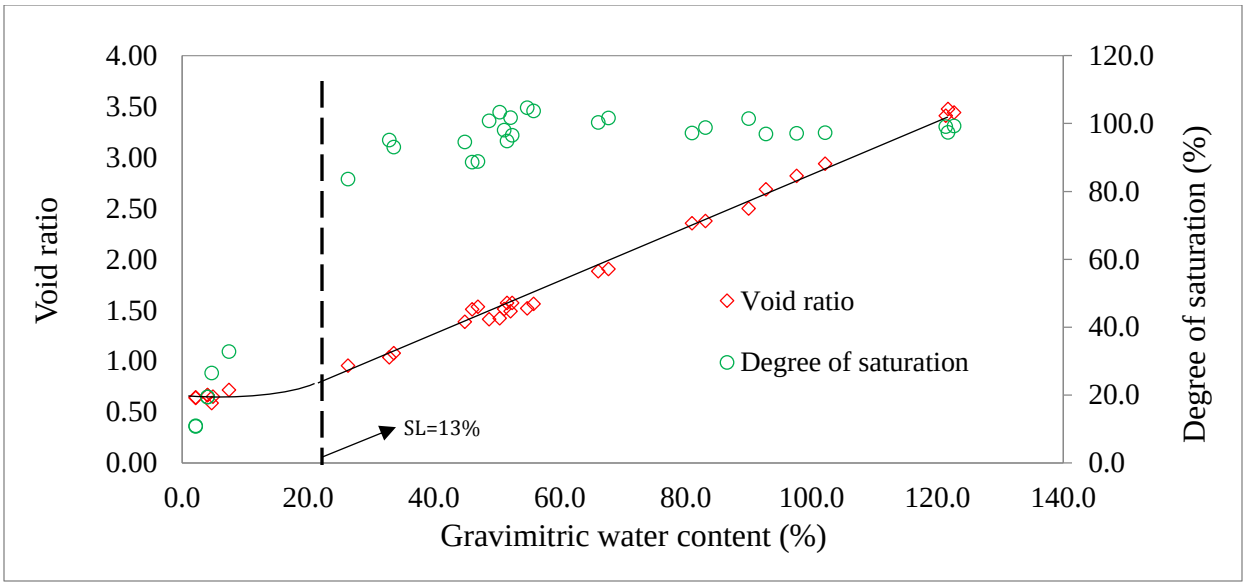

Figure 5.9, Evolution of void ratio and degree of saturation with water content during drying

5.4 Conclusions

This paper presented and discussed the impact of pre-dewatering of MFTs by SAP on its mechanical, physical, and hydraulic properties in a two-lift deposition, by means of a columns experiment. This study highlighted the interactions between evaporation, drainage, suction, strength, and void ratio that occurred in the columns. Surface evaporation can affect physical, hydraulic, and mechanical properties. Evaporation developed tensile stress that led to a decrease in void ratio and drying shrinkage on the surface. Suction development is a significant factor in the evolution of mechanical properties. Based on the obtained results, the filling sequence can temporarily affect MFT properties. Suction started to develop four days after loading the first layer into the column for both pre-dewatered and raw MFTs, and reached 24 kPa for MFTs pre-dewatered with SAP on the fifth day. Water redistribution from the newly added layer eliminated the developed suction, but later, penetration of the cracks caused a higher rate of evaporation that influenced the water content and degree of saturation in the layer beneath, which consequently developed suction and strength. In terms of shear strength, the strength of different depths of 5 cm and 15 cm of MFTs pre-dewatered with SAP (after 30 days) were measured at 3.6 kPa and 7.3 kPa, while the upper part of the column had a strength of around 2.3 MPa. The strength of the lower part of the raw MFTs was 400 Pa and 7 kPa (after 30 days). This shows that the SAP pre-dewatering technique leads to a much faster strength increase rate, and consequently will positively affect the speed of reclamation and thereby reduce tailings management cost as well as the

environmental footprint of heavy oil operations in Canada. An additional advantage of the application of SAP in this context is an 82% reduction in drainage, which can remedy the issue of MFTs seepage into water bodies and ground water. The results of this study highlight this SAP dewatering and densification method as a promising approach to the management of mature fine tailings generated by the oil sand industry.

Acknowledgements

The authors would like to thank the University of Ottawa and the National Natural Sciences and Engineering Research Council of Canada (NSERC) for supporting this research.

5.5 References

Chalaturnyk, R. J., Don Scott, J., and Özüm, B. (2002). Management of oil sands tailings. Journal of Petroleum Science and Technology, 20 (9-10), 1025–1046.

Clark, K. A, and Pasternack, D. S. (1932). Hot water separation of bitumen from Alberta bituminous sand. Journal of Industrial and Engineering Chemistry, 1410–1416.

Cornelis, W. M., Corluy, J., Medina, H., Díaz, J., Hartmann, R., Van Meirvenne, M., and Ruiz, M. E. (2006). Measuring and modelling the soil shrinkage characteristic curve. Geoderma, 137(1-2), 179–191.

Dzinomwa, G., Wood, C., and Hill, D. (1997). Fine coal dewatering using pH- and temperature-sensitive superabsorbent polymers. Journal of Polymers for Advanced Technologies, 8, 767–772.

Fall, M., Célestin, J., and Sen, H. F. (2010). Potential use of densified polymer-pastefill mixture as waste containment barrier materials. Journal of Waste Management, 30(12), 2570–2578.

Farkish, A., and Fall, M., (2014). Consolidation and hydraulic conductivity of oil sand mature fine tailings dewatered by using supeabsorbent polymer. ASCE Geotechnical and Geoenvironmental Engineering Journal 140(7): 06014006.

Farkish, A., and Fall, M. (2013). Rapid dewatering of oil sand mature fine tailings using super absorbent polymer (SAP). Journal of Minerals Engineering, 50–51, 38–47.

Fasking, T., Dunmola, A., Mckay, D., Masala, S., and Langseth, J. (2011). Bench scale drying of multi-layered thickened TSRU tailings. Proceeding in International Conference on Tailings, Edmonton, Canada, 2011.

Fisseha, B., Bryan, R., and Simms, P. (2010). Evaporation, unsaturated flow, and salt accumulation in multilayer deposits of " Paste" gold tailings. ASCE Geotechnical and Geoenvironmental Engineering Journal, 136, 1703–1712.

Hu, Y., Beach, J., Raymer, J., and Gardner, M. (2004). Disposable diaper to collect urine samples from young children for pyrethroid pesticide studies. Journal of Exposure Analysis and Environmental Epidemiology, 14(5), 378–84.

Jeeravipoolvarn, S. (2008). Sedimentation and consolidation of in-line thickened fine tailings. Proceedings in International Oil Sands Tailings Conference, Edmonton, AB, Canada, 1-14.

Jeeravipoolvarn, S., Scott, J. D., and Chalaturnyk, R. J. (2009). 10 M standpipe tests on oil sands tailings: Long-term experimental results and prediction. Canadian Geotechnical Journal, 46(8), 875–888.

Jordaan, S. (2012). Land and water impacts of oil sands production in Alberta. Journal of Environmental Science and Technology, 46, 3611–3617.

Junqueira, F. F., Sanin, M. V., Sedgwick, A., and Blum, J. (2011). Assessment of water removal from oil sands tailings by evaporation and under-drainage, and the impact on tailings consolidation. Proceeding in Tailings and Mine Waste Conference, Vancouver, BC, Canada.

Kayadelen, C., Tekinsoy, M. a., and TaşkIran, T. (2007). Influence of matric suction on shear strength behavior of a residual clayey soil. Journal of Environmental Geology, 53(4), 891–901.

Kuai, L. (2000). Sludge treatment and reuse as soil conditioner for small rural communities. Bioresource Technology Journal, 73(3), 213–219.

Li, J. H., and Zhang, L. M. (2011). Study of desiccation crack initiation and development at ground surface. Engineering Geology Journal, 123(4), 347–358.

Masuda, K., and Iwata, H. (1990). Dewatering of particulate materials utilizing highly water-absorptive polymer. Powder Technology Journal, 63(2), 113–119.

Mikula, R., Kasperski, K., and Burns, R. (1996). Nature and fate of oil sands fine tailings. Journal of American Chemical Society. 677-723.

Nasir, O., and Fall, M. (2010). Coupling binder hydration, temperature and compressive strength development of underground cemented paste backfill at early ages. Journal of Tunnelling and Underground Space Technology, 25(1), 9–20.

Peer, F., and Venter, T. (2003). Dewatering of coal fines using a superabsorbent polymer. Journal of the South African Institute of Mining and Metallurgy, 403–410.

Pó, R. (1994). Water-absorbent polymers: A Patent Survey. Journal of Macromolecular Science, Part C: Polymer Reviews, 34(4), 607–662.

Rayhani, M. H., Yanful, E. K., and Fakher, A. (2008). Physical modeling of desiccation cracking in plastic soils. Journal of Engineering Geology, 97(1-2), 25–31.

Rayhani, M. H., Yanful, E. K., and Fakher, A. (2007). Desiccation-induced cracking and its effect on the hydraulic conductivity of clayey soils from Iran. Canadian Geotechnical Journal, 44(3), 276–283.

Shokri, N., Zhou, P., and Keshmiri, A. (2015). Patterns of desiccation cracks in saline bentonite layers. Journal of Transportation in Porous Media, 110 (2), 333-344.

Sposito, G., and Giráldez, J. V. (1976). Thermodynamic stability and the law of corresponding states in swelling soils1. Soil Science Society of America Journal, 40(3), 352.

Tang, C. S., Shi, B., Liu, C., Suo, W. Bin, and Gao, L. (2011). Experimental characterization of shrinkage and desiccation cracking in thin clay layer. Journal of Applied Clay Science, 52(1-2), 69–77.

Tekinsoy, M. A., Kayadelen, C., Keskin, M. S., and Söylemez, M. (2004). An equation for predicting shear strength envelope with respect to matric suction. Computers and Geotechnics Journal, 31(7), 589–593.

Timoney, K. P., and Lee, P. (2009). Does the Alberta tar sands industry pollute? The scientific evidence. The Open Conservation Biology Journal, 3(1), 65–81.

Vanapali S., D. Fredlund, D. Pufahl, and Clifton, A.(1996). Model for the prediction of shear strength with respect to soil suction. Canadian Geotechnical Journal, 33, 379-392.

Wilson, G., Fredlund, D., and Barbour S. (1994). Coupled soil-atmosphere modelling for soil evaporation. Canadian Geotechnical Journal, 31, 151-161.

Yuan, X. S., and Shaw, W. (2007). Novel processes for treatment of Syncrude fine transition and marine ore tailings. Journal of Canadian Metallurgical Quarterly, 46(3), 265–272.

Zohuriaan-mehr, M. J., and Kabiri, K. (2008). Superabsorbent Polymer Materials: A review. Iranian Polymer Journal, 17(6), 451–477.

6 Impact of drying on geo-environmental properties of mature fine tailings pre-dewatered with SAP

Anis Roshani, Mamadou Fall, Kevin Kennedy

International Journal of Environmental Science and Technology, 14(3), 453-462**.**

ABSTRACT

Oil sand operation in Alberta generates a large amount of waste in the form of slurry that is rich in terms of fine particle. The surface disposal of such waste has created several environmental problems. Strict governmental regulations with regards to the disposal of such a huge amount of waste called mature fine tailings (MFT) in the tailings ponds compel this industry to develop new techniques which are more sustainable and environmentally friendly. Hence, in this study, the new technique of superabsorbent polymer (SAP) for dewatering of MFTs was investigated by adding 1% by weight of polymer to MFTs. Pre-dewatered MFTs was exposed to evaporation and the results in terms of water content, electrical conductivity (EC), geo-chemical evolution, micro-structural observation and permeability are reported. Volumetric water content and electrical conductivity followed the same behavior such that as water content decreases the electrical conductivity decreases. In term of chemical evolution, SAP decreased the ion concentration of pore water by up taking the major cations in its polymer chains. Based on SEM observation, more compacted clay matrix was observed in pre-dewatered MFTs rather than raw material. Hence, by further restriction of flow in SAP pre-dewatered MFTs, hydraulic conductivity decreased.

Keywords: Oil sands, Mature fine tailings, Superabsorbent polymer, Dewatering.

6.1 Introduction

In the oil sand industry, the Clark hot water extraction process has been used on a commercial scale in order to wash the bitumen off the surface-minded oil sand. This process is based on high temperature with the addition of dispersing agent (NaOH) that results in the formation of the extremely dispersed tailings as a by-product stream. When tailings are released into the tailings pond for the containment, a layer forms in; this is referred to as mature fine tailings (MFT). The challenge is that MFTs does not settle within a reasonable timeframe and its consolidation takes decades due to dispersed nature of the clay fraction caused by the extraction process (Mikula et al., 1996; Beier et al., 2013). On average, for every barrel of produced bitumen, 0.25 m^3 of MFTs have been deposited (Beier et al., 2013). MFTs is a mixture of fine particles (< 44 microns), process affected water and residual bitumen. Process affected water includes high concentration of dissolved ions including sodium, calcium, magnesium, potassium chloride, sulphate, bicarbonate and organic chemical consisting of naphthenic acid, BTEX, aromatic hydrocarbons. This polluted stream is released into adjacent surface or water bodies that makes the water toxic to human and aquatic life (Timoney and Lee, 2009; Holden et al., 2011; Holden et al., 2013).

Inevitable expansion of oil sand industry and stricter regulation for environmental compliance (Directive 074) have driven active operators to evaluate the applicable scenarios for reclamation of oil sand tailings and dedicated disposal areas (DDAs). The oil sand industry has developed some dewatering techniques to reduce MFTs inventory. For example, flocculation and coagulation are employed for fines dewatering (Beier et al., 2013; Sworska et al., 2000; Yuan and Shaw, 2007; Jeeravipoolvarn, 2008; Yao et al., 2011; Fasking et al., 2011). Composite or consolidated tailings (CT) are implemented at Suncor and Syncrude and is considered in different studies for addressing different challenges and drawbacks (Caughill et al., 1993; Chalaturnyk et al., 2002; Matthews et al., 2002). In addition of commercially applicable technologies in oil sand fine tailings management, finding new methods for fine tailings dewatering is an ongoing challenge of the industry.

The industrial use of superabsorbent polymer (SAP) to dewater fine particle was studied in 1990 and it was found that SAP is a high water absorptive polymer for dewatering the coal fines (Masud and Iwata, 1990). More investigations approved the effectiveness of SAP in moisture content

reduction of fine coal (Dzinomwa et al., 1997; Peer and Venter, 2003). In 1999, water absorptivity and water retention capacity of SAP was confirmed when its application reduced the water content of the sewage sludge from 96% to 8.5% (Kuai, 2000). Fall et al. (2010) concluded that polymer pastefill (PP) that is a mixture of pastefill and SAP, show encouraging performance properties for barrier design (Fall et al., 2010). Extending this line of research, Farkish and Fall (2013) investigated the feasibility of SAP application in dewatering and densification of MFTs and they found it as a promising approach for rapid dewatering of MFTs (Farkish and Fall, 2013). So, the potential of fine tailings volume reduction by applying SAP with improved geo-environmental behavior provided an environmental incentive for authors to study the effect of polymer pre-dewatered tailings on hydraulic, chemical and microstructural evolution of a two layer deposition of pre-dewatered MFTs with SAP. Till now, no targeted attempt has been made to consider the SAP application in multi-layer MFTs deposition and addressing this knowledge gap can help the better understanding of physical and chemical evolution due to pre-dewatering, evaporation and interlayer flow as the result of placing the fresh layer.

6.2 Material

6.2.1 Mature fine tailings (MFT)

MFTs was delivered from Alberta, Canada and according to wet laser diffraction analysis (Figure 6.1) it is composed of around 95% fine particles. The minerals identified by XRD were kaolinite and illite. This identification is in agreement with the other studies (Mikula et al., 1996; Omotoso and Mikula, 2004; Chertkov, 2007; Kaminsky et al., 2006). The mineralogy of fine tailings is affected only by the oil sand ore and not by extraction process (Miller et al., 2010). The specific gravity was measured 2.36 and the liquid limit and plastic limit were 51.2 and 37.2, respectively. Greater bitumen content causes higher values in Atterberg limits and lower values of specific gravity (Suthaker and Scott, 1996; Jeeravipoolvarn, 2009). Oil sand connate water, make up water and chemicals added during the process determine the MFTs water chemistry that affect the clay interaction and water holding capacity of suspension (Mikula et al., 1996).

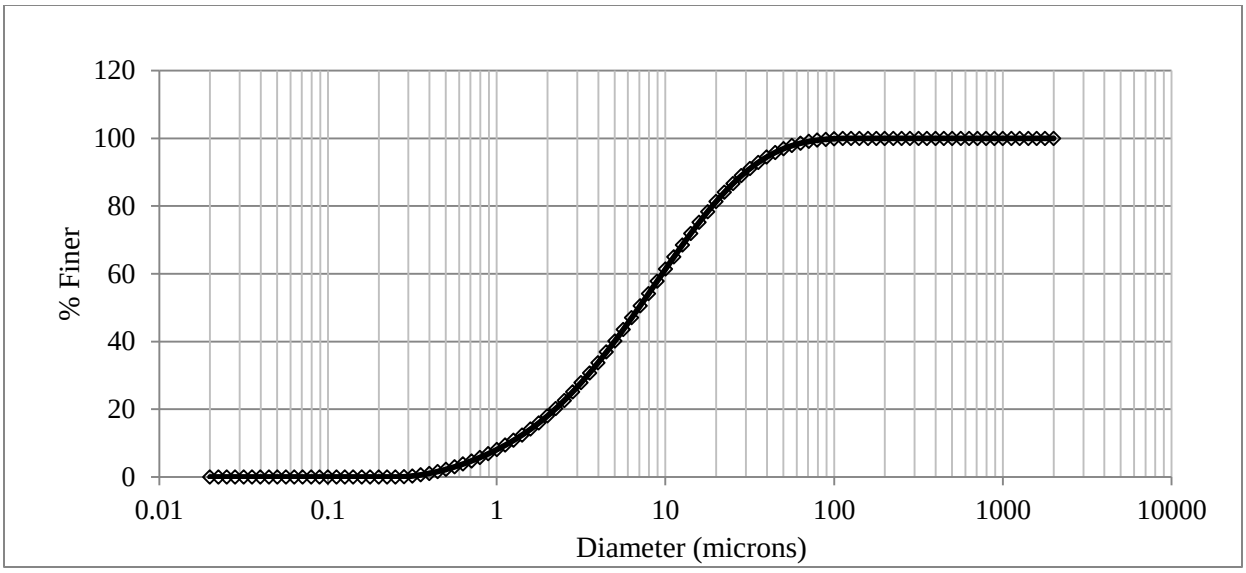

Figure 6.1, Grain size distribution of the used mature fine tailings

The water chemistry of the fine tailings was determined in terms of major ions, cation. pH of the pore water solution was around 8.0 that is high enough to keep the fine tailings in suspended status. Table 6.1 illustrates the concentration of metals measured in pore water by applying inductivity coupled plasma mass spectrometry (ICP-ES/ICP-MS). High concentration of dissolved sodium is due to the caustic addition in the process.

Table 6. 1, MFTs pore water chemistry

Metal	ppm	Metal	ppm	Metal	ppm
Na	617	Ca	4.5	Li	0.11
K	14	Al	3.52	Ti	0.08
Si	8.31	Fe	0.85	Mn	0.07
Mg	6.53	Ba	0.18	Ni	0.012

6.2.2 Polymer material (Sodium poly-acrylates)

Commercially available cross-linked insoluble sodium poly-acrylates with capacity of 250 g/g in deionized water was used. When the powder is dry, the polymer chains are coiled. When hydrated, the sodium ion detaches so that the carboxyl groups (CO_2H) become negatively charged and repel

one another to uncoil the polymer chain to allow more water to associate with more carboxyl groups or sodium atoms (Hu et al., 2004). SAP has a lot of applications in hygienic and agricultural areas (Bowman et al., 1990; Kenawy, 1998). SAP is used in many other fields like entertaining toys and tools, building internal decoration, cryogenic gels, food /meat packaging, concrete strengthening, reduction of the ground-resistance in the electrical industry (Po, 1994; Schröf et al., 2012).

6.2.3 Specimen preparation and mix proportioning

The adopted mixing procedure for this study included mixing of MFTs with 1% SAP (by weight) for 6 days. Permeable sachets were prepared in order to hold the SAP during the mixing process. By applying these sachets, not only removing the polymer from the tailings can be applicable, but also the SAP can be recycled. Mixture of SAP and MFTs was mixed 15 min per day in order to reach a homogenous mixture. After 6 days, by increasing the solid content from 45 % to around 60 %, SAP sachets were removed and pre-dewatered MFTs was loaded to columns as the first or second layer to further dewatering through evaporation and drainage.

6.2.4 Experimental setup, column instrumentation and monitoring

Figure 6.2 portraits the experimental setup developed. The inner diameter of the columns was 25 cm and the height was 55 cm. A thin layer of sand as the drainage layer was considered at the bottom of each column that was separated from the MFTs by a perforated palate covered with a coarse filter paper. In total, 4 columns were manufactured for taking samples at different time intervals of 5, 10, 20 and 30 days. Filling strategy included the placement of the first lift (25 cm) and then 5 days rest. After 5 days, the first column (d) was dismantled and second lift (25 cm) was added to the other three columns. The columns (c), (b) and (a) were dug out after 10, 20 and 30 days, respectively. Monitoring column (a) was instrumented with different types of sensor for measuring the suction, water content, temperature and electrical conductivity. Four MPS-6 sensors (Decagon Devices Inc.) implanted at heights of 5, 15, 35 and 45 cm were monitoring suction while four 5TE sensors (Decagon Devices Inc.) were measuring volumetric water content, electrical conductivity (EC) and temperature. 5TE sensor can measure water content in the range of 0-80%, electrical conductivity in the range of 0-23 dS/m and temperature in the range of -40 to 60℃. All the sensors are connected to the data logger in which the data can be recorded. A dial gage (3058S,

Mitutoyo Co.) on top of the monitoring column can measure the settlement. The arrangement of the sensors and dial gage, filling sequences and the location of the taken samples are shown in Figure 6.2.

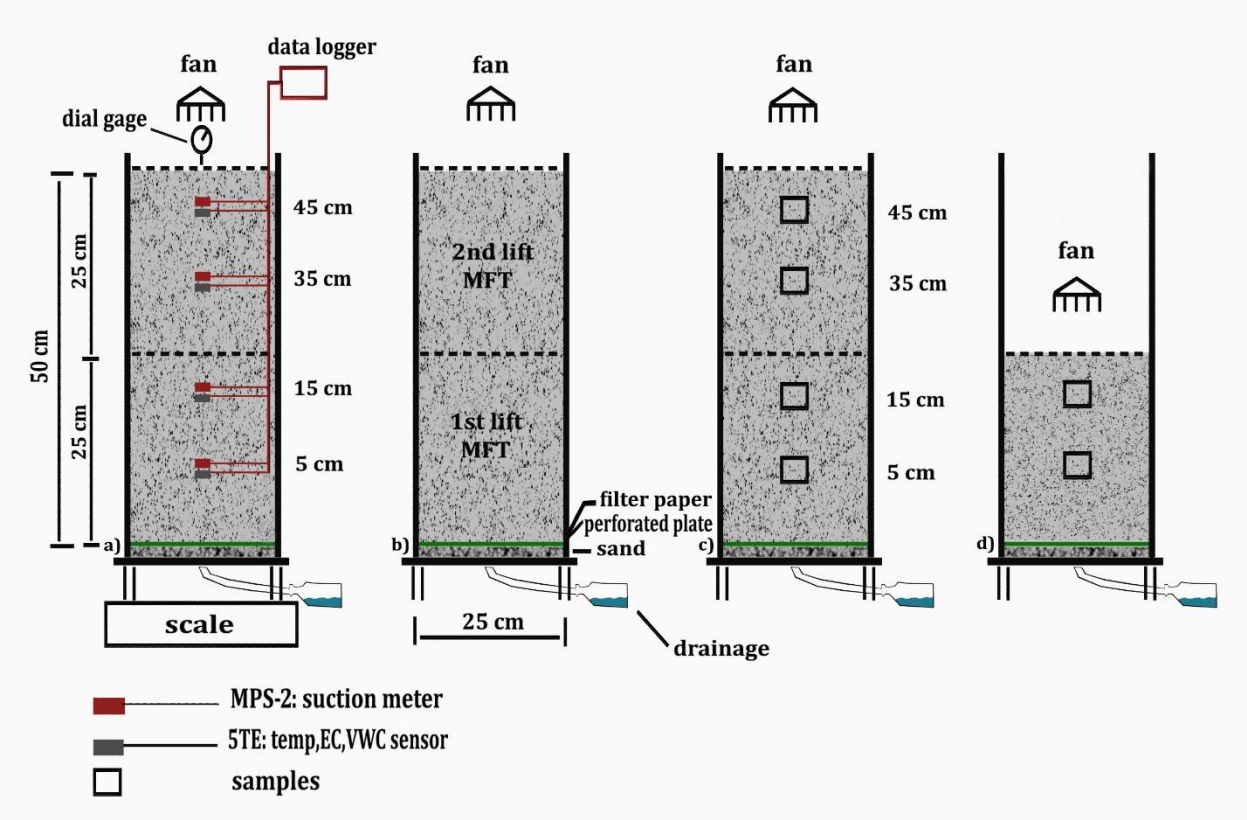

Figure 6.2, Schematic diagram of the experimental setup

6.2.5 Hydraulic conductivity tests

Hydraulic conductivity test was conducted under ASTM D5084 by using TRI-FLEX II on the MFTs samples taken from different heights after each elapsed times. Hydraulic conductivity of porous material decreases with increase of the air in the pores. But this test method applies to water saturated porous material that contains no air. The assumption is that Darcy's law is valid and this test method measures a hydraulic conductivity at a controlled effective stress. Hydraulic conductivity varied with varying void ratio which changes when the effective stress changes. The method of constant head was used and hydraulic conductivity (k) was calculated as below:

$$k = \frac{\Delta Q. L}{A. \Delta h. \Delta t}$$

where:

k = hydraulic conductivity, m/s,

ΔQ = quantity of flow in time interval $\Delta t = (t_2 - t_1)$, taken as the average of inflow and outflow, m^3,

L = length of specimen, m,

A = cross-sectional area of specimen, m^2,

Δh_1 = head loss across the specimen at t_1, m of water,

Δh_2 = head loss across the specimen at t_2, m of water,

Δh = average head loss $((\Delta h_1+\Delta h_2)/2)$, m of water,

The tests were performed with an upward flow. Four values of permeability are obtained in which the steady state condition is reached. Experiences have shown that hydraulic conductivity of small samples are not necessarily the same as larger scale values. So, the results obtained in the lab should be considered with caution for the field (ASTM D5084).

6.2.6 Analysis of chemistry

Due to the close distance of the tailings pond to the water bodies and risk of seepage, chemical analysis of MFTs pore water is a necessity for applying mitigative measures. Sediment possess only a mild capacity to retain potential contaminant (likely Na as dominant cation in tailings ponds), while the concentration of Ca and Mg increases in the water as a result of sodium displacement (Holden et al., 2012). Heavy metals cannot be destroyed as organic pollutants and several technologies like precipitation, ultra-filtration, adsorption and ion exchange are applied for eliminating them from solution (Fonseca et al., 2006).

MFT samples taken from different heights after certain elapsed times were ashed at 500℃ for 24 hours and the ashed residue was grounded to a fine powder with a mortar and a pestle. 0.5 ml concentrated HNO_3 and 1.5 ml of concentrated HCl was added to 0.1 gr of ash in a teflon vial and allowed to stand for 4-5 hours. Mixture was heated (lightly closed) on a hot plate at 100 for 5-6 hours. The acid was evaporated to near dryness. 0.5 ml of concentrated HNO_3 was added and heated for 1 hour. The volume was brought to about 3 ml of water and centrifuged. Supernatant was transferred to another vial. The residue was rinsed with another 3 ml portion of water and

centrifuged for the second time. The solutions from the two centrifugations were merged and the total mass was brought to 10 gr accurately for the measurement by ICP-ES/ ICP-MS (Inductively coupled plasma mass spectrometry).

6.2.7 Microstructural analyses

A series of microstructural analyses that included scanning electron microscope (SEM) and mercury intrusion porosimetry (MIP) were investigated. SEM observation is a type of electron microscope in which a focused beam of electron scans the surface of the sample to detect the surface topography. The SEM analyses conducted on the oven dried MFTs samples to reveal the micro surface structures with a Hitachi 3500-N microscope. MIP tests were performed on oven dried MFTs samples to evaluate pore size distribution using a micromeritics auto-pore III 9420 mercury porosimeter. Moreover, by employing the brass ring with known volume for taking samples, void ratio (e), porosity (n) and saturation (s) for entire the columns can be determined.

6.3 Results and discussion

6.3.1 Evaporation and volumetric water content evolution

Basically, desiccation is the removal of water by evaporation which increases density and promotes strength. Increase in density and consequent decrease in void ratio improves the traffic ability of the soft clay or MFTs (Fujiyasu and Fahey, 2000; Lee et al., 2003; Fisseha et al., 2010). Figure 6.3 shows evolution of water content in different column heights with respect to the time. The initial water content of the MFTs pre-dewatered with SAP decreased from 130% (raw MFTs) to around 50%. Water content of the top portion of the first lift (15 cm) of pre-dewatered MFTs with SAP fell to 0.21 m^3/m^3 from the initial value of 0.45 m^3/m^3; this is obviously associated with an increase of the suction while the water content of raw MFTs dropped to 0.28 m^3/m^3. Loading the second lift increased water content of top portion of the former lift due to water drainage and gravity. Water content increased to 0.23 m^3/m^3 for pre-dewatered MFTs and to 0.41 m^3/m^3 for raw one. Pre-dewatered MFTs showed a lower increase in water content gradient due to lower initial water content of added MFTs. By casting the second lift, cracking and lateral shrinkage away from the wall started on day 2. At the height of 45 cm, water content decreased sharply in the first 5 days while the height of 35 cm showed a slight decreasing trend during the first 10 days and then declined steeply to zero. In the early stages of both SAP pre-dewatered and raw MFTs (first lift) a

crust formed on the top layers (15 cm) imply that higher rate of evaporation occurred on top while the beneath layers (5 cm) remained almost unaffected. In term of crack, more developed cracks were observed in raw MFTs. These cracks were deep enough to affect the water content of raw MFTs at height of 15 cm that showed a decreasing trend in the last 12 days.

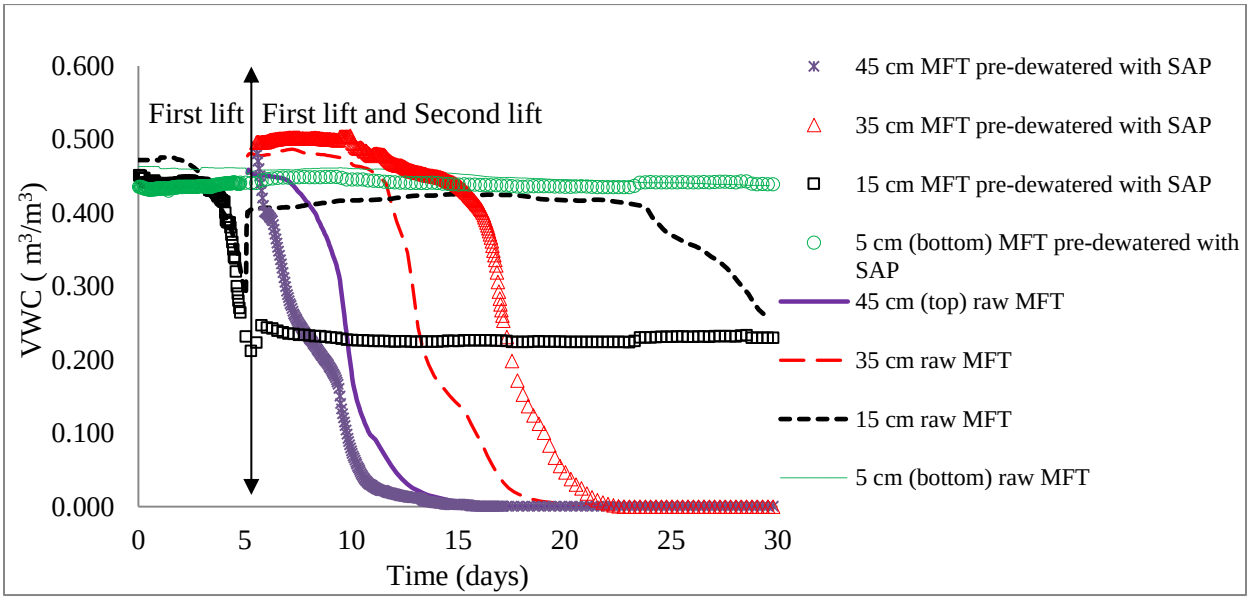

Figure 6.3, Evolution of volumetric water content of pre-dewatered and control MFTs with respect to the height and time

6.3.2 Changes in electrical conductivity

Electrical conductivity (EC) of a soil solution is an indicator of its cation and anion concentration. In aqueous systems, most of the clay minerals have a degree of electrical conductance due to the mobility of accumulated ions on their surface. Increasing water content promotes the ionic mobility that makes the clay more conductive (Miyamoto et al., 2009). As soil solution is the only conducting phase, the water content and electrical conductivity of the soil solution are major factors that affect the electrical conductivity of the bulk (Friedman, 2005; Tabbagh and Cosenza, 2007). Figure 6.4 shows the evolution of EC within the columns. Electrical conductivity followed the same trend as volumetric water content. This is explained by the fact that when the degree of saturation decreases, the water film around the solid particles become thinner and as far as the solid phase of the porous medium and of course air are non-conductive, electrical conductivity decreases (Friedman, 2005).

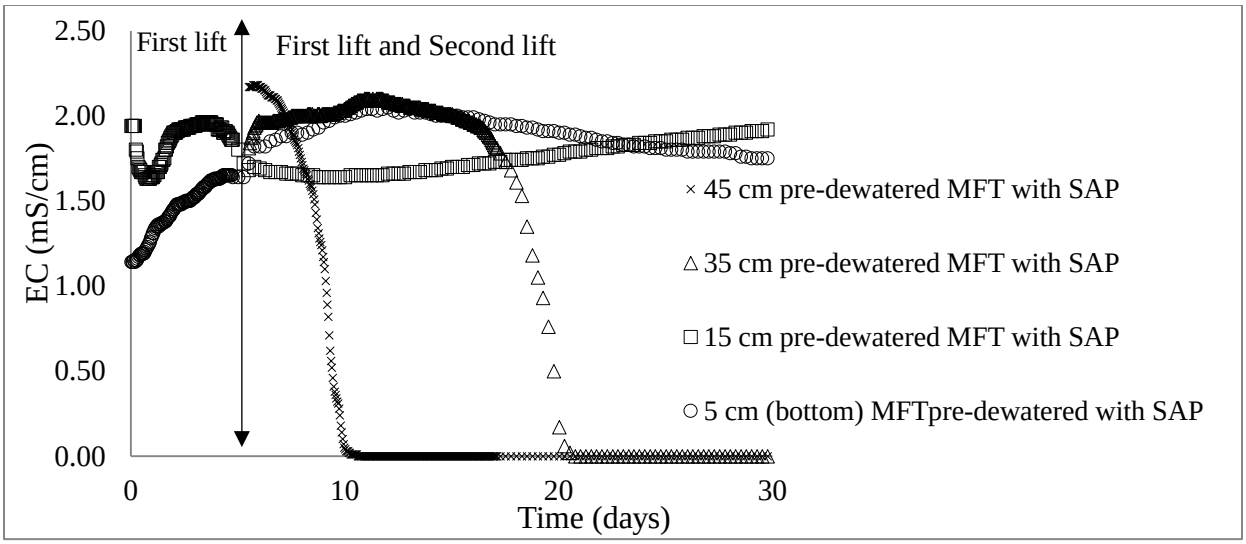

Figure 6.4, Evolution of the electrical conductivity with respect to the heights and time

6.3.3 Changes in geochemistry

By considering the vast inventory of fluid fine tailings, the fate and transport of oil sand process affected water into adjacent water bodies has become an important aspect to environmental protection and impact assessment of this industry. The total concentration of various major cations (B, Na, Mg, Al, Si, P, S, K, Ca, Ti, V, Cr, Mn, Fe, Co, Ni, Cu, Zn, Sr and Ba) were determined for each MFT sample pre-dewatered by SAP. The purpose of this stage was to assess the potential for uptake or release of major ions and trace elements by SAP. Preliminary assessment of trace elements behavior reveals that concentration of Ti, V, Cr, Mn, Co, Ni, Cu and Zn in pore water are less than 0.1 ppm. This data are in agreement with Holden et al. (2013) that showed there is no release of Co, Ni and Ti into ground water, despite the presence of these metals in the soil phase. In pore water fluid, the major cations in decreasing order of presence are: Na > S > K> Si > Mg > Ca. Table 6.2 shows concentration of the aforementioned elements in MFTs pore water without SAP pre-dewatering and pre-dewatered MFTs with SAP. After pre-dewatering of MFTs with SAP, major cations in pore water can replace sodium in the polymer chain. The ease of replacement depends mainly on the cation size, abundance and ion size (Mitchell and Soga, 2005). A typical replicability series is:

$$Na^{+} < K^{+} < Mg^{2+} < Ca^{2+} < Ba^{2+} < Al^{3+} < Fe^{3+}$$

According to Table 6.2, percent reduction of cations in pore water after pre-dewatering with SAP for trivalent cations Fe, Al and Cr are 100%, 98% and 97%, respectively. Percent reduction of divalent cations Mn and Ba are 95% and 87%, respectively. In contrast, monovalent cations Na and K that are held less tightly in polymer chains showed lower absorption by SAP. Table 6.3 compares concentration of cations in SAP before and after MFTs pre-dewatering. Concentration of all the elements increased due to up taking the cations by polymer chain except sodium. Sodium is one of the low replacing power cations and in contact with MFTs pore water, some sodium tend to displace large cations with high replacing power. Hence, polymer chain releases some sodium ions and as a result, concentration of sodium decreased. This is a great achievement since SAP not only decreases the MFTs pore water seepage up to 80% (Roshani et al., 2017), but also it can reduce the concentration of dissolved cations in seepage stream. Decreasing ion concentration in MFTs water drainage reduces the risk associated with ion accumulation in recycled water to the extraction process (Chalaturnyk, 2002; Mackinnon et al., 2001).

Table 6. 2, Comparison between concentration in pore water chemistry for raw MFTs and pre-dewatered MFTs with SAP

	Na	**S**	**K**	**Si**	**Mg**	**Ca**	**B**	**Al**	**P**	**Ti**	**Cr**	**Mn**	**Fe**	**Ba**
Concentration in pore water of raw MFT (ppm)	594	48.3	13.2	7.3	6.3	4.7	2.36	1.8	0.09	0.04	0.03	0.03	0.48	0.17
Concentration in pore water of MFTs pre-dewatered with SAP(ppm)	250	19.0	7.5	1.5	5.6	6.1	0.61	0.02	0.04	0.0009	0.0009	0.001	0.0	0.02
Percentage decrease	57	60	43	79	11	-30	73	98	48	97	97	95	100	87

Table 6. 3, Comparison between concentration of fresh SAP and recycled SAP after MFTs pre-dewatering

	Na	S	K	Si	Mg	Ca	B	Al	P	Ti	Cr	Mn	Fe	Ba
Concentration of fresh SAP (ppm)	439,738	3,834	1,694	51	28	16.72	5.48	164	6	16	0.42	0.17	10	5
Concentration of recycled SAP (ppm)	331,727	4,732	5,711	151	6,190	19,053	265.4	12,174	81	761	9	216	6,276	619

Evaporation in a freshly layer deposition can develop strength by increasing density and void ratio reduction (Simms et al., 2007). However, salt can strongly influence evaporation by supressing evaporation. In addition of pore water analyses, assessment of major cations in solid phase (soil matrix) was studied as well. Figure 6.5 shows the concentration of Na, Ca, Fe and K in soil matrix. Higher concentration of these elements can be seen on the surface where salt precipitates in evaporation boundaries. It's worth mentioning that due to non-uniform distribution of ions in the tailings matrix that will discuss later, four different samples were taken per each depth and the average was reported.

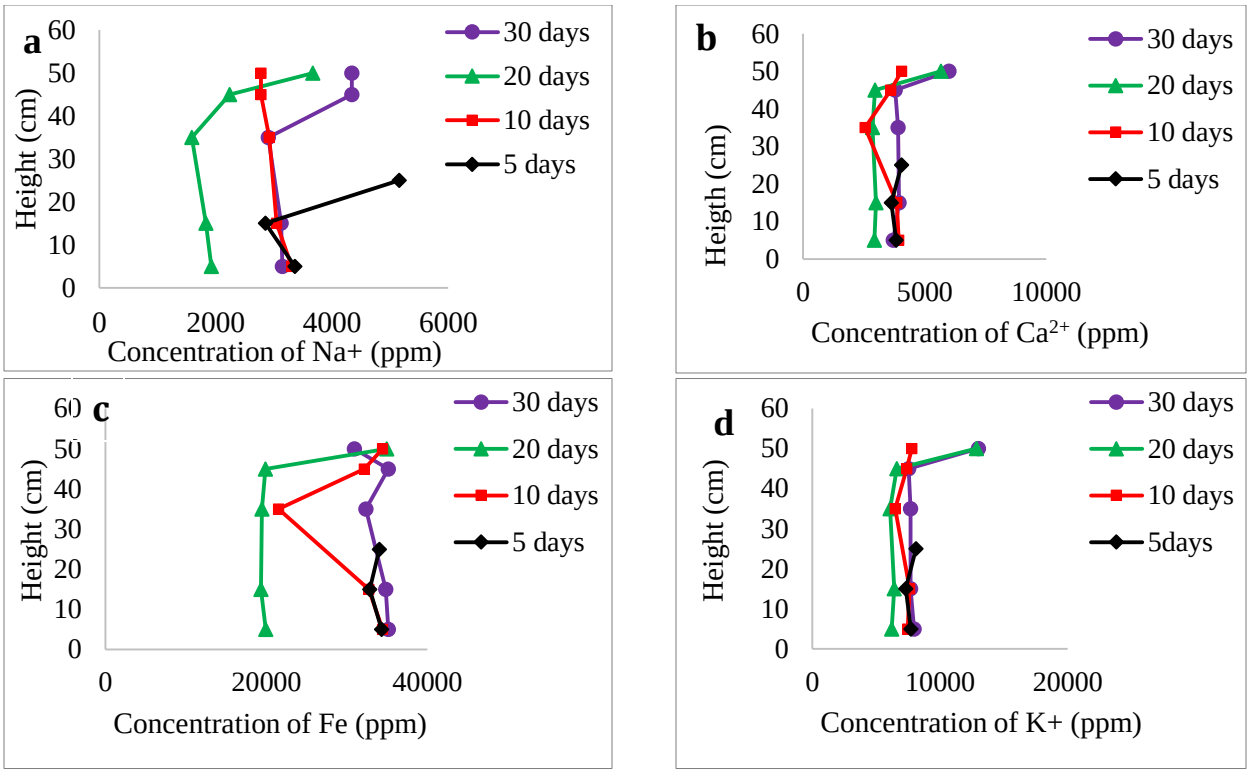

Figure 6.5, Evolution of ions concentration with respect to the height and time a) Sodium b) Calcium c) Iron d) Potassium

6.3.4 Microstructural changes

6.3.4.1 SEM observations

The effect of evaporation on the MFTs micro-fabric is seen in the SEM micrographs in Figure 6.6. As depicted in this figure, the MFTs ped structure changes by evaporation and subsequent developed suction. Figure 6.6a illustrates the raw MFTs located at the bottom (5 cm) of the column which was not affected by evaporation. Void ratio for this sample was measured 2.3 that showed reduction from the initial value of 3.44. Self-weight consolidation and seepage were responsible mechanisms for void ratio reduction. In comparison, Figure 6.6b presents the micro-fabric for MFTs pre-dewatered with SAP for the same height (5 cm). Up-taking pore water by SAP and self-weight consolidation reduced void ratio from initial value of 3.44 (before pre-dewatering with SAP) to around 1.68. Figures 6.6c and 6.6d show comparison between the raw MFTs and pre-dewatered MFTs on the column surface (45 cm) after 30 days in which void ratio was measured 0.67 and 0.58, respectively. In both cases, the compacted and dense MFTs matrix can be observed. Decrease of water content, i.e suction increase induced by evaporation on the surface, made the solid phase rigid and completely compacted. By increasing suction and decreasing void ratio, the

fissures closed and hydraulic conductivity (see section 6.3.5) decreased since fluid flow was further restricted. The lower evaporation rate may be due to lower void ratio and more compacted structure.

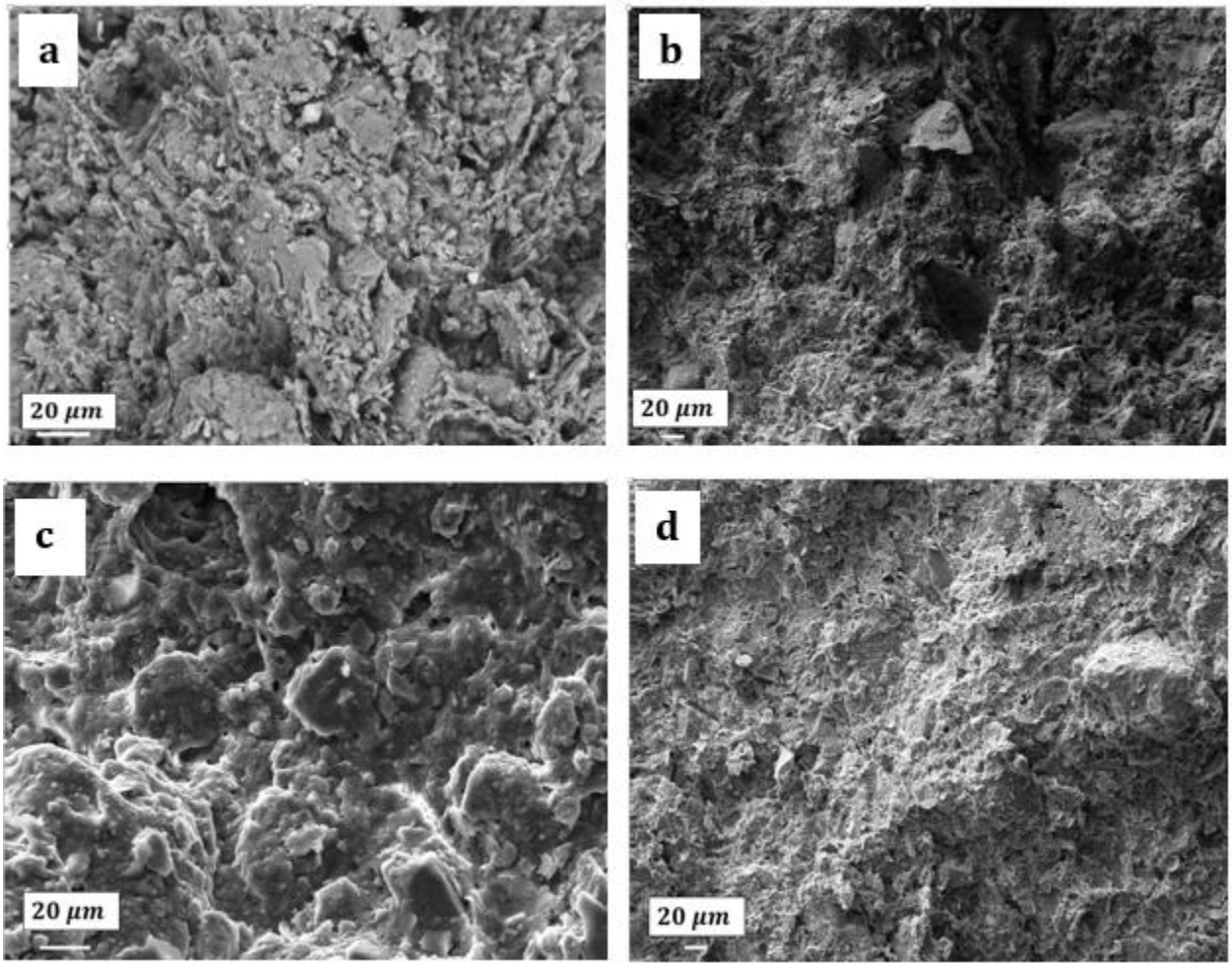

Figure 6.6, Scanning electron micrographs of MFTs micro-fabric (a) 5 cm height after 30 days for raw MFTs (b) 5 cm height after 30 days pre-dewatered MFTs with SAP (c) surface of the column after 30 days without SAP (d) surface of the column after 30 days for MFTs pre-dewatered with SAP

6.3.4.2 Mercury intrusion porosimetry tests

Mercury intrusion porosimetry has been commonly applied to analyse pore size distribution and total porosity of porous samples. Total volume of intruded mercury gives total porosity and the pore width that corresponds to the highest rate of intrusion is named threshold diameter (Fall et al., 2005; Ouellet et al., 2007). Figure 6.7 presents MIP test results for four different MFTs pre-dewatered samples taken after 10 days and 30 days. Based on the results, the finest pore structure

was related to the sample from 45 cm of the test column after 30 days. Void ratio and porosity for this sample were measured 0.58 and 0.37, respectively. By analysing the pore distribution, the fraction of pores with diameter less than 0.1 microns was around 23%, and 60% of pores have pore diameter between 0.1-0.3 microns while only 8% of pores have the diameter between 0.3-0.7 microns. For raw MFTs, pore abundance for diameters less than 0.1 micron and 0.1-0.3 micron were the same as pre-dewatered MFTs with SAP but the percentage of pore with diameter 0.3-0.7 micron is around 16%. This difference can imply the higher void ratio of raw MFTs than pre-dewatered MFTs with SAP. High rate of evaporation and developed suction are the main mechanisms responsible for micro fabric shrinkage. Furthermore, the pre-dewatered MFT sample taken from the bottom (5 cm) of the column after 10 days, showed coarser pore diameter. 14% of pores were smaller than 0.1 micron and pore fraction with diameter of 0.1-0.3 micron and 0.3-0.7 micron were 39% and 31%, respectively.

Threshold diameter (d_{th}) is the first inflection point on the cumulative mercury intrusion curve. Below d_{th}, the great portion of intrusion commences (Pipilikak and Beazi-Katsioti, 2009). According to Fall et al. (2005) more fraction of fine particle reduces the threshold diameter. The smallest threshold diameter was equal to 0.5 micron correspond to the sample taken from 45 cm height of column after 30 days where evaporation fully developed suction and void ratio caught the smallest value of 0.58. d_{th} for the sample from 45 cm height of column with 10 days age and 15 cm height of column with 30 days age were both around 1 micron.

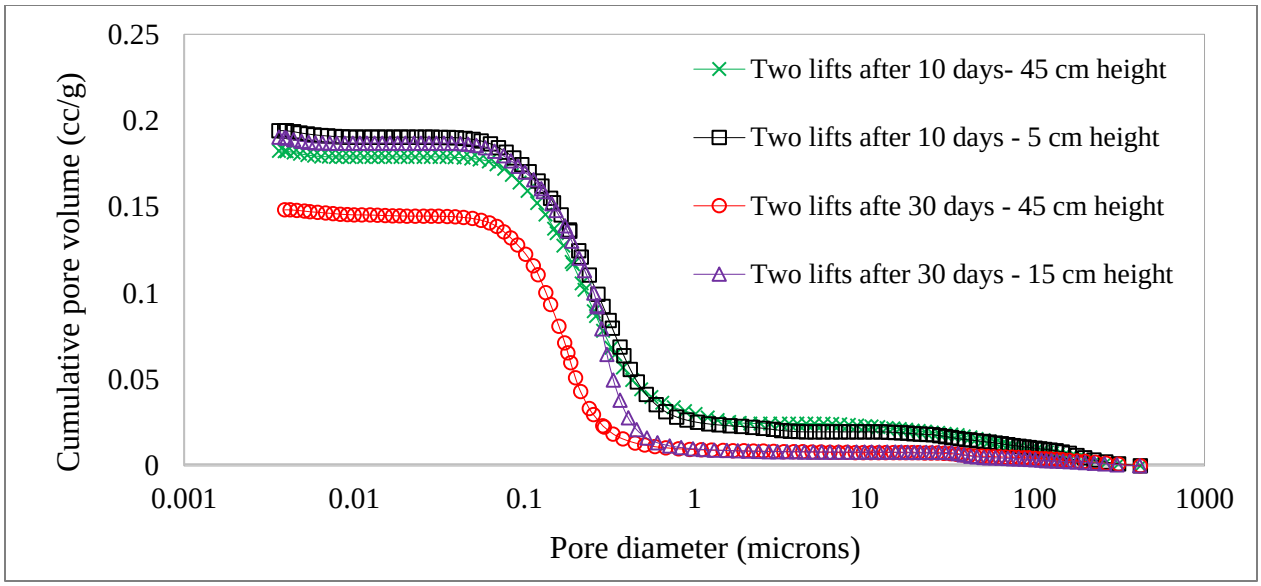

Figure 6.7, MIP test results for cumulative pore volume

6.3.5 Changes in permeability

Variation in the void ratio-hydraulic conductivity has a strong impact on rate of MFTs settlement and pore pressure dissipation rather than consolidation (Miller et al., 2010; Jeeravipoovarn et al., 2009). MFTs has very low permeability that is due to the extensive clay dispersion and concentration of uncovered bitumen (Mikula et al., 1996; Jeeravipoolvarn et al., 2009; Suarez et al., 1984) and permeability reduces as bitumen content increases (Suthaker and Scott, 1996). According to Miller et al., (2010) non-caustic oil sand tailings had a greater hydraulic conductivity at void ratios more than 3. Suarez et al., (1984) found that hydraulic conductivity of clays decreased when pH increased from 6 to 9. Figure 6.8 shows the comparison between hydraulic conductivity (k_{sat}) of pre-dewatered and raw MFTs. From this figure it can be found that k_{sat} decreases with void ratio reduction. Some fluctuation of k_{sat} in the same void ratios might be due to the difference in bitumen content of the samples. Hydraulic conductivity were measured 1.54*E-9 cm/s, 2.34*E-8 cm/s and 6.23*E-8 cm/s at void ratio of 0.58, 1.5 and 2, respectively.

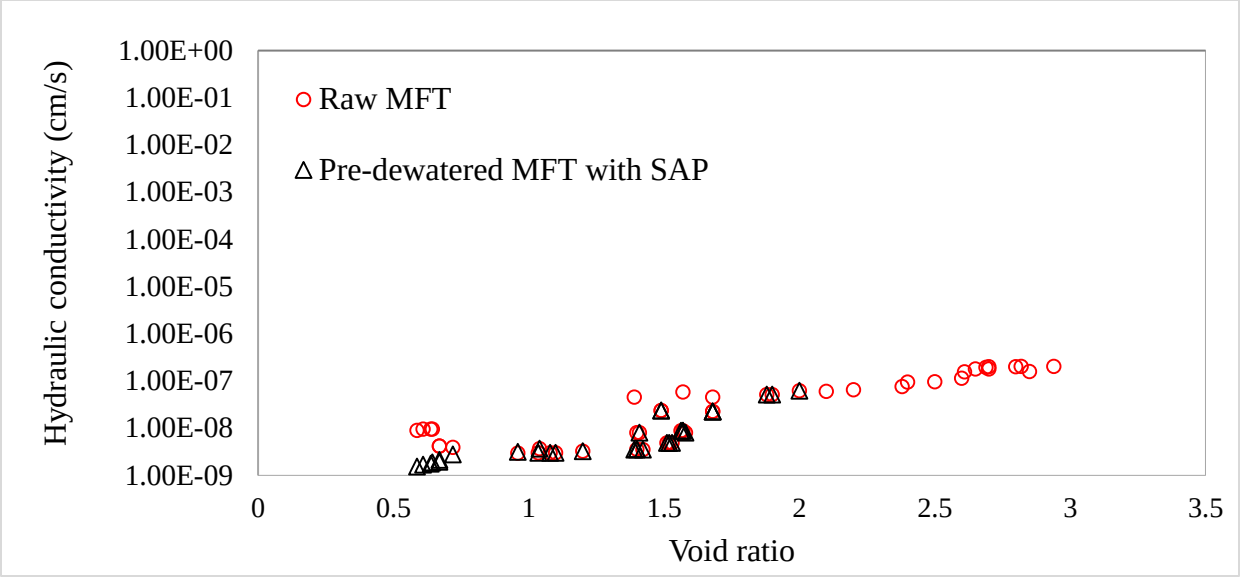

Figure 6.8, Hydraulic conductivity with respect to the void ratio

6.4 Conclusions

With the goal of enhancing dewatering of MFTs and production of a geo-technically stable waste, new technique of SAP was studied in this research. The volumetric water content of pre-dewatered MFTs was monitored in a two lift deposition system exposed to atmospheric evaporation. It was found that addition of the new lift could not impact the water content of the former lift because the initial water content of pre-dewatered MFTs with SAP was around 50% that is much lower than initial water content of raw MFTs (130%). High rate of evaporation on top decreased the water content and consequently EC of the second load to zero after around two weeks. In term of geo-chemical evolution, the concentration of major ions such as K, Mg, Ca, Al, Ti, Cr, Mn Fe, etc. in polymer chain of SAP increased and as a result, the concentration of aforementioned cations decreased in pore water that can be released to ground water by seepage. For example, the concentration of Na, S, K and Mg in raw MFTs pore water were 594 ppm, 48 ppm, 13 ppm and 6ppm, respectively, while by pre-dewatering with SAP, their concentrations felt to 250 ppm, 19 ppm, 7 ppm and 5.6 ppm, respectively. by employing SEM and MIP technique, the finest pore structure was observed in the sample taken from 45 cm height of the column after 30 days in which 60% of pores had diameter between 0.1-0.3 micron and diameter of 8% of pores were in the range of 0.3-0.7 micron. Sample taken from the bottom after 10 days where the suction could not develop had coarser structure. But, pre-dewatered MFTs showed compacted pore structure in comparison with raw MFTs. Hydraulic conductivity of pre-dewatered MFTs with SAP is slightly less than raw

MFTs that is might due to the more compacted structure. The proposed technique can enhance MFTs dewatering as an environmentally acceptable solution for dedication and reclamation of dedicated disposal area.

6.5 References

Beier, N., Wilson, W., Dunmola, A., and Sego, D. (2013). Impact of flocculation-based dewatering on the shear strength of oil sands fine tailings. Canadian Geotechnical Journal, 50, 1001–1007.

Bowman, D. C., Evans, R. V., and Paul, J. L. (1990). Fertilizer salts reduce hydration of polyacrylamide gels and affect physical properties of gel-amended container media. Horticultural Science Journal, 115, 382–386.

Caughill, D., Morgenstern, N. and Scott, J. (1993). Geotechnics of non-segregating oil sand tailings. Canadian Geotechnical Journal, 30(5), 801–811.

Chalaturnyk, R. J., Don Scott, J., and Özüm, B. (2002). Management of oil sands tailings. Journal of Petroleum Science and Technology, 20 (9-10), 1025–1046.

Chertkov, V. Y. (2007). The reference shrinkage curve of clay soil. Theoretical and Applied Fracture Mechanics, 48, 50–67.

Dzinomwa, G., Wood, C., and Hill, D. (1997). Fine coal dewatering using pH- and temperature-sensitive superabsorbent polymers. Journal of Polymers for Advanced Technologies, 8, 767–772.

Fall, M., Benzaazoua, M., and Ouellet, S. (2005). Experomental characterizaton of ther influence of tailings fineness and density on the quality of cemented paste backfill. Journal of Minerals Enginering, 18, 41- 44.

Fall, M., Célestin, J., and Sen, H. F. (2010). Potential use of densified polymer-pastefill mixture as waste containment barrier materials. Journal of Waste Management, 30(12), 2570–2578.

Farkish, A., and Fall, M. (2013). Rapid dewatering of oil sand mature fine tailings using super absorbent polymer (SAP). Journal of Minerals Engineering, 50–51, 38–47.

Fasking, T., Dunmola, A., Mckay, D., Masala, S., and Langseth, J. (2011). Bench scale drying of multi-layered thickened TSRU tailings. Proceeding in International Conference on Tailings, Edmonton, Canada, 2011.

Fisseha, B., Bryan, R., and Simms, P. (2010). Evaporation, unsaturated flow, and salt accumulation in multilayer deposits of "Paste" gold tailings. Journal of Geotechnical and Geoenvironmental Engineering, 136, 1703–1712.

Fonseca, M. G., Oliveira, M., Arakaki, N. H. (2006). Removal of cadmium, zinc, manganese and chromium cations from aqueous solution by a clay mineral. Journal of Hazardous Materials, 137, 288–292.

Friedman, S. (2005). Soil properties influencing apparent electrical conductivity: a review. Journal of Computers and Electronics in Agriculture, 46, 45–70.

Fujiyasu, Y., and Fahey, M. (2000). Experimental study of evaporation from saline tailings. Jornal of Geotechnical and Geoenvionmental Engineering, 126, 18-27.

Holden, A. A., Donahue, R. B., and Ulrich, A.C. (2011). Geochemical interactions between process-affected water from oil sands tailings ponds and north Alberta surficial sediments. Journal of Contaminant Hydrology, 119, 55–68.

Holden, A. A., Mayer, K. U., Ulrich, A. C. (2012). Evaluating methods for quantifying cation exchange in mildly calcareous sediments in northern Alberta. Journal of Applied Geochemistry, 27, 2511–2523.

Holden, A. A., Haque, S. E., Mayer, K. U., and Ulrich, A. C. (2013). Biogeochemical processes controlling the mobility of major ions and trace metals in aquitard sediments beneath an oil sand tailings pond: Laboratory studies and reactive transport modeling. Journal of Contaminant Hydrology, 151, 55–67.

Hu, Y., Beach, J., Raymer, J., and Gardner, M. (2004). Disposable diaper to collect urine samples from young children for pyrethroid pesticide studies. Journal of Exposure Analysis and Environmental Epidemiology, 14(5), 378–84.

Jeeravipoolvarn, S. (2008). Sedimentation and consolidation of in-line thickened fine tailings. Proceedings in International Oil Sands Tailings Conference, Edmonton, AB, Canada, 1-14.

Jeeravipoolvarn, S., Scott, J. D., and Chalaturnyk, R. J. (2009). 10 M standpipe tests on oil sands tailings: Long-term experimental results and prediction. Canadian Geotechnical Journal, 46(8), 875–888.

Kaminsky, H., Etsella, T., Ivey, D. G., and Omotoso, O. (2006). Fundamental particle size of clay minerals in Athabasca oil sands tailings, Clay Science Journal, 12, 217-222.

Kenawy, E. R. (1998). Recent advances in controlled release of agrochemicals. Journal of Macromolecular Science, Part C: Polymer Reviews, 38, 365–390.

Lee, I., Lee, H., Cheon, J., and Reddi, L. (2003). Evaporation theory for deformable soils. Journal of Geotechnical and Geo-environmental Engineering, 129, 1020–1027.

Mackinnon, M., Matthews, J., Shaw, W., and Cuddy, R. (2010). Water quality issues associated with composite tailings (CT) technology for managing oil sands tailings. International Journal of Surface Mining, Reclamation and Environment, 15 (4), 235–256.

Matthews, J., Shaw, W., Mackinnon, M., and Cuddy, R. (2002). Development of composite tailings technology at Syncrude. International Journal of Surface Mining, Reclamation and Environment, 16(1), 24–39.

Miller, G. (2010). Comparison of geoenvironmental properties of caustic and noncaustic oil sand fine tailings. PhD. thesis, department of Civil and Environmental Engineering, University of Alberta, Edmonton, Alberta, Canada.

Mitchell, J. K, Soga, K. (2005). Fundamentals of soil behavior (3rd ed.). New York, NY: John Wiley and Sons Inc.

Miyamoto, H., Chikushi, J., and Kanayama, M. (2009). Coupled measurements of water content and electrical conductivity in dielectrically Lossy clay slurry using a coated TDR probe. Journal of Soils and Foundations, 49, 175–180.

Omotoso, O. E., and Mikula, R. J. (2004). High surface areas caused by smectitic interstratification of kaolinite and illite in Athabasca oil sands. Applied Clay Science, 25(2004) 37–47.

Ouellet, S., Bussière, B., Aubertin, M., and Benzaazoua, M. (2007). Microstructural evolution of cemented paste backfill: Mercury intrusion porosimetry test results. Cement and Concrete Research Journal, 37, 1654–1665.

Pipilikak, P., and Beazi-Katsioti, M. (2009). The assessment of porosity and pore size distribution of limestone Portland cement pastes. Journal of Construction and Building Materials, 23, 1966–1970.

Roshani, A., Fall, M., and Kennedy, K. (2017). Drying behavior of mature fine tailings pre-dewatered with superabsorbent polymer (SAP): column experiments. Geotechnical Testing Journal, 40 (2), 210-220.

Schröf, C., Mechtcherine, V., Gorges, M. (2012). Relation between the molecular structure and the efficiency of superabsorbent polymers (SAP) as concrete admixture to mitigate autogenous shrinkage. Cement and Concrete Research, 42, 865–873.

Simms, P., Grabinsky, M., and Zhan, G. (2007). Modelling evaporation of paste tailings from the Bulyanhulu mine. Canadian Geotechnical Journal, 44, 1417–1432.

Suarez, D. L., Rhoades, J., Lavado, R., and Grieve, C. M. (1984). Effect of pH on saturated hydraulic conductivity and soil dispersion1. Soil Science Society of America Journal, 48, 50-55.

Suthaker, N., and Scott, J. (1996). Measurement of hydraulic conductivity in oil sand tailings slurries. Canadian Geotechnical Journal, 33, 642–653.

Sworska, S., Laskowski, J. S., and Cymerman, G. (2000). Flocculation of the Syncrude fine tailings Part I. Effect of pH, polymer dosage and Mg^{2+} and Ca^{2+} cations. International Journal of Mineral Processing, 60, 143–152.

Tabbagh, A., and Cosenza, P. (2007). Effect of microstructure on the electrical conductivity of clay-rich systems. Journal of Physics and Chemistry of the Earth, 32, 154–160.

Timoney, K., and Lee, P. (2009). Does the Alberta tar sands industry polute? The scientific evidence. Journal of Open Conservation Biology, 3, 65-81.

Yao, Y., Tol, F., and Paassen, L. (2012). The effect of flocculant on the geotechnical properties of mature fine tailings: an experimental study. Proceeding in the 3rd International Oil Sand Tailings Conefernce, Edmonton, Canada, 391–398.

7 Effect of wetting-drying cycles on the desiccation behavior of oil sands mature fine tailings pre-dewatered with a superabsorbent polymer

Anis Roshani, Mamadou Fall, Kevin Kennedy

Submitted

ABSTRACT

The main objective of this investigation is to understand the desiccation behavior of mature fine tailings (MFT) pre-dewatered with superabsorbent polymer (SAP) with respect to wetting-drying cycles. Raw MFTs and pre-dewatered MFTs were subjected to five cycles of wetting and six cycles of drying. Evaporation was found to be the dominant mechanism in the dewatering of raw MFTs as well as MFTs dewatered with SAP. In both cases, the suction developed in each drying cycle was eliminated temporarily by the succeeding wetting cycle. The solids content of the MFTs pre-dewatered with SAP increased to 98% (from an initial 50%) after 25 days of drying the second lift. The minimum solids content within the column was found to be around 70 %, which corresponded to a vane shear strength of 4.5 kPa. Based on the digital images of the surface, the crack intensity factors (CIF) of the raw MFTs and MFTs pre-dewatered with SAP were calculated to be 26% and 14%, respectively. At the same time, wetting-drying cycles did not affect the initiation and development of cracks. Scanning electron microscopy (SEM) and mercury intrusion porosimetry (MIP) analysis, indicate that the MFTs pre-dewatered with SAP after 25 days of evaporation in the second lift exhibits the most compacted texture. It was found in this study, that seasonal precipitation could not prevent suction from being developed in the two-lift deposition system. Hence, dewatering of MFTs with SAP in combination with atmospheric drying might be a promising approach for MFTs management and reclamation of dedicated disposal areas.

Keywords: Evaporation, Mature fine tailings, Superabsorbent polymer, Dewatering, Strength

7.1 Introduction

The process of oil sand extraction has been an on-going challenge in Alberta, Canada for the past five decades. Bitumen production from oil sands is commonly based on open-pit mining and a water-based process, the so called Clark Hot Water Extraction process (CHWE) (Clark and Pasternack, 1932). The process produces a tailings stream that consists of water, sand, silt, clay and residual bitumen. The by-product stream either is discharged directly into tailings ponds or goes through a cyclone or thickener. In the tailings pond, the deposited tailings undergo segregation (Beier et al., 2013). Coarse sands settle quickly while clays and fine particles (< 45 μm) deposit slowly and form a gel-like suspension, which is referred to as mature fine tailings (MFT). the solids content in MFTs reaches about 30% within two years and further consolidation (or creep) takes several decades (Jeeravipoolvarn et al., 2009).

After mining, large pits, tailings ponds, and overburden are left behind, which makes it necessary to reclaim the affected area. Strict regulations have driven scientists to better understand the environmental impact of oil sands mining operations. The treatment and management of mature fine tailings were undertaken to meet Directive 074 (Tailing Performance Criteria and Requirement for Oil Sand Mining Schemes) issued by the Energy Resources Conservation Board (ERCB). It is referred to as the first step in regulating tailings management. The directive mandated a minimum undrained shear strength of 5 kPa for any fine tailings deposited in the previous year. Five years after active deposition, the deposit must reach an undrained vane shear strength of 10 kPa and be ready for reclamation. Thus, the treatment of MFTs to improve its consolidation behavior and strength has received significant attention in recent years. Different reclamation strategies are currently being used or tested to reduce the MFTs inventory.

Consolidated tailings (CT) technology was the first commercial process to be used for oil sand tailings management. In this process, coarse sand and gypsum are mixed with MFTs to form a non-segregating mixture that can release pore water through self-weight consolidation (Mackinnon et al., 2010; Chalaturnyk et al., 2002; Caughillet al., 1993). The released water, which is rich in calcium and sulphates, is recycled during the extraction process. However, the recycled water has a detrimental impact on the extraction process and interferes with bitumen extraction efficiency (Mackinnon et al., 2010; Pramanik, 2016). Hence, chemical modification (use of polymeric

flocculants) is being considered as an alternative for CT. A number of studies (Botha and Soares, 2015; Demoz and Mikula, 2012; Salam et al., 2016; Al-Hashmi et al., 2013; Sworska et al., 2000; Beier et al., 2013) were carried out to evaluate the flocculation performance and behavior of MFTs as well as the effect of water chemistry, bitumen content, and particle size distribution on tailings flocculation. It has been shown that the use of flocculants results in faster dewatering, drying, and consolidation of MFTs. Although flocculation is commercially implemented by the industry, the chemically modified deposits may exhibit metastable and sensitive behavior (Beier et al., 2013).

One of the primary drying (dewatering) technologies for MFTs is environmental (atmospheric) drying which can be applied either during initial deposition or during the thickening process (Beier et al., 2013; Fasking et al., 2011). Evaporation and self-consolidation are the main mechanisms involved in the atmospheric drying process. The relatively low operational cost of atmospheric drying makes it an economically viable approach. The deposited materials, however, relies on additional dewatering techniques, such as settlement, drainage, and freeze-thawing. The major drawback in this process is that the efficiency of atmospheric drying is dependent on the weather conditions. Moreover, warm and dry weather condition are generally short in northern Alberta, the province with the largest oil sands reserves in Canada.

Conceptually, the drying efficiency of thin lifts (<30 cm) is much greater than that of thick lifts (>30 cm) because the formation of a crust on the tailings surface inhibits evaporation from saturated zones (Junqueira et al., 2011; Caldwell et al., 2014). Therefore, the buried layer needs a longer time to gain strength than the unburied one. Furthermore, from an operational point of view, the soft material beneath the crust controls the geotechnical behavior of the deposit. Thus, a multi-lift deposition technique cannot be applied if the freshly deposited lift eliminates the suction developed in the previously buried lift as this causes instability (Fasking et al., 2011; Gidley, 2016). However, thin-lift drying alone is not an efficient dewatering method and should be combined with other techniques to meet both operational and reclamation closure goals.

Previous studies (Farkish and Fall, 2013) have shown that a superabsorbent polymer (SAP) can significantly dewater MFTs and speed up the atmospheric drying process. Subsequent investigations by Roshani et al. (2016a,b) and (2017a,b) also indicated that the combination of SAP-based dewatering of MFTs with a two-lift deposition system considerably increases the drying of the MFTs layers, which could be a promising approach for MFTs management and

reclamation of dedicated disposal areas. However, to determine the field efficiency of the aforementioned approach (multi-lift deposition of MFTs pre-dewatered with SAP), investigating the desiccation behavior of MFTs pre-dewatered with SAP under the climatic conditions prevalent in northern Alberta is essential. As mentioned earlier, the multi-lift deposition technique relies on atmospheric conditions. Although the highest drying potential exists in summer, the negative effect of precipitation on the evaporation rate and developed suction should not be discounted. Till date, no targeted attempt has been made to understand the effect of wetting-drying cycles on the desiccation behavior of MFTs pre-dewatered with SAP in multi-lift deposited tailings. Thus, addressing this knowledge gap is a critical step forward in understanding the evaporation and drying mechanism in multi-lift deposition systems with respect to wetting-drying cycles and subsequent strength gain. This can help in optimizing land use and maximizing storage capacity. The need to understand the effect of wetting-drying cycles on the desiccation behavior of MFTs pre-dewatered with SAP resulted in the present experimental study, which utilizes column experiments to investigate the effect of wetting and drying cycles on the desiccation behavior of thin lifts of MFTs pre-dewatered with SAP. This study highlights the impact of wetting-drying cycles on the water distribution, strength gain and loss, settlement, and crack formation with respect to testing time and column height. Moreover, the initiation and evolution of cracks in periodic wetting-drying cycles induced by seasonal rainy and sunny weather were monitored and the mechanisms involved are discussed.

7.2 Materials and methods

7.2.1 Material characteristics and preparation

7.2.1.1 Mature fine tailings

The MFTs used in this particular study was procured from an oil sand company in Alberta, Canada. The fraction of fines (<44 μm) in the MFTs was around 95%. The initial solids content was 45% and the average specific gravity of the tailings was 2.37. The liquid limit (LL) and plastic limit (PL) of the MFTs were 51.2 and 37.2, respectively. The plasticity index (PI) of the MFTs was 14 while the activity (A) was 0.77, which is the value reported for a normal clay. Based on mineralogical analysis, the mineral content was found to be composed of 33.6% quartz, 31.3% kaolinite, and 21.8% muscovite.

7.2.1.2 Superabsorbent polymer (SAP)

A superabsorbent polymer is a high molecular weight crosslinked hydrophilic network that can absorb and retain huge amounts of water or aqueous solutions, as high as 10–1000 grams per gram of polymer. The water imbibing mechanism of an SAP is based on the physical entrapment of water via capillary forces in its macroporous structure and hydration of its functional groups. Hence, squeezing or pressure does not impact the SAP water absorption capacity. The high water removal efficiency of SAP has been beneficial in the dewatering of fine coal slurry and domestic sludge as well as in the densification of barrier design (Masuda and Iwata, 1990; Kuai, 2000; Dzinomwa et al., 1997; Peer and Venter, 2003; Fall et al., 2010). In addition, SAP is capable of absorbing large quantity of MFTs pore water (Farkish and Fall, 2013). A commercially available crosslinked insoluble sodium polyacrylate was used as the SAP in this study; 1 g of the polyacrylate SAP can absorb 107 g of MFTs water (Farkish and Fall, 2013).

7.2.1.3 Pre-dewatering of MFTs with SAP

MFTs was mixed with 1% SAP (wt. %) for five days in a mixer with a mixing period of one hour per day. For the rest of the day, the mixture was allowed to rest in the mixer, which was covered to prevent evaporation. In this study, small sachets were used to hold the polymer. These sachets serve to separate the swollen polymer from the dewatered MFTs.

7.2.2 Column setup and procedures

A schematic diagram of the developed column is shown in Figure 7.1. A Plexiglas column (45 cm x 45 cm) with a 50 cm height and bottom drainage was equipped with a network of sensors. Four 5TE sensors (Decagon Devices Inc.) were employed to monitor the volumetric water content and electrical conductivity while four MPS-6 sensors (Decagon Devices Inc.) were used to monitor the suction and temperature. The sensors were placed at heights of 2 cm, 10 cm, 17 cm, and 25 cm for monitoring suction and water content. A 3 cm thick layer of saturated gravel was placed at the bottom of the column covered with a coarse filter paper for holding the tailings and preventing them from going through the drainage layer. The rate of drainage was monitored by measuring the amount of water that was collected from the drainage outlet located at the base of the column. The setup is mounted on a scale to record water loss by evaporation and calculate the evaporation rate.

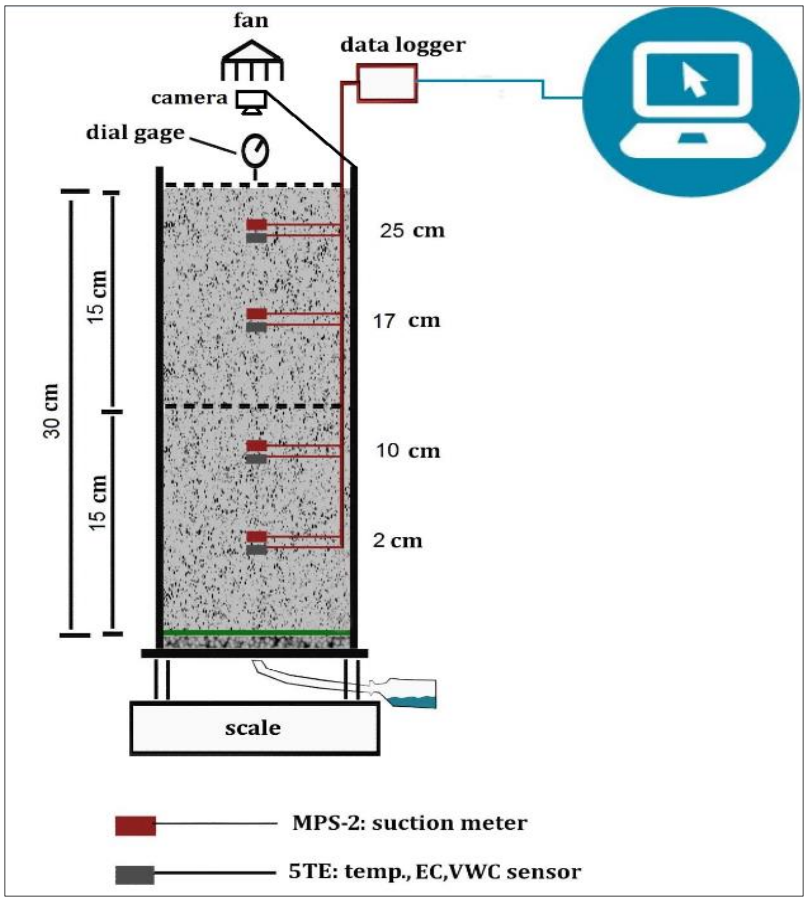

Figure 7. 1, Schematic diagram of the developed experimental setup

In the lab-scale test, the initial layer was dried for 5 days. After 5 days of drying, the second lift of the MFTs pre-dewatered with SAP was placed on top of the previously placed lift and allowed to dry for 25 more days. Each lift was 15 cm high. A digital camera was fixed above the column to monitor the crack patterns. Image processing techniques were used to calculate the crack intensities at different water contents. Rainfall simulation system was manually. A regular soil auger (5 cm x 5 cm) was used to take samples after 4, 13, 18, and 30 days without disturbing the rest of the column. The walls of the dug hole were covered with metal sheets in a precise manner to prevent evaporation. Samples taken from different locations at heights of 2 cm, 10 cm, 17 cm, and 25 cm were subjected to various analytical techniques or tested to analyze the water content (ASTM D2216), void ratio, morphology (by scanning electron microscopy (SEM)), porosity (by mercury intrusion porosimetry (MIP)), and vane shear strength (ASTM D4648).

7.2.3 Application of wetting-drying cycles

The period of wet and warm weather is short in northern Alberta and 70% of the total annual precipitation occurs during June to August (Owolagba and Azam, 2015). The average values of the precipitation, relative humidity, and wind speed in the region for the last 30 summers have been reported to be 67 mm, 68%, and 34 km/h, respectively (Owolagba and Azam, 2015). The wetting-drying cycles adopted in this study are based on the average precipitation pattern in Fort McCurry during the last ten years. In the last 10 years period, the average number of rainy days in August was ten and the average precipitation period in each day was one hour. On an average, in each August, six cycles of drying and five cycles of wetting could be identified, as shown in Table 7.1.

Table 7. 1, Average wetting-drying cycles in August in northern Alberta, Canada

Day	**1**	**2**	**3**	**4**	**5**	**6**	**7**	**8**	**9**	**10**	**11**	**12**	**13**	**14**	
Precipitation (mm)	0		7	0	5	0	10	4	0					5	
Wetting (W) Drying (D)	D		W	D	W	D	W		D					W	
Day	**15**	**16**	**17**	**18**	**19**	**20**	**21**	**22**	**23**	**24**	**25**	**26**	**27**	**28**	**29**	**30**
Precipitation (mm)	0				2	4	20	7	0							
Wetting (W) Drying (D)	D				W				D							

7.2.4 Microstructural analyses and mechanical tests

The particle size distribution and morphology of the samples were analyzed by SEM using a Hitachi 3500-N microscope. In addition, the pore size distribution and porosity of the soil matrix were analyzed by MIP on an Auto-pore III 9420 mercury porosimeter.

A vane shear test was conducted to determine the strength of the MFT samples in accordance to (ASTM D4648). This method is based on measuring the torque required to shear the sample.

7.3 Results and discussion

7.3.1 Evaporation and drainage

Sedimentation, self-weight consolidation, evaporation from the surface, and downward drainage are the mechanisms responsible for dewatering in the tailings deposits (Fisseha et al., 2010; Theriault et al., 2003; Hoz et al., 2013). However, evaporation is the most dominant drying mechanism and is mainly responsible for the increase in the solids content (Junqueira et al., 2011; Gidley and Jeeravipoolvarn, 2016).

The results of the evaporation rate and cumulative evaporation analysis are shown in Figure 7.2. The initial evaporation rate of the raw MFTs and pre-dewatered MFTs were approximately 1.04 and 0.84 cm/day, respectively. The difference in the initial evaporation rates of the raw MFTs and the MFTs pre-dewatered with SAP could be due to the higher initial water content of raw MFTs. This initial rate of evaporation is followed by a moisture limiting period in which evaporation reached a residual value unless the next wetting period took place or another lift was added. After casting the second lift on day 5 and after the 2^{nd} and 3^{rd} wetting cycles on days 7 and 8, the evaporation rates increased to 1.23 and 1.5 cm/day for raw and pre-dewatered MFTs, respectively. The fluctuations in the evaporation rate from day 15 to 25 are related to the 4^{th} and 5^{th} wetting cycles. The residual evaporation rates of raw and pre-dewatered MFTs are 0.43 and 0.32 cm/day, respectively. Cumulative water loss by evaporation was measured to be around 30 kg for raw MFTs and 27 kg for MFTs pre-dewatered with SAP. The average room temperature and humidity were maintained at 21.5 °C and 45%, respectively, throughout these experiments.

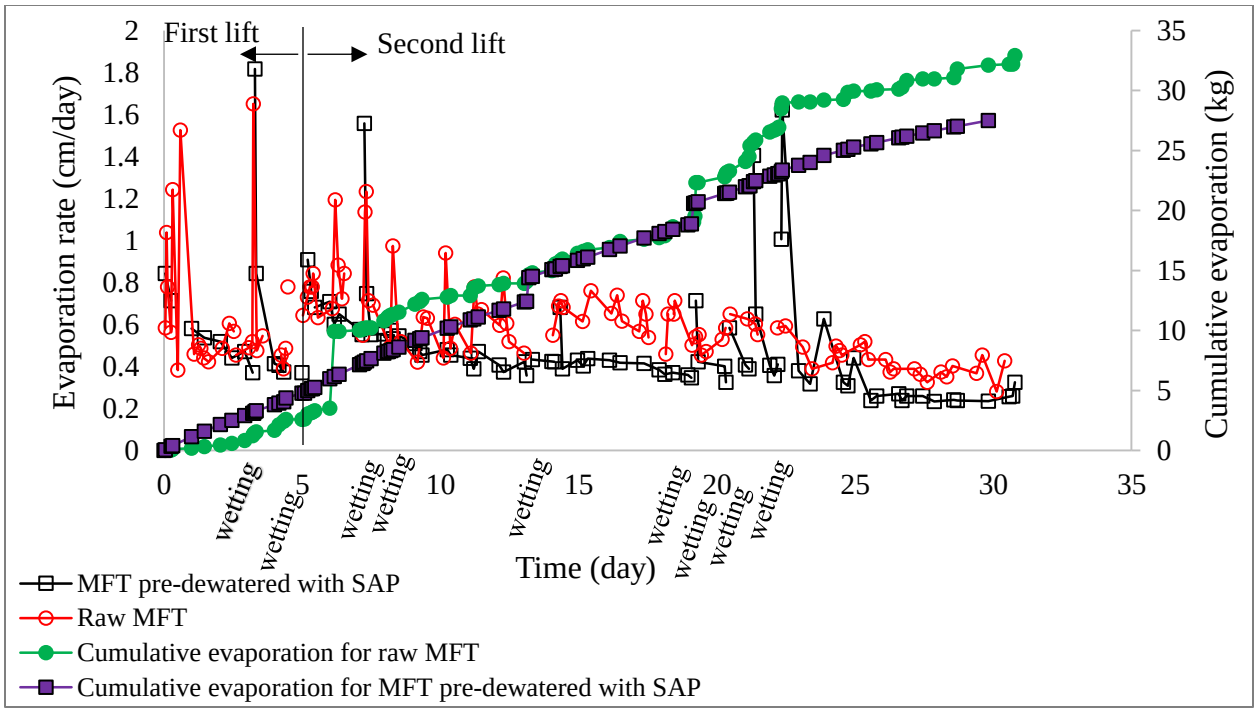

Figure 7.2, Evaporation rate for the raw MFTs and dewatered MFTs

Figure 7.3 shows the rate of drainage and cumulative drainage of raw MFTs and MFTs pre-dewatered with SAP. The two big shifts in the drainage rate of the MFTs pre-dewatered with SAP are related to two intensive wetting cycles on day 7 (10 mm/day) and day 21 (20 mm/day). The cumulative drainages of raw MFTs and pre-dewatered MFTs after 30 days were 3.4 kg and 1.3 kg, respectively. Such high reduction (62%) in the drainage water in MFTs pre-dewatered with SAP can minimize the risk of seepage of toxic tailings water from the tailings ponds which can cause groundwater contamination.

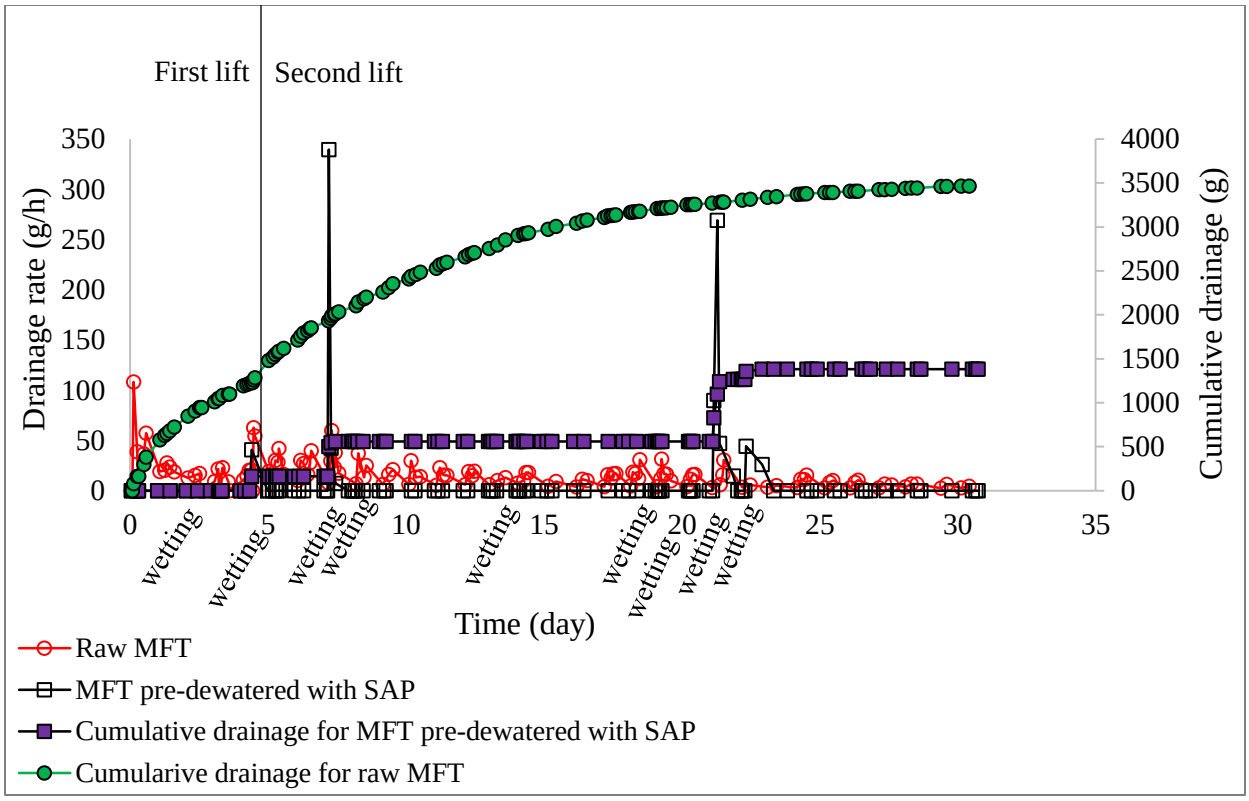

Figure 7.3, Drainage rate for the raw MFTs and dewatered MFTs

7.3.2 Suction

MFTs and pre-dewatered MFTs are shown in Figures 7.4 and 7.5, respectively. The results for raw MFTs showed that no suction was developed in the first lift (2 cm and 10 cm). A freshly added layer on top of the first lift that covers the evaporation boundary of the first lift and water drainage from the new lift due to gravity into the first lift are the main factors that prevent suction from being developed in the first lift. At the end of six wetting cycles (day 30), suction in the raw MFTs varied from 150 kPa to 27000 kPa in the height range of 17 cm to 25 cm.

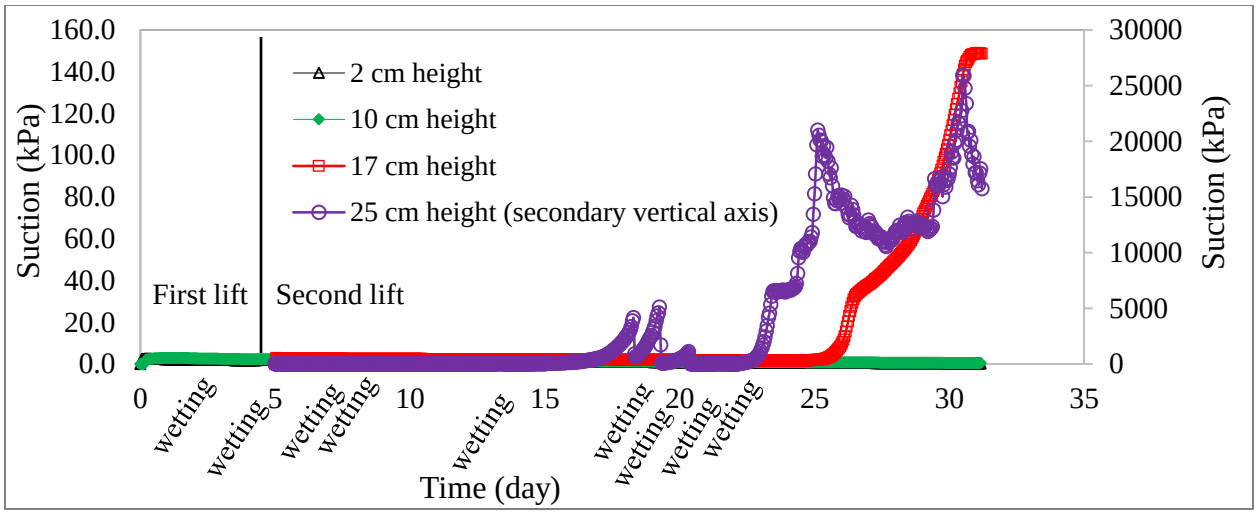

Figure 7.4, Suction evolution for raw MFTs with respect to the wetting-drying cycles

In contrast, in the case of pre-dewatered MFTs, a more uniform suction could be observed in the entire column. The higher value of suction may due to the lower initial water content of the MFTs pre-dewatered with SAP (50%) in comparison with the raw MFTs (120%). Suction was developed on top of the first lift (10 cm) immediately after casting the first lift and it showed an increasing trend until the second lift was added. In addition to the infiltration of water from the freshly added lift into the previously placed lift, wetting cycles on the 5^{th}, 7^{th}, 8^{th}, and 14^{th} days of the test period eliminated the developed suction at this location. At a height of 2 cm from the bottom of the column, suction was not developed until day 27 when cracks reached the lower part. After this time period, suction increased and reached a value of 50 kPa on the last day. A rapid divergence could be observed in the suction at a height of 25 cm on day 11 and after a sharp decrease on day 14 (wetting cycle), it was almost zero. The rise and fall in the measured suction between days 14 and 24 is due to the fifth cycle of wetting and drying. Again, on day 24, the developed suction exhibited an increasing trend (at 25 cm height) until cavitation took place at 100,000 kPa. At a height of 17 cm, after fluctuations between days 16 and 21, suction started to increase at day 23 and reached a maximum on day 25 after which cavitation occurred.

The dewatering of MFTs with SAP created a highly heterogeneous texture in the tailings, which may significantly influence the desiccation behavior. Figure 7.11e shows an aggregated MFTs with a patchy and clogged matrix in which cracks act as the boundaries of the aggregates. The binding inside each aggregate is much stronger than the adhesion between separate aggregates. As a result, the contact regions between the aggregates contained macropores. These macropores are

drained easily and consequently, suction developed faster and more uniformly in MFTs pre-dewatered with SAP in comparison to raw MFTs. Similar observations were reported previously by other researchers (Li & Zhang, 2011; Bajwa and Simms, 2013; Carminati et al., 2008; Lebron et al., 2002).

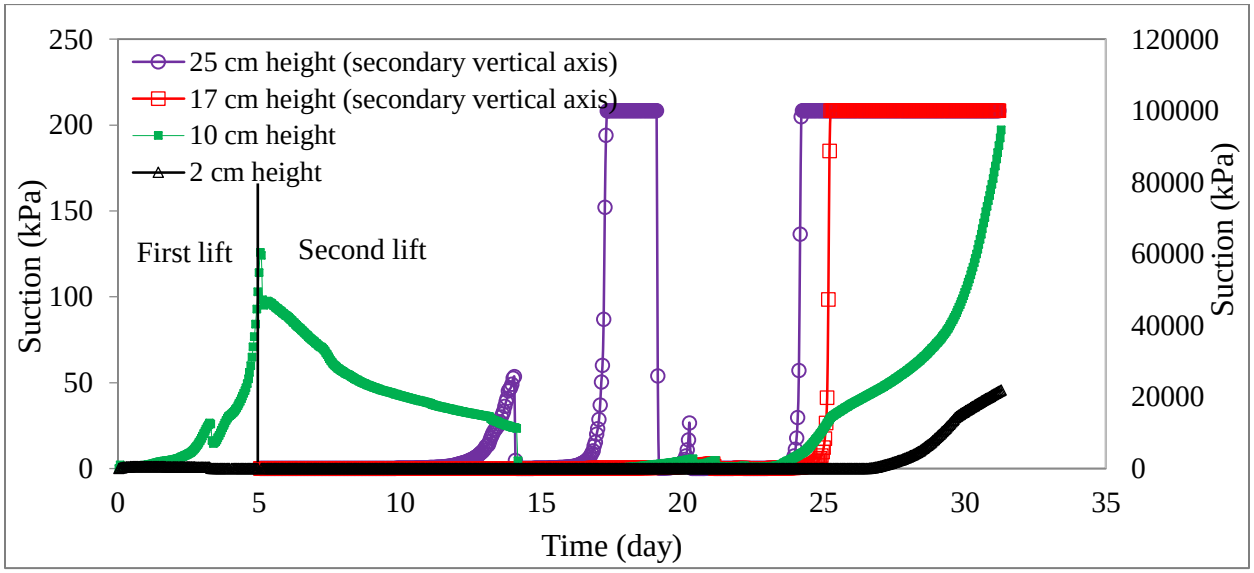

Figure 7.5, Suction evolution for MFTs pre-dewatered with SAP with respect to the wetting-drying cycles

7.3.3 Volumetric water content

Figures 7.6 and 7.7 show the evolution of water content in the raw and pre-dewatered MFTs, respectively. In both cases, an expected pattern was observed. The top portion of the first lift dried faster than the lower parts due to evaporation at the evaporation boundary. As can be seen in Figure 7.6, the addition of the second lift strongly affected the top portion of the first lift (10 cm), most likely due to the high water content of the freshly added layer draining into the first lift due to gravity; the upper part of the first lift and lower part of the second lift had very similar water contents until day 22. At this stage, cracks penetrated deeper and the drying front progressed downwards. Thus, the water content decreased at a height of 17 cm and the solids content increased from 53% on day 22 to 79% on the final day of the test period.

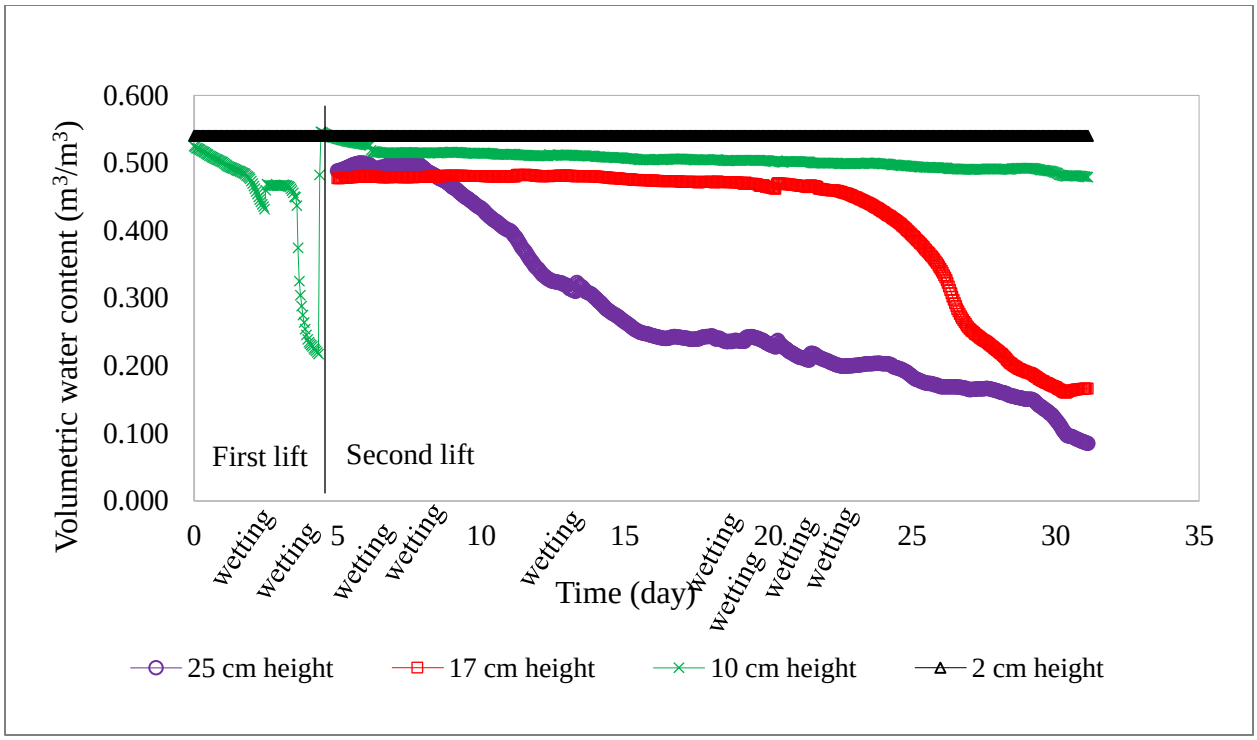

Figure 7.6, Variation of water content with time with respect to the wetting-dying cycles for raw MFTs

In pre-dewatered MFTs (Figure 7.7), the water content at a height of 25 cm decreased sharply immediately after casting the second lift and was almost zero on day 23 in the second lift. By the end of the test period, the minimum solids content in the column was measured to be around 70% (Figure 7.8). According to Figures 7.6 and 7.7, the wetting effects of the added lift and wetting cycles are temporary and previously developed suction can be satisfactorily made up in the next drying cycle.

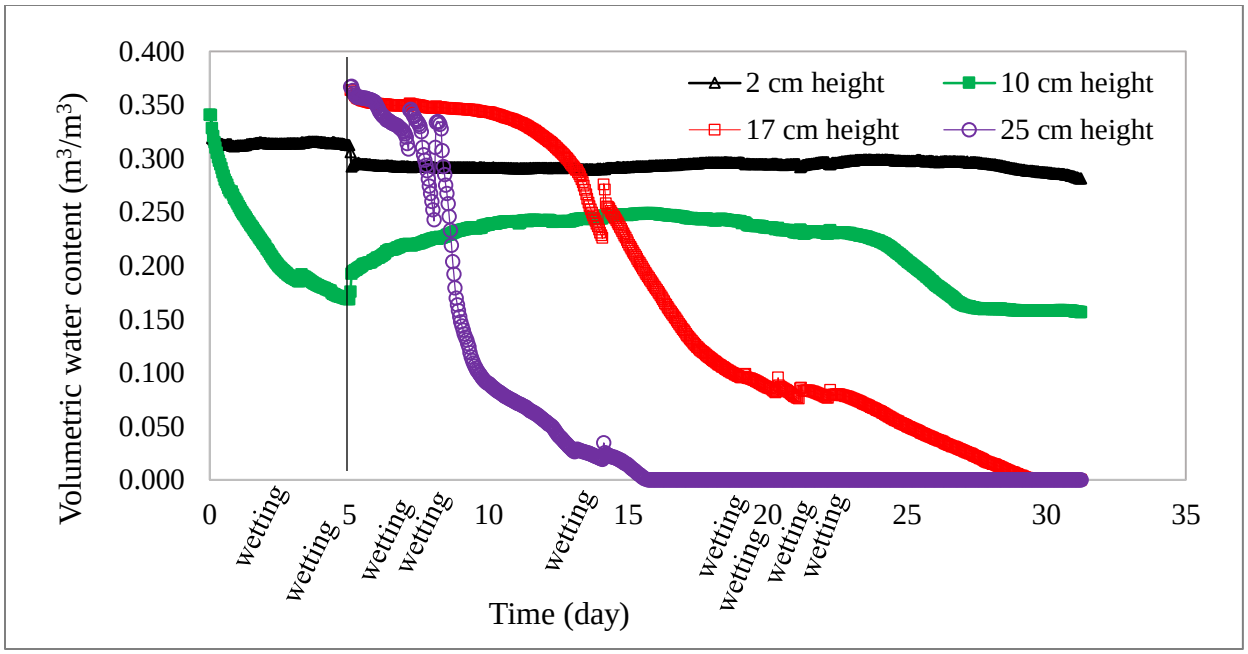

Figure 7.7, Variation of water content with time with respect to the wetting-dying cycles for MFTs pre-dewatered with SAP

The lower water content in the MFTs pre-dewatered with SAP as compared to raw MFTs is most likely due to the lower initial water content of MFTs pre-dewatered with SAP (52%) than raw MFTs (120%).

7.3.4 Vane shear strength

The test results of the vane shear strengths of the raw MFTs and the MFTs pre-dewatered with SAP are shown in Figure 7.8. In both raw and pre-dewatered MFTs, the solids contents in the upper locations are higher than those at lower locations. The highest solids content (98%) was found in the sample sourced at a height of 25 cm in pre-dewatered MFTs with a shear strength of 1.0 MPa. In the same column, the lowest measured solids content was 70% corresponding to a vane shear strength of 4500 Pa. On the other hand, in the case of raw MFTs, the highest solids content was 85% and half of the column (first 15 cm) exhibited a strength less than 2 kPa.

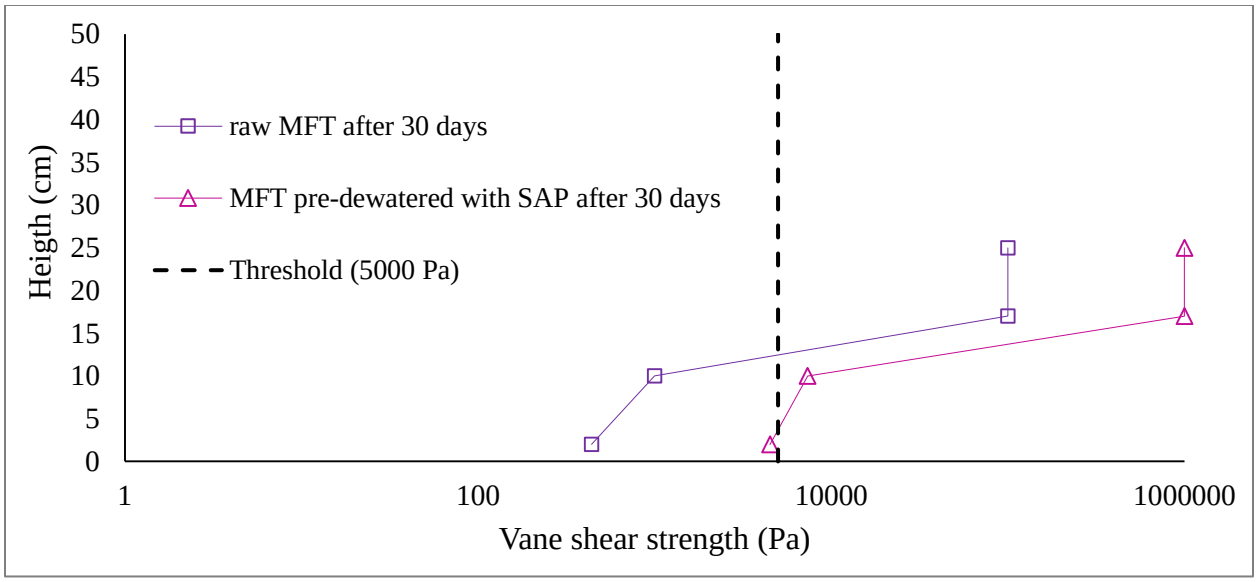

Figure 7.8, Vane shear strength with respect to the column height

7.3.5 Cracking

Desiccation cracks formed as a result of matrix suction induced by drying and shrinkage penetrate the MFTs layer slowly towards the base of the deposit (Carol et al., 1999). Cracking is a key dewatering process that reduces the flow path and compensates for the negative impact of the crust (Simms et al., 2007; Fujiyasu and Fahey, 2000; Gidley, 2016).

The extent of surficial cracking is described by the crack intensity factor (CIF) which is defined as the ratio of the surface crack area to the total surface area of the clay (Miller et al., 1999). Figures 7.9 and 7.10 illustrate the variation in CIF with respect to the testing time and wetting-drying cycles in raw MFTs and MFTs pre-dewatered with SAP, respectively. Three distinct stages of crack initiation and development can be identified in these graphs. In the initial stage (Figures 7.11a and 7.11e), cracks developed slowly upon decreasing the water content and based on its heterogeneity, new cracks appeared randomly in the matrix (Li and Zhang, 2011). The desiccation process can be accelerated in the primary stage. In this stage, the cracks became wider and deeper and formed a polygonal network; furthermore, new cracks were formed (Figures 7.11b and 7.11f). As shown in Figure 7.2, the rate of evaporation in the first five days after loading each lift (the primary stage) increased rapidly. The reason for this phenomenon can be described as follows - in addition to vertical evaporation from the surface, horizontal evaporation from the crack walls takes place, thus increasing the rate of evaporation (Li and Zhang, 2011). When the water vapour

concentration gradient between the soil and the atmosphere was almost zero, the evaporation rate and crack propagation were limited and consequently a steady state was attained. In this study, ImageJ software, which works on the principle of image segmentation, was used to measure the CIF. More precisely, during image segmentation, cracks were depicted in white and the MFTs surface matrix was depicted in black.

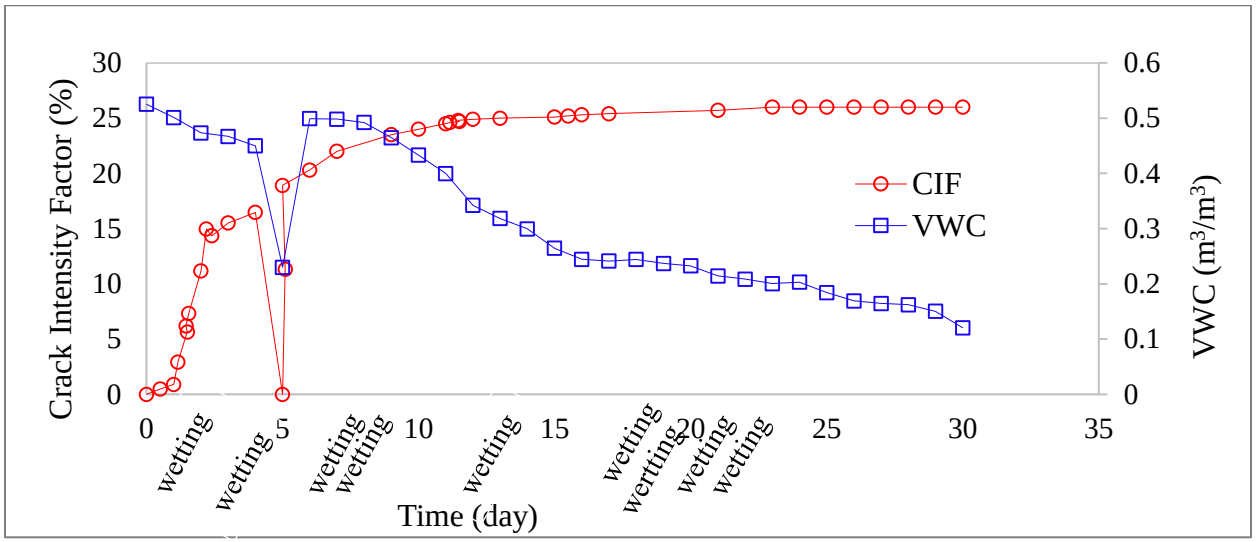

Figure 7.9, Relationship between CIF and surface water content (25 cm height) for the raw MFTs

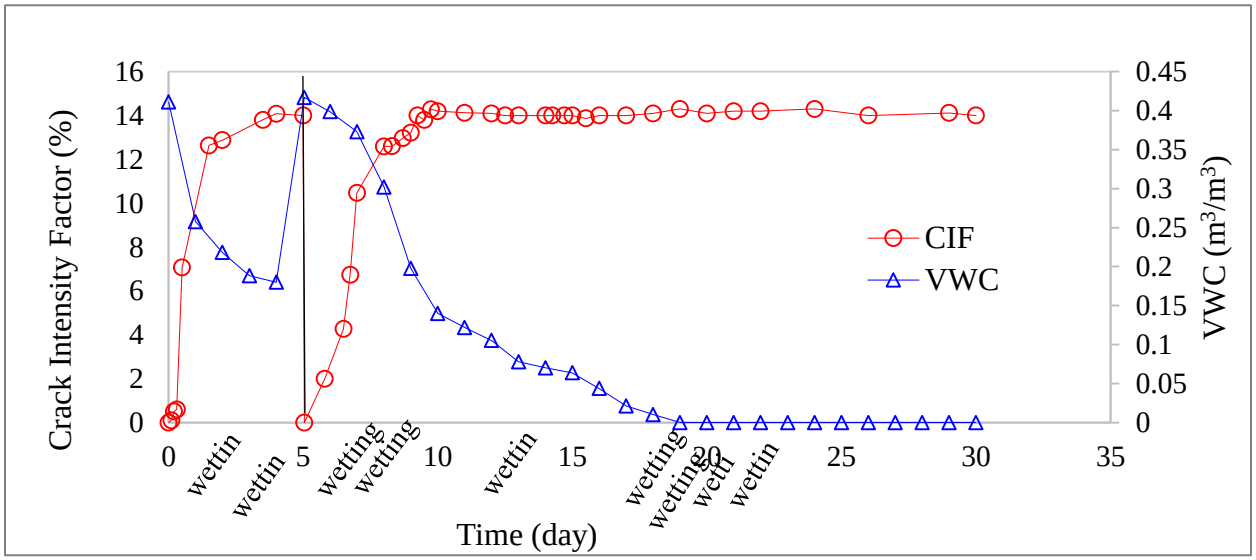

Figure 7.10, Relationship between CIF and surface water content (25 cm height) for the pre-dewatered MFTs

As shown in Figure 7.9, during the first day of drying, the CIF increased slowly (this time period is considered to be the initial stage). The CIF increased rapidly during the next four drying days. On the fifth day, the second lift was added and subsequently crack formation started after 2 h; the

CIF increased from zero to 19% in the same day. The surface crack area increased from 19% (volumetric water content of 0.4 m^3/m^3) to 25.7% (volumetric water content of 0.2 m^3/m^3) on day 21. On approaching the shrinkage limit of 13% gravimetric water content (Roshani et al., 2017), a steady state was attained. At the end of the test period, the CIF approached a steady state of approximately 26% and although suction increased and water content decreased, there was no change in the CIF. In this stage, the development of cracks is affected by moisture conduction from the depths of the MFTs and hence, it lasted longer. Rewetting did not close or reduce the volume of the cracks.

In the case of the MFTs pre-dewatered with SAP, cracking and lateral shrinkage away from the wall started almost 6 h after casting the first lift. As depicted in Figure 7.10, during the first day of drying, crack initiation and propagation increased slowly to 0.5% (initial stage). From the end of the first day to the fourth day, the CIF increased rapidly until it reached a value of 13.8%. The high rate of increase in the crack surface area indicates the onset of the primary stage in crack development. After casting the second lift on day 5, cracks started forming within 5 h after the placement of the second lift. Five days after loading the second lift, crack development was limited and from day 10 to the end of the test period, the CIF exhibited a constant value of 14%, which implies that the crack development reached a steady state. Based on the graph in Figure 7.10, in the initial stage, the volumetric water content decreased from 0.40 m^3/m^3 to 0.35 m^3/m^3 and in the primary stage, the water content decreased from 0.35 m^3/m^3 to 0.18 m^3/m^3, after which it remained constant (steady state). With good deviation, the shrinkage limit of 0.17m^3/m^3 (Roshani et al., 2017) is close to the water content in the steady state.

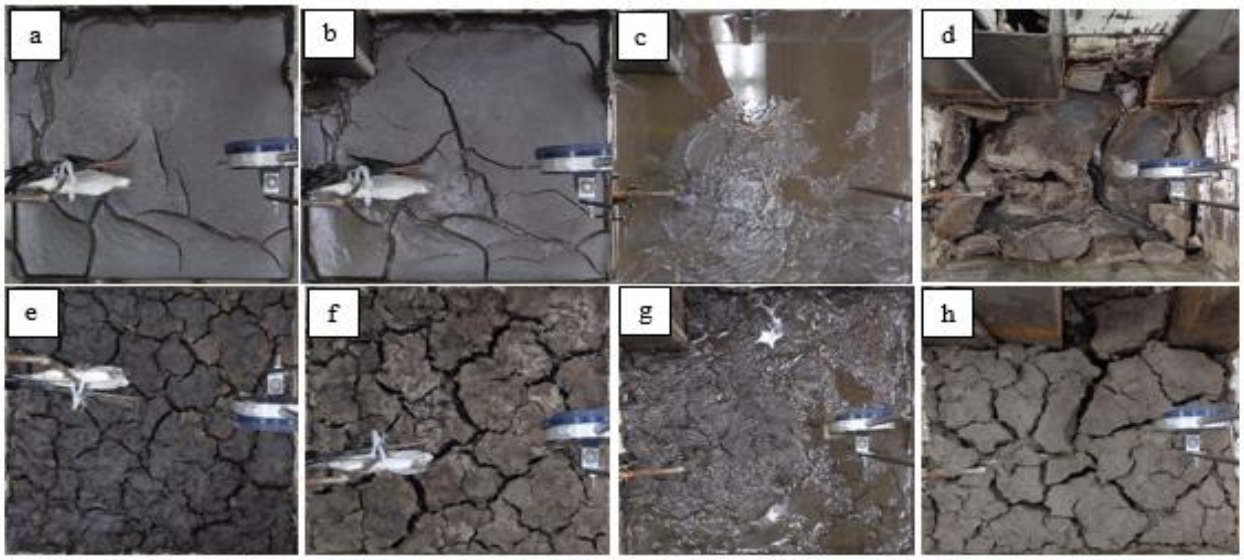

Figure 7.11, Surface desiccation crack pattern - a) raw MFTs after two days of drying the first lift, b) raw MFTs after 5 days of drying the first lift, c) raw MFTs after casting the second lift and second cycle of wetting, d) raw MFTs after 30 days, e) MFTs pre-dewatered after one day of drying the first lift, f) MFTs pre-dewatered after 5 days of drying the first lift, g) MFTs pre-dewatered after casting the second lift and second cycle of wetting, and h) MFTs pre-dewatered after 30 days of drying

7.3.6 Settlement

In the saturated state, volume change is related to the volume of removed water. Due to the development of suction, additional volume changes that result in further shrinkage occur (Junqueira et al., 2011). Figure 7.12 shows the cumulative settlement of raw MFTs and MFTs pre-dewatered with SAP. The cumulative settlements of raw MFTs and pre-dewatered MFTs in the test period were measured to be around 100 mm and 40 mm, respectively. The higher settlement of raw MFTs is due to its higher water content and higher drainage (Figure 7.3). The higher rate of settlement for raw MFTs can be explained by its higher rate of evaporation and drainage (Figures. 7.2 and 7.3).

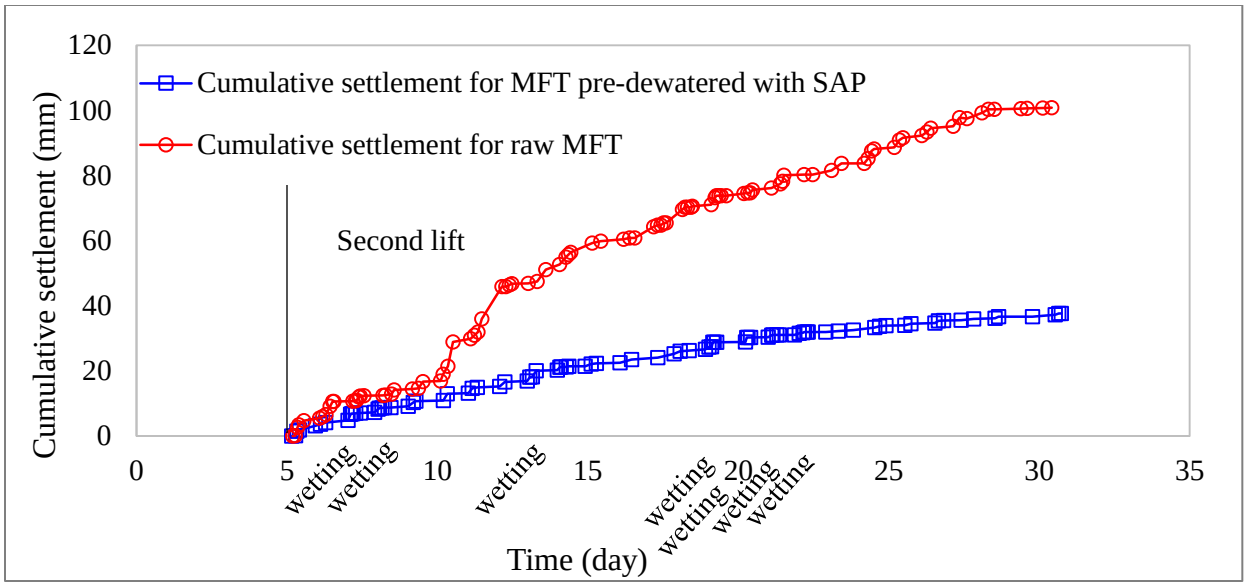

Figure 7.12, Cumulative settlement for the raw MFTs and pre-dewater MFTs

7.3.7 Mercury intrusion porosimetry

MIP was carried out to determine the pore size distribution and analyze the arrangement and distribution of pores and their connectivity in different soils. A non-wetting fluid (mercury) under pressure is allowed to intrude the voids of a porous medium and the pore width related to the highest rate of intrusion is defined as the threshold diameter (TD). It has been experimentally proven that an increase in the fine content leads to a decrease in the TD value (Fall et al., 2005). The MIP tests were carried out on different samples obtained at 25 cm from raw MFTs and pre-dewatered MFTs after 13 days (at the end of the 4th drying cycle) and 30 days (at the end of the 6th drying cycle). This allows us to understand the effect of SAP pre-dewatering and evaporation on the microstructure of the MFTs matrix. The MIP results are presented in Figures 7.13 and 7.14. It can be understood from Figure 7.13 that the MFTs pre-dewatered with SAP after 30 days had the finest pore structure. This can be due to the coupled effect of pre-dewatering and evaporation. Associated drying shrinkage on the surface of the column by evaporation can reduce the porosity, which consequently resulted in a finer pore structure. The median pore diameters (based on surface area) of the raw MFTs and the MFTs pre-dewatered with SAP after 13 days were 0.0093 µm and 0.0069 µm, respectively. Furthermore, the median pore diameters after 30 days were found to be 0.0077 µm and 0.0052 µm for raw MFTs and SAP pre-dewatered MFTs, respectively. It is worth mentioning that the median pore diameter and the diameter at the maximum value of dv/dlogD (which is called TD) of the raw MFTs unaffected by evaporation are 0.6 µm and 0.9 µm,

respectively. The measured TD of the densified MFTs with SAP dewatering after 30 days was 0.12 µm, which is the lowest measured value among all the samples.

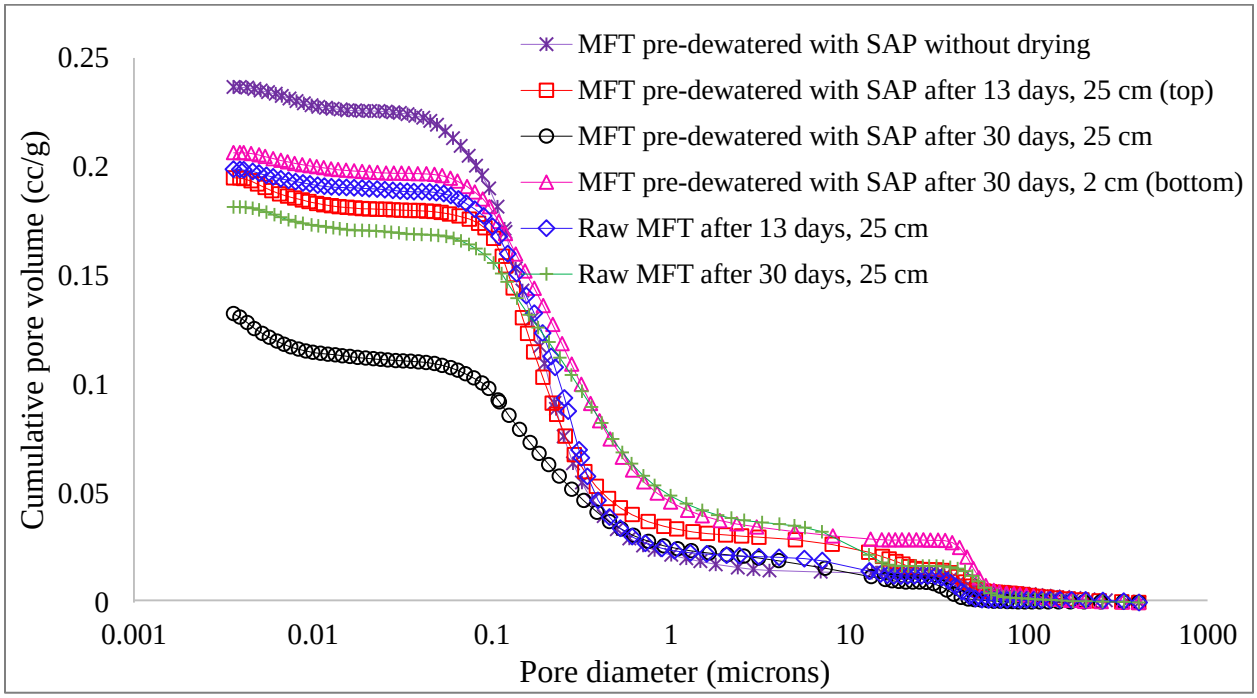

Figure 7.13, MIP test results for pore volume distribution

Figure 7.14 compares the pore size distribution of the raw MFTs and the MFTs pre-dewatered with SAP after 30 days of drying. It can be observed from this graph that in the MFTs pre-dewatered with SAP, 18% of the pores had diameters of less than 0.01 µm. Around 8% of the pores had diameters in the range of 0–0.005 µm and 6.5% of the pores had diameters in the range of 0.005–0.007 µm. In raw MFTs at the same location (25 cm after 30 days), only 6% of the pores had diameters less than 0.01 µm. The pore distribution shifted to a coarser size when suction induced by evaporation decreased.

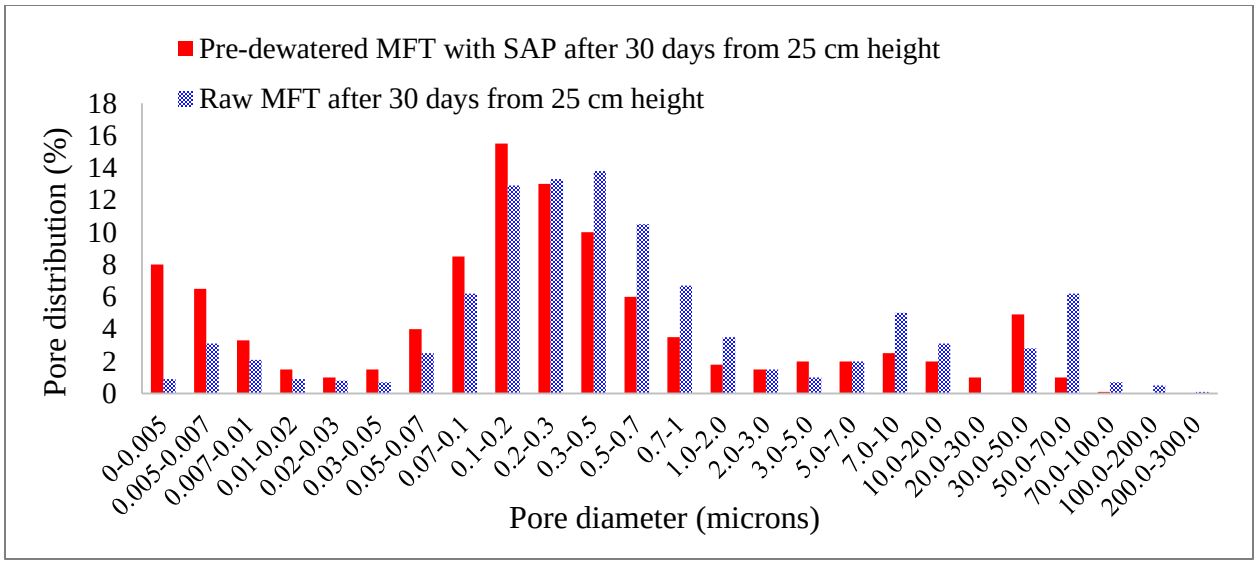

Figure 7.14, Pore size distribution

These results suggest that any changes in the moisture content lead to temporary changes in the macroporous structure, while leaving the micro pores unaffected

7.3.8 Scanning electronic microscopy

The effect of evaporation on the MFTs micro-fabric can be understood from the SEM micrographs in Figure 7.15. As expected, MFTs pre-dewatered with SAP after 13 days and 30 days at 25 cm height and raw MFTs after 30 days at 25 cm height showed the densest and most compacted structures. Suction induced by evaporation altered the card house fabric to a compact and aggregated fabric. High water retention capacity is observed in those samples whose microstructures are shown in Figures 7.15a, 7.15d, and 7.15e. In these MFTs samples, suction is not fully developed and the fissures and voids are not blocked. The void ratios in the samples corresponding to Figures 7.15a, 7.15b, 7.15c, 7.15d, 7.15e, and 7.15f are 1.39, 0.98, 0.58, 1.21, 1.89, and 0.72, respectively.

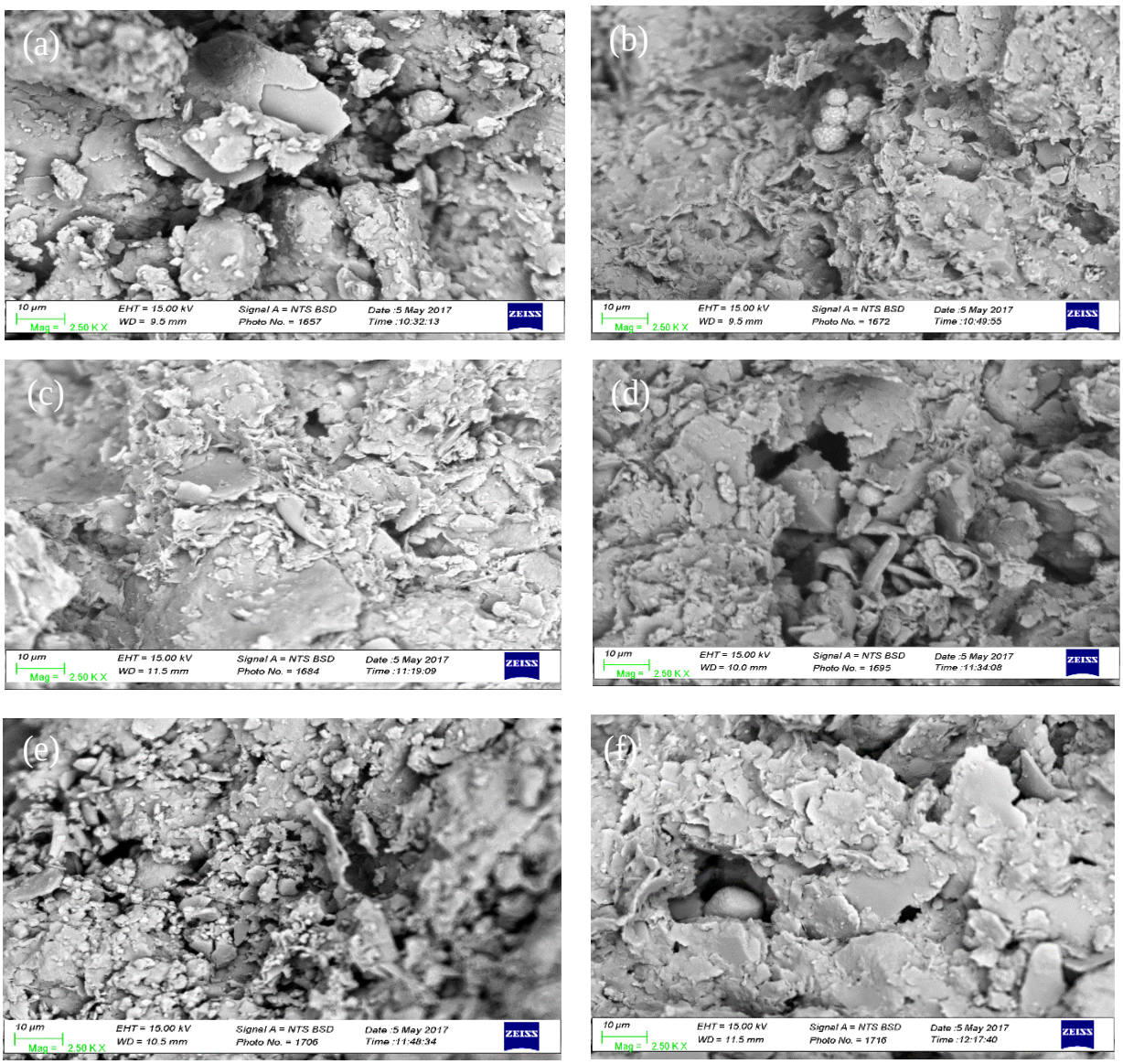

Figure 7.15, a) MFTs pre-dewatered with SAP with no impact of evaporation, b) MFTs pre-dewatered with SAP after 13 days at 25 cm height, c) MFTs pre-dewatered with SAP after 30 days at 25 cm height, d) MFTs pre-dewatered with SAP after 30 days at 2 cm height, e) raw MFTs after 13 days at 25 cm height, and f) raw MFTs after 30 days at 25 cm height

7.4 Conclusions

In this study, the effects of wetting-drying cycles, interlayer flow, and cracking on the evaporation, drainage, settlement, and microstructure of raw MFTs and MFTs pre-dewatered with SAP in a two-lift deposition system were investigated. The following conclusions are drawn after a detailed analysis:

- This study suggests that evaporation has a major role in drying process. However, crust formation on evaporation surfaces severely reduces the drying efficiency.
- The negative impact of wetting cycles or freshly added lift on the developed suction and consequently the strength is not permanent.
- Desiccation crack development occurred in three different stages. In the initial stage, few cracks appeared on the MFTs surface. Due to crack development and propagation in the initial stage, the rate of evaporation increased and consequently, cracks developed faster in the next stage, which is called the primary stage. Upon decreasing the water pressure in the soil matrix, the evaporation rate was limited and crack development reached a steady state. When the shrinkage limit was approached, the soil particles came into contact with each other and further drying occurred. Hence, any changes in the void ratio are small and as a consequence, crack formation and development reached a steady state.
- The crack intensity factor of the raw MFTs was twice that of the MFTs pre-dewatered with SAP. The higher water content, rate of evaporation, and drainage of raw MFTs can account for the larger crack surface area in raw MFTs.
- SAP pre-dewatering leads to a much faster increase in strength, which can accelerate reclamation and reduce the environmental footprint of the oil sands industry. An additional advantage of the SAP technique is that it leads to a 62% reduction in drainage and thus can remedy the issue of MFTs seepage into ground water and main water bodies. Based on the results of the present study, the SAP dewatering technique can be considered as a promising approach for densification and dewatering of MFTs generated by the oil sands industry.
- It is recommended to study the effect of freeze-thaw cycles at a large scale in the future.
- The information gained in this study can assist in MFTs management for the reclamation of designated lands and tailings ponds for a sustainable development of the oil sands industry.

7.5 References

Al-Hashmi, A. R., Luckham, P. F., Heng, J. Y. Y., Al-Maamari, R. S., Zaitoun, A., Al-Sharji, H. H., and Al-Wehaibi, T. K. (2013). Adsorption of high-molecular-weight EOR polymers on glass surfaces using AFM and QCM-D. Journal of Energy and Fuels, 27(5), 2437–2444.

Beier, N., Wilson, W., Dunmola, A., and Sego, D. (2013). Impact of flocculation-based dewatering on the shear strength of oil sands fine tailings. Canadian Geothenical Journal, 50, 1001–1007.

Botha, L., and Soares, J. B. P. (2015). The influence of tailings composition on flocculation. Canadian Journal of Chemical Engineering, 93(9), 1514–1523.

Caldwell, J., Revington, A., McPhail, G., Charlebois, L. (2014). Optimised seasonal deposition for successful management of treated mature fine tailings, 1–18.

Caughill, D. L., Morgenstern, N. R., and Scott, J. D. (1993). Geotechnics of nonsegregating oil sand tailings. Canadian Geotechnical Journal, 30(5), 801–811.

Chalaturnyk, R. J., Don Scott, J., and Özüm, B. (2002). Management of oil sands tailings. Journal of Petroleum Science and Technology, 20(9–10), 1025–1046.

Clark, K. A, and Pasternack, D. S. (1932). Hot water separation of bitumen from Alberta bituminous sand. Journal of Industrial and Engineering Chemistry, 1410–1416.

Demoz, A., and Mikula, R. J. (2012). Role of mixing energy in the flocculation of mature fine tailings. Journal of Environmental Engineering, 138(1), 129–136.

Dzinomwa, G. P. T., Wood, C. J., and Hill, D. J. T. (1997). Fine coal dewatering using pH- and temperature-sensitive superabsorbent polymers, 8, 767–772.

Fall, M., Benzaazoua, M., and Ouellet, S. (2005). Experimental characterization of the influence of tailings fineness and density on the quality of cemented paste backfill. Journal of Minerals Engineering, 18(1), 41–44.

Fall, M., Célestin, J., and Sen, H. F. (2010). Potential use of densified polymer-pastefill mixture

as waste containment barrier materials. Journal of Waste Management, 30(12), 2570–2578.

Farkish, A., and Fall, M. (2013). Rapid dewatering of oil sand mature fine tailings using super absorbent polymer (SAP). Journal of Minerals Engineering, 50–51, 38–47.

Fasking, T., Dunmola, A., Mckay, D., Masala, S., and Langseth, J. (2011). Bench scale drying of multi-layered thickened TSRU tailings. Proceeding in International Conference on Tailings, Edmonton, Canada, 2011.

Fisseha, B., Bryan, R., and Simms, P. (2010). Evaporation, unsaturated flow, and salt accumulation in multilayer deposits of "Paste" gold tailings. Journal of Geotechnical and Geoenvironmental Engineering, 136, 1703–1712.

Fujiyasu, Y., and Fahey, M. (2000). Experimental study of evaporation from saline tailings. Jornal of Geotechnical and Geoenvionmental Engineering, 126, 18-27.

Gidley, I. D. C., and Jeeravipoolvarn, S. (2014). Key dewatering mechanisms of the environmental drying scheme for oil sands fine tailings. Proceeidng in Tailings and Mine Waste, Colorado, US.

Jeeravipoolvarn, S., Scott, J. D., and Chalaturnyk, R. J. (2009). 10 M standpipe tests on oil sands tailings: long-term experimental results and prediction. Canadian Geotechnical Journal, 46(8), 875–888.

Junqueira, F. F., Sanin, M. V., Sedgwick, A., and Blum, J. (2011). Assessment of water removal from oil sands tailings by evaporation and under-drainage, and the impact on tailings consolidation. Proceeding in Tailings and Mine Waste Conference, Vancouver, BC, Canada.

Kuai, L. (2000). Sludge treatment and reuse as soil conditioner for small rural communities. Journal of Bioresource Technology, 73(3), 213–219.

Li, J. H., and Zhang, L. M. (2011). Study of desiccation crack initiation and development at ground surface. Journal of Engineering Geology, 123(4), 347–358.

Mackinnon, M., Matthews, J., Shaw, W., and Cuddy, R. (2010). Water quality issues associated with composite tailings (CT) technology for managing oil sands tailings. International Journal of Surface Mining, Reclamation and Environment, 15 (4), 235–256.

Masuda, K., and Iwata, H. (1990). Dewatering of particulate materials utilizing highly water-absorptive polymer. Journal of Powder Technology, 63(2), 113–119.

Miller, C., Mi, H., Yesiller, N. (1999). Experimental analysis of desiccation crack propagation in clay liners, 34(3), 677–686.

Owolagba, J., and Azam, S. (2015). Effect of seasonal weather variations on the desiccation behavior of treated oil sand fine tailings. Journal of Environmental Earth Sciences, 74, 1711–1717.

Peer, F., and Venter, T. (2003). Dewatering of coal fines using a superabsorbent polymer. Journal of the South African Institute of Mining and Metallurgy, 403–410.

Pramanik, S. (2016). Review of biological processes in oil sands: a feasible solution for tailings water treatment. Journal of Environmental Reviews, 24, 274-284.

Roshani, A., Fall, M., and Kennedy, K. (2016). Impact of drying on geo-environmental properties of mature fine tailings pre-dewatered with superabsorbent polymer. International Journal of Environmental Science and Technology, 14 (3), 453-462.

Roshani, A., Fall, M., and Kennedy, K. (2017a). Drying behavior of mature fine tailings pre-dewatered with superabsorbent polymer (SAP): Column experiments. Geotechnical Testing Journal, 40(2), 210-220.

Roshani, A., Fall, M., and Kennedy, K. (2017b). A column study of the hydro-mechanical behavior of mature fine tailings under atmosphere drying. International Journal of Mining Science and Technology, 27(2), 203-209.

Roshani, A., Fall, M., and Kennedy, K. (2017c). Microstructural, hydraulic conductivity and geochemical changes of drying mature fine tailings in column experiments. International

Journal of Mining, Reclamation and Environment, ISSN: 1748-0930, 1-15.

Salam, A. M., Örmeci, B., and Simms, P. H. (2016). Determination of the optimum polymer dose for dewatering of oil sands tailings using UV-vis spectrophotometry. Journal of Petroleum Science and Engineering, 147, 68–76.

Simms, P., Grabinsky, M., and Zhan, G. (2007). Modelling evaporation of paste tailings from the Bulyanhulu mine. Canadian Geotechnical Journal, 44(12), 1417–1432.

Sworska, a., Laskowski, J. S., and Cymerman, G. (2000). Flocculation of the Syncrude fine tailings Part I. Effect of pH, polymer dosage and Mg^{2+} and Ca^{2+} cations. International Journal of Mineral Processing, 60(2), 143–152.

8

Synthesis and integration of the results

8.1 Introduction

In order to facilitate the understanding of the drying behavior of mature fine tailings (MFTs) and feasibility application of superabsorbent polymer (SAP) as a novel dewatering management technique in the oil sand industry, the obtained results from this study, which have been discussed in detail in chapters 3 to 7, are synthesized in this chapter. A corresponding comparative analysis of the obtained results is carried out to demonstrate the behavior of MFTs with and without polymer use under atmospheric drying and wetting-drying cycles.

8.2 Effect of atmospheric drying

When subjected to atmospheric drying, MFTs demonstrates significant changes in chemical, mechanical, hydraulic, and thermal behavior. Correspondingly, the accurate understanding of MFTs behavior is one of the primary tasks for researchers who are working on developing new plans in oil sands tailings management. Based on a comparison of the results, the influence of the atmospheric drying on the geo-environmental and geotechnical behavior or properties of MFTs without SAP and MFTs pre-dewatered with SAP are summarized in sections 8.2.1 and 8.2.2, respectively.

8.2.1 Raw MFTs

8.2.1.1 Raw MFTs behavior under atmospheric drying

Based on the obtained results, MFTs behavior under atmospheric drying is summarized in the following paragraphs.

For the thermal response, the changes in MFTs temperature are determined by latent heat of vaporization. Figure 3.10 is selected as a representative example to analyze the thermal response of MFTs to evaporation. From this figure, it can be seen that the temperature difference between the monitored points became gradually less pronounced during the last 10 days. Lower temperature in the upper parts of the column (evaporation boundaries) indicates the high rate of evaporation, which is an endothermic process. The location of the drying front was then advanced toward the bottom. By decreasing the water vapor gradient between the ambient air and MFTs, the evaporation rate was restricted in the last 10 days (Figure 3.4), and thus the entire column reached room temperature.

For the hydraulic response, the pore water pressure variation is very important because it has a significant impact on strength development and deposit stability. The hydraulic response was analyzed by pore water pressure, evaporation, drainage, and hydraulic conductivity. As shown in Figure 3.9, the most significant changes in negative pore water pressure (suction) occurred after 5 days of casting each lift (at the upper part). The high rate of evaporation (Figure 3.4) and drainage (Figure 3.6) during the first days after adding the fresh lift built up the suction within the upper parts. Based on these figures, when the evaporation reached stage III, in which the soil surface became sufficiently desiccated, the slow rate of evaporation caused the liquid phase to become discontinuous. As a result, suction reached the maximum value in the upper part of the column in this period. It is worth mentioning that suction in the first lift (upper part) reached around 17kPa after 5 days, but after casting the second lift, and drainage of the water from the upper part eliminated the suction that had been built up. However, at the end of the test period, suction in this depth could be developed to around 21 kPa and exceeded the former value. This may be due to the fact that the micro-cracks induced by evaporation increased the suction. This outcome could be highlighted from the practical point of view, and two-lift depositions with less than 25 cm height (each lift) are recommended.

The hydraulic conductivity of MFTs decreased by decreasing the void ratio. In the upper parts where the suction was fully developed, the soil matrix became dense and less permeable. By increasing the solids content and decreasing the void ratio, water flow was restricted, and hydraulic conductivity decreased (Figures 3.8, 4.11, and 4.12). At the same time, in the lower part, suction was not developed, and connected voids became a channel for water flow, causing higher hydraulic conductivity

Mechanical strength and its magnitude are of great importance for MFTs deposit stability. Undrained vane shear strength increased with time (Figure 3.11). Figures 3.9 and 3.11 showed the coupled relationship between mechanical and hydraulic properties and that by developing suction, strength increased. At the end of the test period (after 30 days), only 10 cm thickness of the bottom could not reach the threshold strength (5 kPa). Moreover, according to Figure 3.13, the solids content of more than 70% for MFTs is required to meet the performance criterion of 5 kPa.

In terms of chemical properties, the concentration of major cations and trace elements showed that regardless of the elapsed time and the height of the samples, the concentration of the elements was

almost constant within the column. It was believed that very low hydraulic conductivity of MFTs and high concentration of fine particles restricted the movement of the elements toward the evaporation boundaries.

8.2.1.2 Microstructural changes of atmospheric drying MFTs

To clearly demonstrate the influence of atmospheric drying on microstructural properties of MFTs, SEM images and MIP results were presented in section 4.3.4. As depicted in Figure 4.8, along with suction development, the card house structure of the voids was altered into a dense and compacted matrix. At the upper parts of the column where suction induced by evaporation was fully developed, the edge to face card house fabric became compact and aggregated. At the bottom, however, well-developed and interconnected voids can be seen. Thus, the drying alters the MFTs microstructure, which, in turn, influences the strength.

Furthermore, the SEM observation was confirmed by the MIP results. As illustrated in Figures 4.9, 4.10(a), and 4.10(b), samples taken from the bottom in the early stage showed the coarser pore structure. However, the samples from the upper part had the finest pore matrix after 30 days due to the surface evaporation that developed the suction and correspondingly reduced the porosity and void ratio. Threshold diameters were also measured. Threshold diameters for samples taken from the upper parts of the monitoring column and the bottom of the column at early stages were 0.4 micron and 3 microns, respectively. This difference is due to the fully developed suction and precipitates on the evaporation surfaces.

8.2.2 MFTs pre-dewatered with SAP

8.2.2.1 MFTs pre-dewatered with SAP under atmospheric drying

As previously mentioned in sections 5.2.1 and 5.2.2, pre-dewatering MFTs with SAP decreased the initial water content from 130% to around 57%. The drying behavior of MFTs pre-dewatered with SAP in terms of hydraulic properties was discussed in detail in sections 5.3.1 and 5.3.2. As depicted in Figure 5.2, the water removal process for MFTs pre-dewatered and non-pre-dewatered with SAP was controlled by evaporation rather than drainage. A decreasing trend of evaporation rate was observed in the first 5 days, which was due to the start of the second stage of evaporation in which the conductive properties of MFTs prevented the flow of sufficient water to the surface.

Cumulative water loss due to evaporation for MFTs pre-dewatered with SAP showed a 56% reduction in comparison with raw MFTs—from a 12.9 kg water loss in raw MFTs to around 7.2 kg in pre-dewatered MFTs. This decrease is due to the lower initial water content of pre-dewatered MFTs and its lower extended cracks, which reduce the flow ability of pore water toward the evaporating front.

Tailings pond seepage is one of the main concerns in the oil sand industry. Due to the proximity of the ponds to key water bodies, notably the Athabasca River, MFTs seepage has always been a critical issue for this industry. Based on Figure 5.3, a comparison between cumulative water loss through drainage for pre-dewatered and non-dewatered MFTs with SAP denoted an 82% reduction in total drainage when the SAP pre-dewatering technique was used. These findings point to the practically efficient application of SAP to absorb and retain MFTs-processed water, and thus considerably mitigate the seepage of MFTs water.

Suction development within the column was illustrated by Figure 5.5. This figure is in agreement with Figures 5.2, 5.3, and 5.7. The high rate of evaporation and drainage during the first 5 days of casting each lift built up the suction, and, as a result, strength developed in the upper part of the column (Figure 5.7). As shown in this graph, suction increased faster in pre-dewatered MFTs with SAP, which is attributed to the lower initial water content of pre-dewatered MFTs.

Figure 6.9 presented comparative values of hydraulic conductivity for pre-dewatered and non-dewatered MFTs. Hydraulic conductivity decreased with the decreasing void ratio, and values still remained very low.

Mechanical properties have a crucial role in tailings management in terms of slope stability and reclamation policy. Figure 5.7 showed that MFTs pre-dewatered with SAP had a much higher strength increase rate at early stages. After 10 days of drying, the undrained shear strength at all column depths exceeded or was close to 5 kPa (Figure 5.7a). This may have significant practical implications with respect to accelerating the dewatering process and consolidation of MFTs, thereby increasing the pace of reclamation and reducing the cost of tailings management.

The maximum rate of desiccation-induced settlement was observed in the first 4 to 5 days after loading the second lift (Figure 5.4), which is compatible with Figures 5.2, 5.3, and 5.5. These figures

showed that the maximum rate of evaporation, drainage, and developed suction occurred at the same time.

Chemical analysis of MFTs has always been a concern, and the transportation of the oil sands–affected water into main water bodies has become an important issue. Tables 6.2 and 6.3 showed the effectiveness of SAP to capture and hold the dissolved cations and prevent them from transportation to underground water. The concentration of some trivalent cations (Fe^{3+}) and divalent cations (Mn^{2+}) in MFTs pore water decreased by 100% and 95%, respectively, after pre-dewatering with SAP. This is a notable result because the SAP application not only reduced the seepage stream by 80% but also reduced ion concentration in the MFTs drainage water. Consequently, the associated risk with ion accumulation in recycled water will be remedied as well.

8.2.2.2 Microstructural evolution of atmospheric drying MFTs pre-dewatered with SAP

As predicted, the SEM observation and MIP results for pre-dewatered and non-dewatered MFTs showed the same results. The obtained results were fully described in section 6.3.4, and, as Figure 6.6 showed, the developed suction induced by evaporation altered the MFTs matrix into a compact and rigid soil fabric.

8.2.3 Wetting –drying cycles

8.2.3.1 MFTs under wetting-drying cycles

Evaporation and drainage of MFTs in the presence of the wetting-drying cycles were fully explained in section 7.3.1. The results of the evaporation and drainage illustrated in Figures 7.2 and 7.3 showed that evaporation is the main drying mechanism for MFTs subjected to drying-wetting cycles. The cumulative drainages of MFTs pre-dewatered with SAP showed a 62% reduction when compared to non-dewatered MFTs. This reduction is of great importance from a practical point of view because it can minimize the risk of seepage of toxic tailings water from the tailings ponds, which can cause groundwater contamination.

Suction development in MFTs pre-dewatered and non-dewatered showed two different behaviors. In raw MFTs (Figure 7.4), suction only developed on top of the column, and the half bottom had no suction after 30 days. With pre-dewatered MFTs, a more uniform suction was observed in the

entire column (Figure 7.5). The main reason may be that dewatering of MFTs with SAP created a highly heterogeneous texture with aggregates in the tailings, which may significantly influence MFTs desiccation behavior. Cracks formed within the boundaries of the aggregates immediately after loading each lift. These cracks helped to drain pore water easily, and, consequently, suction developed faster and more uniformly in MFTs pre-dewatered with SAP in comparison to raw MFTs.

The vane shear strengths of the raw MFTs and MFTs pre-dewatered with SAP were shown in Figure 7.8. The highest solids content (98%) was found in the sample sourced at a height of 25 cm in pre-dewatered MFTs with a shear strength of 1.0 MPa. In the same column, the lowest measured solids content was 70%, corresponding to a vane shear strength of 4500 Pa. Whereas for raw MFTs, the highest solids content was 85%, and half of the column (first 15 cm) exhibited a strength less than 2 kPa.

The extent of surficial cracking was described by the crack intensity factor (CIF) illustrated in Figures 7.9 and 7.10. Initial stage, primary stage, and steady stage as three distinct stages of crack formation were clearly shown in these graphs. CIF for pre-dewatered and non-dewatered MFTs were measured as 14% and 25.7%, respectively. Rewetting did not close or reduce the volume of the cracks.

8.2.3.2 Microstructural evolution of atmospheric drying MFTs subjected to wetting-drying cycles

The effect of evaporation on MFTs micro-fabric can be understood from the SEM micrographs as well as MIP results. As expected, MFTs pre-dewatered with SAP after 30 days showed the densest and most compacted structures due to the suction induced by evaporation, which altered the card house fabric to a compacted matrix. Furthermore, the median pore diameters after 30 days were found to be 0.0077 μm and 0.0052 μm for raw MFTs and SAP pre-dewatered MFTs, respectively, and the pore distribution shifted to a coarser size when suction induced by evaporation decreased.

9

Conclusions and recommendations

9.1 Conclusions

The main goal of this research was to experimentally analyze the atmospheric drying of MFTs with and without SAP as well as determine the influence of wetting-drying cycles on their desiccation behavior.

In the first phase of this study, the hydro-mechanical behavior of MFTs was studied in the column. Interaction among the mechanical, hydraulic, and physical properties of the two successive lifts of raw MFTs was investigated under atmospheric drying. The main outcomes of this part are summarized as follows:

- Evaporation was considered as the main mechanism in the dewatering process rather than drainage. The initial rate of evaporation from MFTs was relatively high (close to the potential rate of evaporation), but when the water was limited on the evaporation boundary, the rate of evaporation showed a gradual decreasing trend and finally reached a residual value.
- Evaporation, drainage, and self-weigh consolidation were the three main mechanisms responsible for the high rate of settlement during the early stages of deposition.
- The freshly added lift had two negative effects on the strength of the first lift. Water drainage from the latter lift into the former lift and covering the evaporation boundaries of the former lift were destructive effects on the developed suction.
- The negative effect of the new lift deposition on eliminating the developed suction of the former lift in multi-lift deposition was not permanent. Strength and suction could be recovered and exceed the previous values.
- Increases in suction increased the strength. On the upper parts of the column where suction induced by evaporation developed, the vane shear strength was high. In contrast, at the bottom, where cracks could not be penetrated and suction remained close to zero, the measured strength was very low.

Microstructural, hydraulic conductivity, and geochemical changes of drying MFTs were analyzed in the second phase of the study. The main results are provided as follows:

- Slightly higher concentrations of anions and cations were measured in the evaporation boundaries.

- The finest microstructure was found on top of the column where the fully developed suction altered the card house void structure into the dense and compacted fabric.
- Finer pores restricted the water flow, and, consequently, hydraulic conductivity decreased on the top portion of the column.
- Solid content in the column varied significantly from very high on the top to very low on the bottom. As a result, the top exhibited very high strength, whereas the bottom could not meet the minimum requirement of Directive 074.

In the third phase of the study, the novel technique of dewatering MFTs with SAP was investigated for a two-lift deposition system by means of a column experiment. The main outcomes include the following:

- Filling sequence can affect MFTs properties temporarily. Redistribution of water from the newly added layer eliminated the developed suction, but later, penetration of the cracks increased the rate of evaporation, and, consequently, strength developed.
- In the multi-lift deposition system for pre-dewatered MFTs with SAP, addition of the fresh lift did not increase the water content of the former lift as much as the multi-lift deposition for raw MFTs. This is due to the much lower water content of the pre-dewatered MFTs in comparison with raw MFTs.
- The SAP dewatering technique leads to a much faster strength increase rate, and strength could be developed even in the lower parts. This can positively affect the pace of reclamation.
- An 82% reduction in drainage for MFTs pre-dewatered with SAP in comparison with raw MFTs can address the challenge of MFTs seepage into water bodies and groundwater.

In the fourth phase, the microstructure of MFTs pre-dewatered with SAP in a two-lift deposition with atmospheric drying was studied. The highlighted results are summarized as follows:

- Pre-dewatered MFTs showed a more compacted pore structure in comparison with raw MFTs. The finest pore structure was found in the samples from the top of the column. At the bottom, where suction was not fully developed, coarser structure was identified.
- In term of changes in geochemistry, the concentration of major ions in the polymer chains of SAP significantly increased, and the concentration of these cations decreased in the pore

water. This might be a remarkable result because SAP can prevent pollutant agents from being discharged into water bodies.

In the fifth and last phase of this study, the effects of wetting-drying cycles, interlayer flow, and cracking on the evaporation, drainage, settlement, and microstructure of raw MFTs and MFTs pre-dewatered with SAP in a two-lift deposition system were investigated. The results are as follows:

- For both raw MFTs and MFTs pre-dewatered with SAP, the negative impact of the wetting cycle or freshly added lift on developed suction and, consequently, strength is not permanent.
- For both raw MFTs and MFTs pre-dewatered with SAP desiccation, crack development showed three different stages: i) In the initial stage, the evaporation rate was small, and few cracks appeared on the soil surface. ii) In the primary stage, cracks formed in the initial stage became more developed and propagated. In this stage, the rate of evaporation increased, and, consequently, the cracks developed faster. iii) By decreasing the water pressure in the soil matrix, the evaporation rate was limited, and crack development reached the steady-state stage. By approaching the shrinkage limit, the soil particles came into contact, along with further drying, thus changes in the void ratio were small, and, as a consequence, cracks approached the steady-state stage.
- The crack intensity factor in raw MFTs was measured as twice that of pre-dewatered MFTs with SAP. Higher water content of raw MFTs and consequently its higher rate of evaporation and drainage could account for the higher crack surface in raw MFTs.
- Obtained results place the SAP dewatering and densification method as a promising approach to oil sands tailings management.

9.2 Recommendations for future work

Significant advancements in the understanding of atmospheric drying of MFTs pre-dewatered with SAP in a two-lift deposition system have been made by means of this thesis. However, some areas remain in which more research is required. The following summarizes recommendations for future work:

- The effect of freeze-thaw as a natural dewatering technique for further dewatering of multi-lift deposition of pre-dewatered MFTs with SAP should be taken into consideration.
- Interaction between freshly added lifts with the former lifts in terms of evaporation, drainage, suction, and water content should be studied for multi-lift deposit with more than two lifts.
- Different percentages of SAP in combination with different lift thicknesses of MFTs as a multi-lift deposition system can be performed to find the optimum dosage of SAP that addresses the requirement in oil sands tailings management for reduction of dedicated disposal areas.
- A numerical model can be developed to provide a better understanding of the desiccation process in a multi-lift deposition system of MFTs pre-dewatered with SAP. A numerical model can integrate all the tailings and atmospheric parameters for predicting the drying behavior of fine tailings.